CONDUCTION-ELECTRON LOCALIZED-MOMENT INTERACTION IN PALLADIUM-SILICON BASE AMORPHOUS ALLOYS CONTAINING TRANSITION METALS

Thesis by

Ryusuke Hasegawa

In Partial Fulfillment of the Requirements

For the Degree of

Doctor of Philosophy

California Institute of Technology

Pasadena, California

1969

(Submitted May 9, 1969)

To my wife and parents

ACKNOWLEDGEMENT

The author would like to express his sincere gratitude to Professor Pol E. Duwez and Dr. C. C. Tsuei for their kind advice and never-ending encouragement throughout this work. He is also grateful to Drs. P. L. Maitrepierre, A. K. Sinha and J. D. Speight for useful discussions. Several communications with Dr. J. Kondo of the Electrotechnical Laboratory of Japan are very much appreciated. This work was made possible through the assistance of R.N.Y. Chan and P. K. Kuan in resistivity measurements; Y. Moriwaki in magnetoresistivity measurements; J. E. Brown in preparing the alloys; C. Geremia, S. Kotake and J. A. Wysocki in technical skills and Mrs. F. S. Williams in typing the manuscript.

Financial aid was gratefully received from the Atomic Energy Commission, the Radio Corporation of America, the Fulbright Commission and the California Institute of Technology.

He is grateful to his wife Pamela for her encouragement during the present work.

ABSTRACT

The electrical and magnetic properties of amorphous alloys obtained by rapid quenching from the liquid state have been studied. The composition of these alloys corresponds to the general formula $M_xPd_{80-x}Si_{20}$, in which M stands for a metal of the first transition series between chromium and nickel and x is its atomic concentration. The concentration ranges within which an amorphous structure could be obtained were: from 0 to 7 for Cr, Mn and Fe, from 0 to 11 for Co and from 0 to 15 for Ni. A well-defined minimum in the resistivity vs temperature curve was observed for all alloys except those containing nickel. The alloys for which a resistivity minimum was observed had a negative magnetoresistivity approximately proportional to the square of the magnetization and their susceptibility obeyed the Curie-Weiss law in a wide temperature range. For concentrated Fe and Co alloys the resistivity minimum was found to coexist with ferromagnetism. These observations lead to the conclusion that the present results are due to a s-d exchange interaction. The unusually high resistivity minimum temperature observed in the Cr alloys is interpreted as a result of a high Kondo temperature and a large s-d exchange integral. A low Fermi energy of the amorphous alloys (3.5 eV) is also responsible for the anomalies due to the s-d exchange interaction.

TABLE OF CONTENTS

I. INTRODUCTION

The interaction between the conduction electrons (s-electrons) and the unfilled shell electrons (d-electrons) localized on a transition metal atom was first considered by Zener[1] to explain metallic magnetism. In this concept, conduction electrons are polarized through the s-d exchange interaction and hence have magnetic moments which align the spins of the d-electrons parallel or antiparallel. One can therefore expect some anomalies in the transport and magnetic properties of alloys containing transition metals due to the s-d exchange interaction. One of these anomalies is a resistivity minimum phenomenon[2, 3]. It has been found[4] also that alloys with an anomaly in the zero magnetic field resistivity show a decrease of resistivity in a magnetic field (negative magnetoresistivity) at low temperature. Korringa and Gerritsen[5] explained this resistivity anomaly by postulating that a transitional metal dissolved dilutely in a non-magnetic host metal introduces spatially localized states with energies near the Fermi energy.

The first attempt to explain the anomalous resistivity and magnetic properties by use of the s-d exchange interaction is due to Owen et al.[6, 7]. Based on the position and width of the electron spin resonance line observed in dilute alloys of Mn in Cu, they concluded that the s-d exchange interaction was of the order of 0.2 of the interaction in the free ion. They also found that the dilute alloys were antiferromagnetic by measuring the magnetic susceptibility and the elec-

tron spin resonance spectrum. Taking into consideration the s-d exchange interaction, Kasuya[8] developed a theory which explains the anomalous resistivity of ferromagnetic metals below the ferromagnetic transition temperature. This theory, however, cannot explain the resistivity minimum in magnetic dilute alloys. Schmitt[9] proposed a phenomenological theory in which the anomalous resistivity in dilute alloys could be a result of a co-operative magnetic transition at low temperature. Schmitt and Jacobs[10] extended this theory to explain anomalous magnetic behavior in Cu-Mn alloys. They also found that the negative magnetoresistivity is proportional to the square of the magnetization. Along similar lines Yosida[11] developed a theory in which he considered a perturbing potential consisting of the spin-dependent and the spin-independent interactions between the 4s conduction electrons and the 3d electrons localized on the transition metal atoms. Although this theory gives a negative magnetoresistivity which is proportional to the square of the magnetization, it does not explain the resistivity minimum.

Friedel[12] pointed out that the residual resistivity of Cu or Al containing a transition metal varies with the atomic number of the metal in a somewhat different way from that of a non-transition metal. The strong peaks observed in the curve of residual resistivity vs the transition metal atomic number suggest some resonance process between the conduction and the d-electrons of the transition metal. Friedel[12, 13] considers that the introduction of a transition metal in metals such as Al or Cu results in "virtual bound states" which are not well defined in

energies nor in space, and that this virtual bound state resonates with the conduction electron state which has the same energy. Friedel[13] also calculated the residual resistivity by introducing the phase-shift sum rule.

A number of alloys of Cu, Ag, Au, Mg and Zn with small concentrations of V, Cr, Mn, Fe, Co, Mo, Re and Os have been found[2, 3, 14] to have a minimum in the resistivity-temperature curve. It has also been found that the resistivity minimum phenomenon is always accompanied by the existence of localized magnetic moments. From these observations Kondo[15] considers that the resistivity minimum must be deduced from a simplified s-d exchange model consisting of localized spins and conduction electrons. Thus, he obtained a temperature-dependent term ($\propto \ln T$) by calculating the transition probability to the second Born approximation. When this logarithmic term is combined with the lattice resistivity, it gives rise to a resistivity minimum.

The problem of localized magnetic moments in dilute alloys has been a subject of current interest since Kondo's successful explanation of the effect. Nagaoka[16] has investigated further how conduction electrons in dilute alloys are affected by the s-d exchange interaction. He has shown that, if the s-d exchange interaction is antiferromagnetic, a quasi-bound state is formed below a critical temperature T_K. Therefore it is expected that the spin resistivity obtained by Kondo will saturate for $T \ll T_K$, as has been observed experimentally[17-21]. Some revised theories along this line have been proposed by Suhl and Wong[22] and by Hamann[23].

All the reported studies have been restricted to crystalline alloys containing small concentrations of transition metals. The temperature at which the resistivity minimum occurs is usually below $50^{o}K$ (except for the Au-V alloys[14]). The present study covers the case of non-crystalline alloys containing transition metals. In this case the resistivity minimum temperature is generally higher than for the crystalline case and can be as high as $580^{o}K$. Since Kondo's theory requires only paramagnetic behavior of the transition metal, the results of the theory are applicable to amorphous alloys. The palladium-base amorphous alloys were chosen for this investigation because in these alloys it is possible to replace Pd by an appreciable concentration of a transition metal. In addition it was found that the amorphous $Pd_{80}Si_{20}$ alloy has a low Fermi energy and a negligibly small magnetic susceptibility. The present study provides the first evidence for a Kondo effect in a number of amorphous alloys in the system $M_xPd_{80-x}Si_{20}$ where M represents a metal of the first transition series from Cr to Ni, and x is its atomic concentration.

II. ALLOY AND SPECIMEN PREPARATION

The amorphous alloys prepared for this study have the general composition $M_xPd_{80-x}Si_{20}$ where M stands for a metal of the first transition series and x varies from 0 to 7 for Cr, Mn and Fe, from 0 to 11 for Co and from 0 to 15 for Ni. The alloys were prepared by induction melting of the appropriate quantities (total of about 5g) of the constituents (99.99% purity for the transition metals and 99.999% for Si) in a quartz crucible under an argon atmosphere. Since the weight loss after melting was less than 0.2%, it was assumed that the actual composition of the alloys was the nominal one.

The amorphous state of the alloys was obtained by quenching from the liquid state. The "piston and anvil" technique[24] was used where a small globule of liquid alloy was contained in a fused silica tube for about 30 sec before quenching. This time is short enough to prevent reaction between the liquid alloys and the fused silica tube. However, some reaction was observed for the alloys containing Cr or Mn, which might have some effect on the chemical composition of the quenched foils. Since the rapid quenching technique does not always yield reproducible results[25] every foil used in the present study was carefully checked by X-ray diffraction. A diffraction pattern was recorded with a Norelco diffractometer at 2 θ angles between 34° and 50° and in angular steps of 0.05° (in 2 θ), each step corresponding to a total of 12,800 counts. Within this angular range, the diffraction pattern of the quenched foil exhibits a very broad maximum typical of a liquid structure. The

presence of microcrystals (if any) in the foil can be detected by weak Bragg reflections superimposed to the broad maximum. Therefore the quenched foils which showed any deviations from the liquid structure diffraction pattern were not used in the present study.

A typical amorphous foil quenched from the liquid state is about 2.5 cm in diameter and 40 μ thick. From this foil a rectangular specimen of about 20 x 2 mm was cut for resistivity measurements. Current and potential leads, made of 0.005" Pt wires, were spot welded to the specimen. For the magnetic susceptibility measurements, one or two foils were cut into small pieces (2 x 2 mm) and a total amount of about 100 mg in weight was used.

III. EXPERIMENTAL RESULTS

(1) Electrical Resistivity

The resistivity of the amorphous alloys was measured by the standard four-probe method as a function of temperature ($1.5^{o} \sim 600^{o}K$) and transition metal concentration. The temperature was measured with an accuracy of $\pm 0.2^{o}K$ by a combination of copper-constantan thermocouple and a Ge crystal. Excluding the uncertainty in the dimensions of the specimen, which is about $\pm$ 15%, the results of the resistivity measurements are accurate to $\pm$ 0.01 $\mu\Omega$-cm.

A well-defined resistivity minimum was observed in all the alloys containing Cr, Mn, Fe or Co. Typical resistivity data for these alloys are shown in Figs. 1, 3, 5 and 7 as a function of temperature. No resistivity minimum was observed for $Ni_xPd_{80-x}Si_{20}$ alloys.

To obtain the contribution of the transition metal to the resistivity of the $M_xPd_{80-x}Si_{20}$ alloys, the resistivity of an amorphous $Pd_{80}Si_{20}$ alloy was studied. It was found that the resistivity of $Pd_{80}Si_{20}$ increases linearly with increasing temperature above $\sim 40^{o}K$ and is proportional to the square of temperature between $10^{o}K$ and $\sim 40^{o}K$. In the temperature range from 0 to $10^{o}K$, the resistivity undergoes a slight minimum. This minimum can be attributed to the presence of Fe impurity in Pd, since it did not exist in an alloy of the same composition prepared with higher purity Pd (99.999%). Typical resistivity data of the $Pd_{80}Si_{20}$ alloy can be expressed by $(86.30 + 2.8 \cdot 10^{-4}T^{2})$ $\mu\Omega$-cm for $T < 40^{o}K$ and $(86.40 + 7.5 \cdot 10^{-3}\ T)$ $\mu\Omega$-cm for $T \gg 40^{o}K$. The resistivity

of the $Pd_{80}Si_{20}$ alloys was subtracted from all the resistivity data for $M_xPd_{80-x}Si_{20}$ alloys. Since the resistivity difference $\Delta\rho(=\rho_{M_xPd_{80-x}Si_{20}} - \rho_{Pd_{80}Si_{20}})$ has an error of about $\pm$ 15% due to the uncertainty in the dimension of the specimen, relative values of $\Delta\rho$/at.% are plotted in Figs. 2, 4, 6 and 8 as a function of temperature.

(2) Magnetoresistivity

The specimens used in this study were the same as those used in the resistivity measurement. The transverse magnetoresistivity was measured for all the amorphous $M_xPd_{80-x}Si_{20}$ alloys with the four-probe method at T = 4.2°, 77° and 295°K. The magnetic field was applied perpendicular to the current and varied from 0 to 10 kOe. Since the negative magnetoresistivity is very small, special attention was given to the selection of a current source. A voltage/current reference source (Model Tc-100.2 BR, Princeton Applied Research) was used in the present experiments.

To obtain the effective negative magnetoresistivity due to the transition metal in the alloys, measurements were made on several specimens of amorphous $Pd_{80}Si_{20}$ alloy. It was found that this alloy exhibits no positive or negative magnetoresistivity at T = 77° and 295°K and a very small positive magnetoresistivity ($\Delta\rho_{H=10kOe}/\rho_{H=0} \sim 0.0025\%$) at T = 4.2°K. Therefore all the magnetoresistivity data for the $M_xPd_{80-x}Si_{20}$ alloys at T = 4.2°K were corrected by subtracting the magnetoresistivity of the $Pd_{80}Si_{20}$ alloy. The corrected negative magnetoresistivity $\Delta\rho_H$ was divided by the zero field resistivity $\rho_{H=0}$ and $\Delta\rho_H/\rho_{H=0}$ at T = 4.2°K

is plotted as a function of magnetic field in Figs. 9, 10, 11 and 12 for alloys containing Cr, Mn, Fe or Co. No negative magnetoresistivity was observed at 77° and 295°K for Cr and Mn alloys and at 295°K for Fe alloys. An appreciable negative magnetoresistivity was observed at 77°K for the concentrated Fe alloys and at 77° and 295°K for Co alloys. The alloys containing Ni showed no negative magnetoresistivity at any temperature. There was no saturation of the negative magnetoresistivity for all the alloys studied in fields ranging from 0 to 10 kOe.

(3) Magnetic Properties

Magnetic moments of the $M_xPd_{80-x}Si_{20}$ alloys were measured between 1.8° and 300°K and in magnetic fields up to 8.40 kOe. The measurements were made in the null-coil pendulum magnetometer whose design and performance are described in detail in Ref. 26.

Since Pd used in the present study contained Fe as an impurity (order of 0.01 wt.%), a measurement on the $Pd_{80}Si_{20}$ alloy was performed to obtain the net contribution of the transition metal in $M_xPd_{80-x}Si_{20}$ alloys. The susceptibility of the $Pd_{80}Si_{20}$ alloy was found to be negligibly small ($\chi \approx 10^{-7} \sim 10^{-8}$ e.m.u./g) between 20° and 300°K and increased as $\chi \sim (1.4 \cdot 10^{-5})T^{-1}$ e.m.u./g for $T < 20°K$. The magnetic moment and susceptibility of the $Pd_{80}Si_{20}$ alloy were subtracted from those measured for the $M_xPd_{80-x}Si_{20}$ alloys.

The magnetization vs temperature at H = 8.4kOe for various compositions of the alloys containing Cr, Mn or Fe is shown in Figs. 13, 15 and 17. The magnetic susceptibility is obtained from the magnetic

isothermals (magnetization vs magnetic field for various temperatures) and inverse of the susceptibility difference $\Delta\chi (= \chi_{M_xPd_{80-x}Si_{20}} - \chi_{Pd_{80}Si_{20}})$ is plotted as a function of temperature in Figs. 14, 16 and 18 for alloys containing Cr, Mn or Fe. Since the magnetic measurements for $Co_xPd_{80-x}Si_{20}$ alloys were already available for $x \geq 3$[26] only the $Co_1Pd_{79}Si_{20}$ alloy was measured. The $Ni_xPd_{80-x}Si_{20}$ alloys showed no magnetic moments.

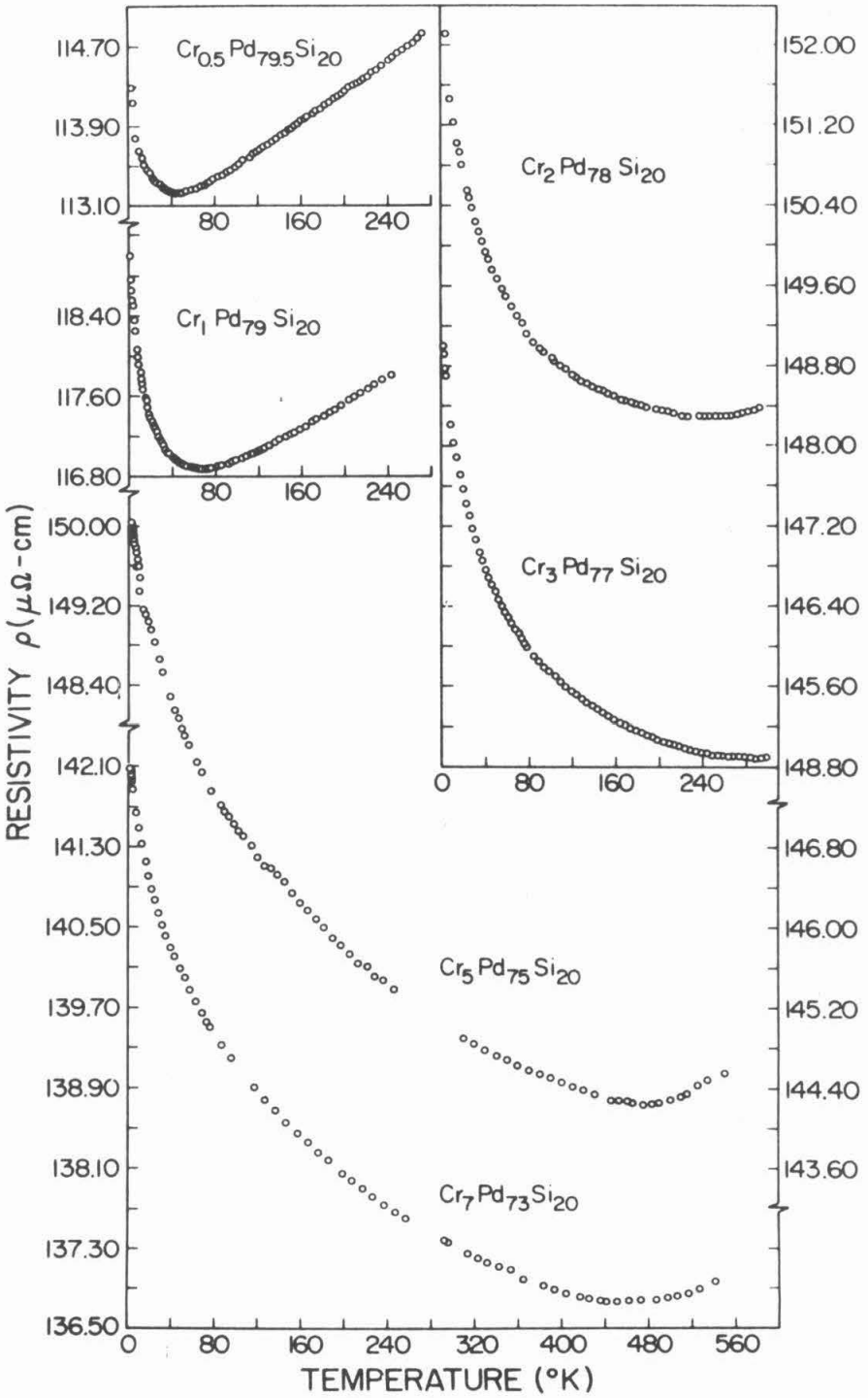

Fig. 1. Resistivity vs temperature curves for the $Cr_xPd_{80-x}Si_{20}$ alloys

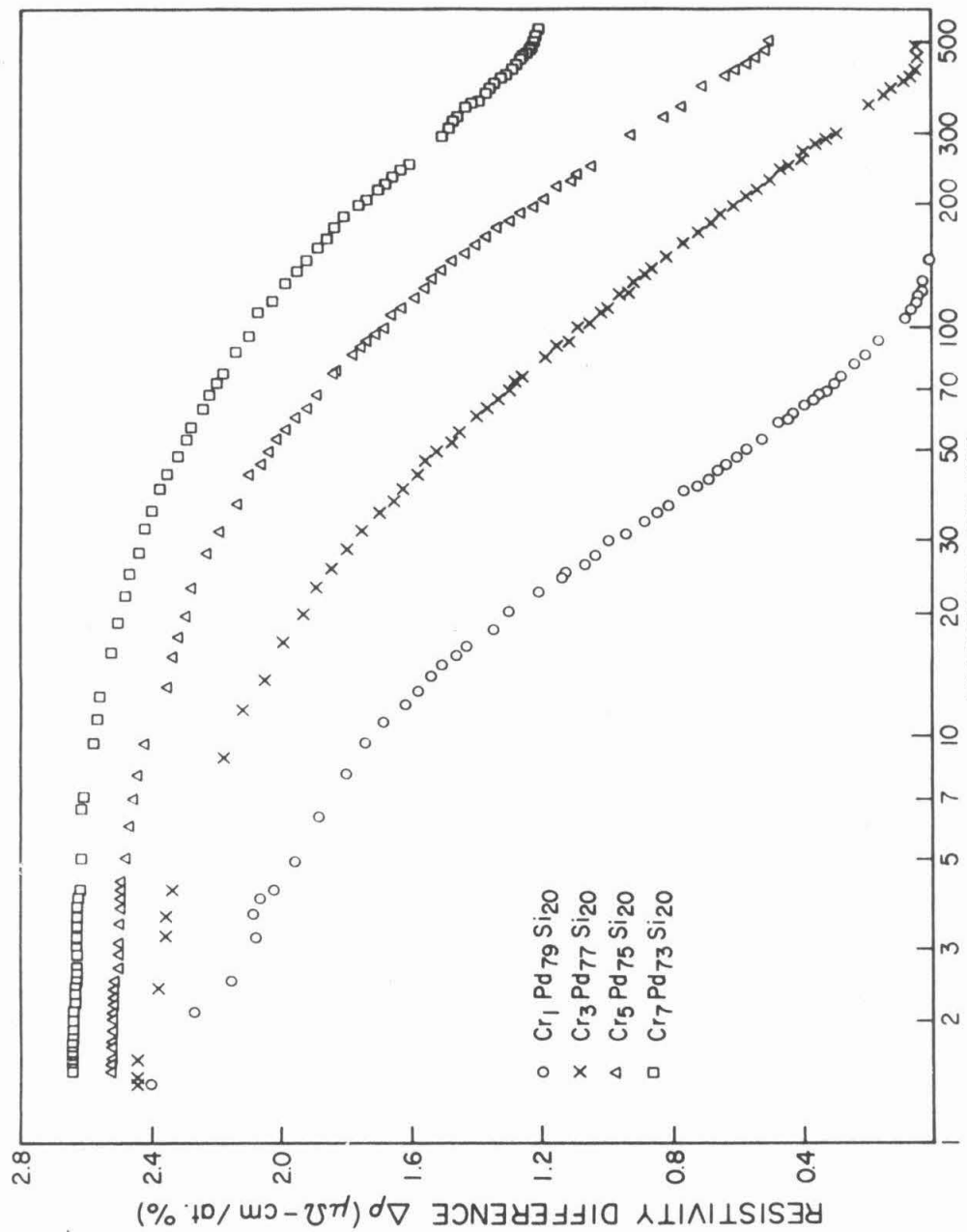

Fig. 2. Resistivity difference per at.% Cr vs temperature curves for the $Cr_x Pd_{80-x} Si_{20}$ alloys

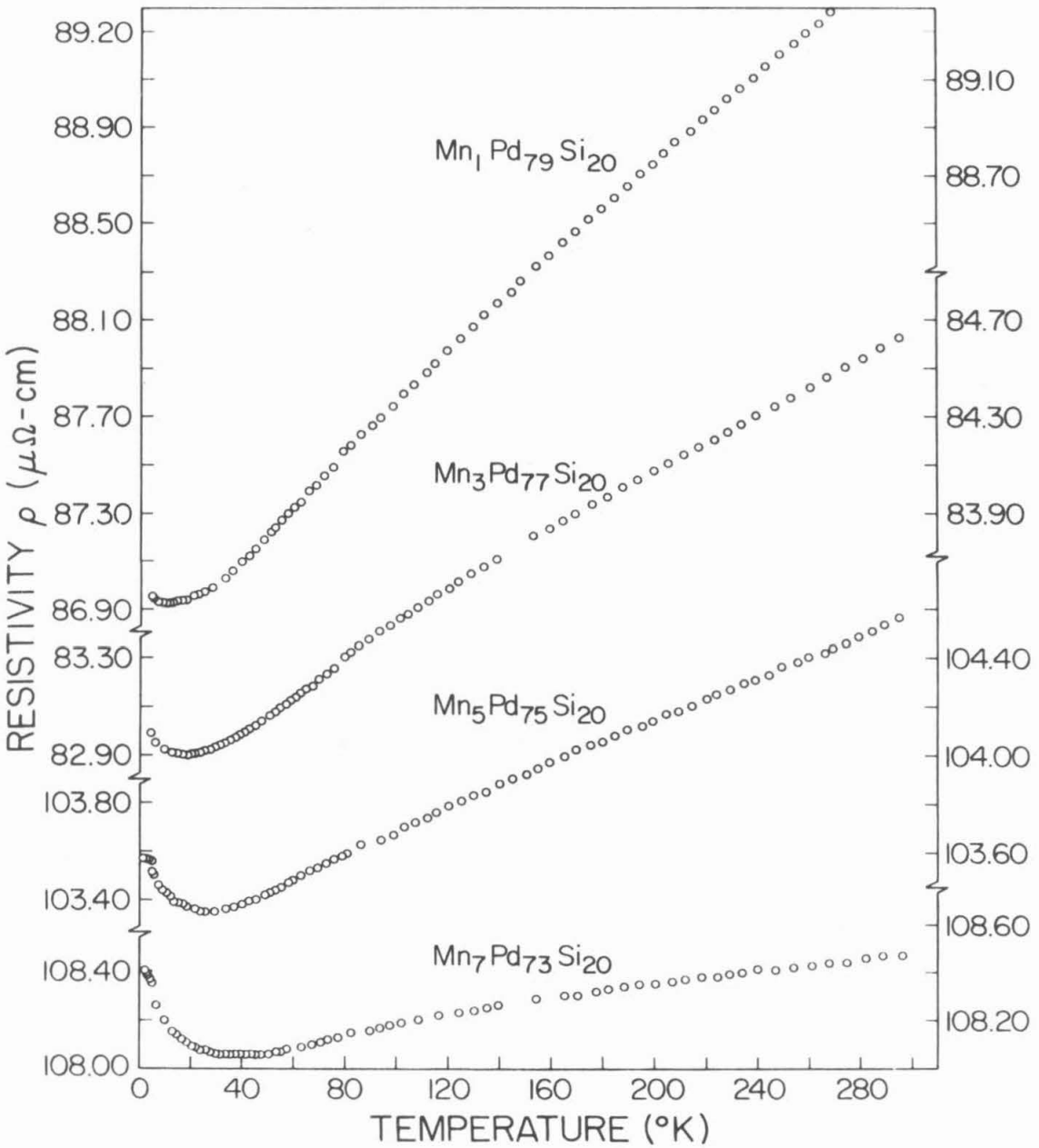

Fig. 3. Resistivity vs temperature curves for the $Mn_xPd_{80-x}Si_{20}$ alloys

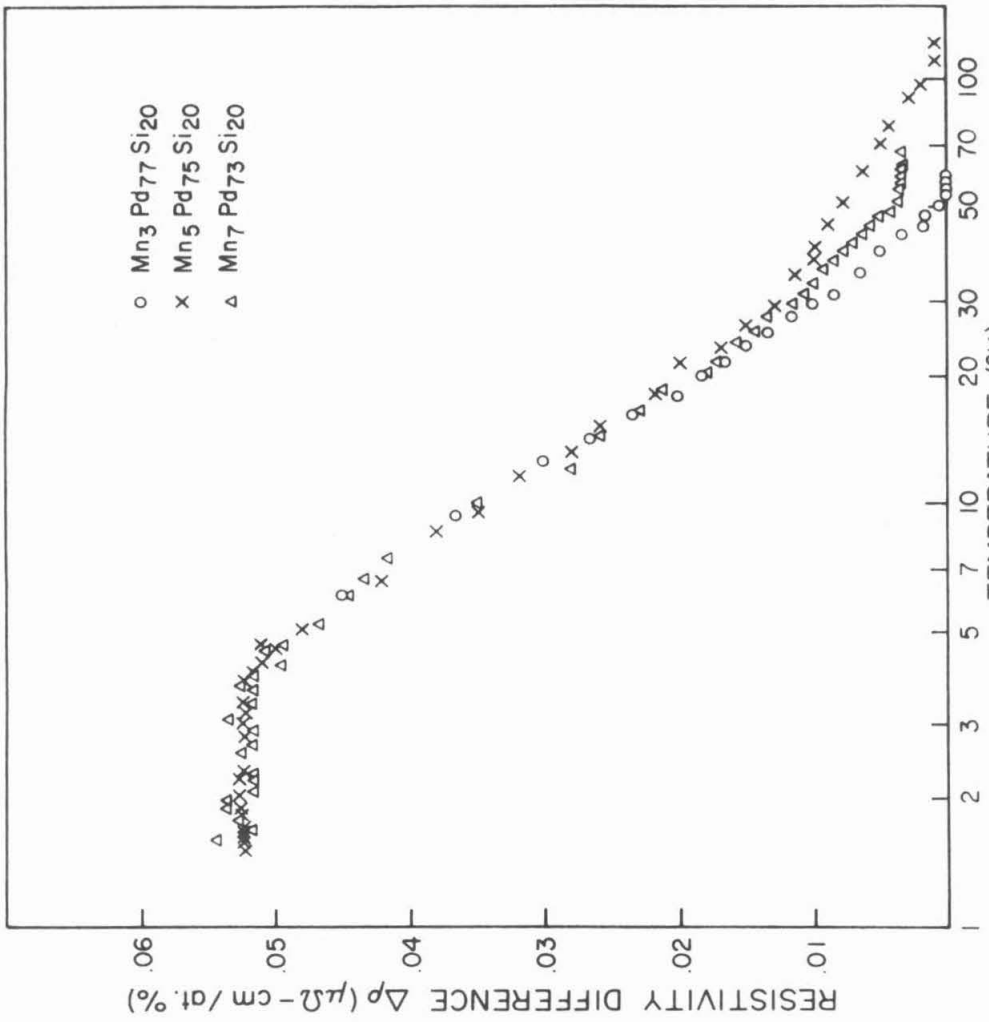

Fig. 4. Resistivity difference per at.% Mn vs temperature curves for the $Mn_xPd_{80-x}Si_{20}$ alloys

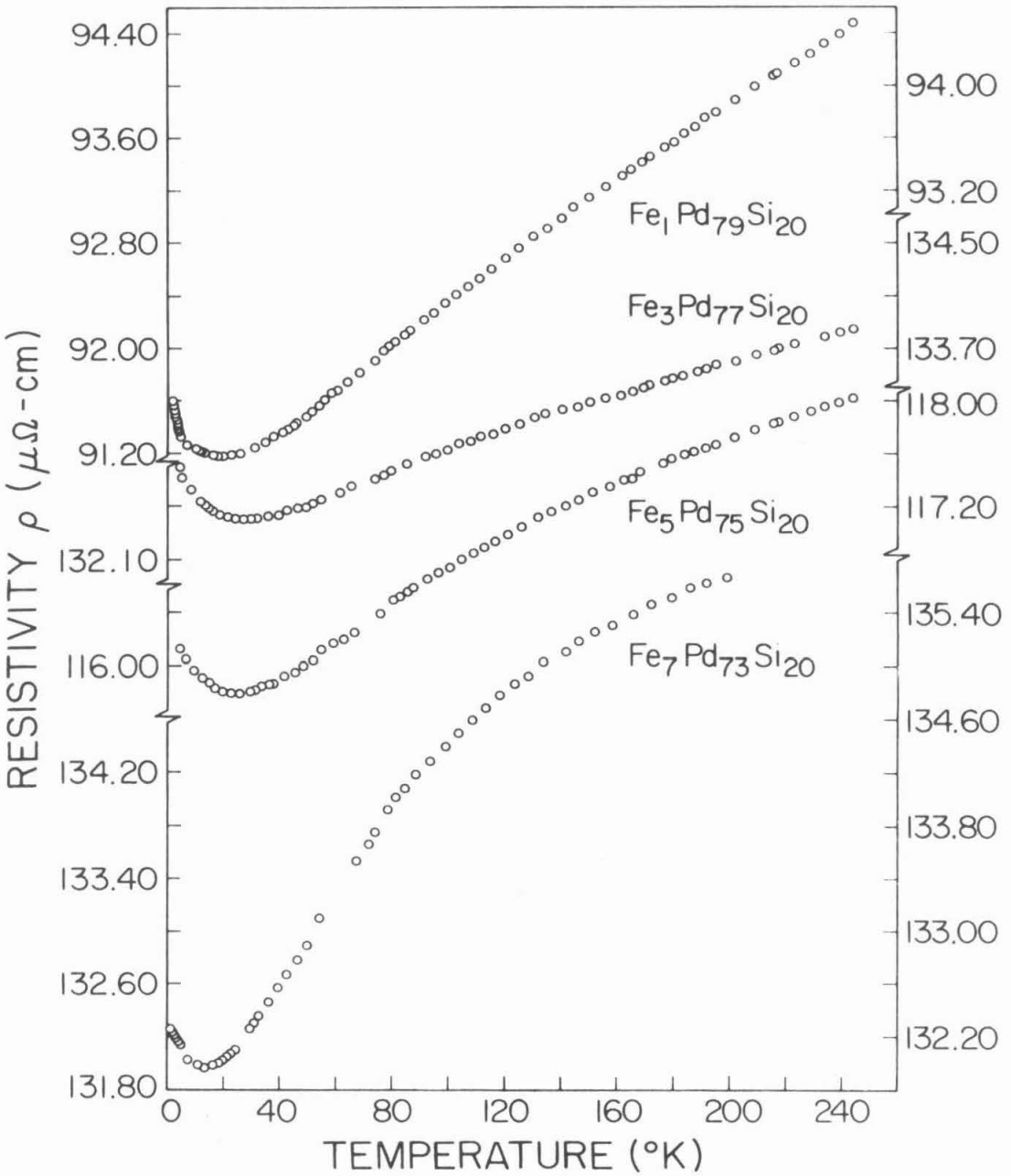

Fig. 5. Resistivity vs temperature curves for the $Fe_xPd_{80-x}Si_{20}$ alloys

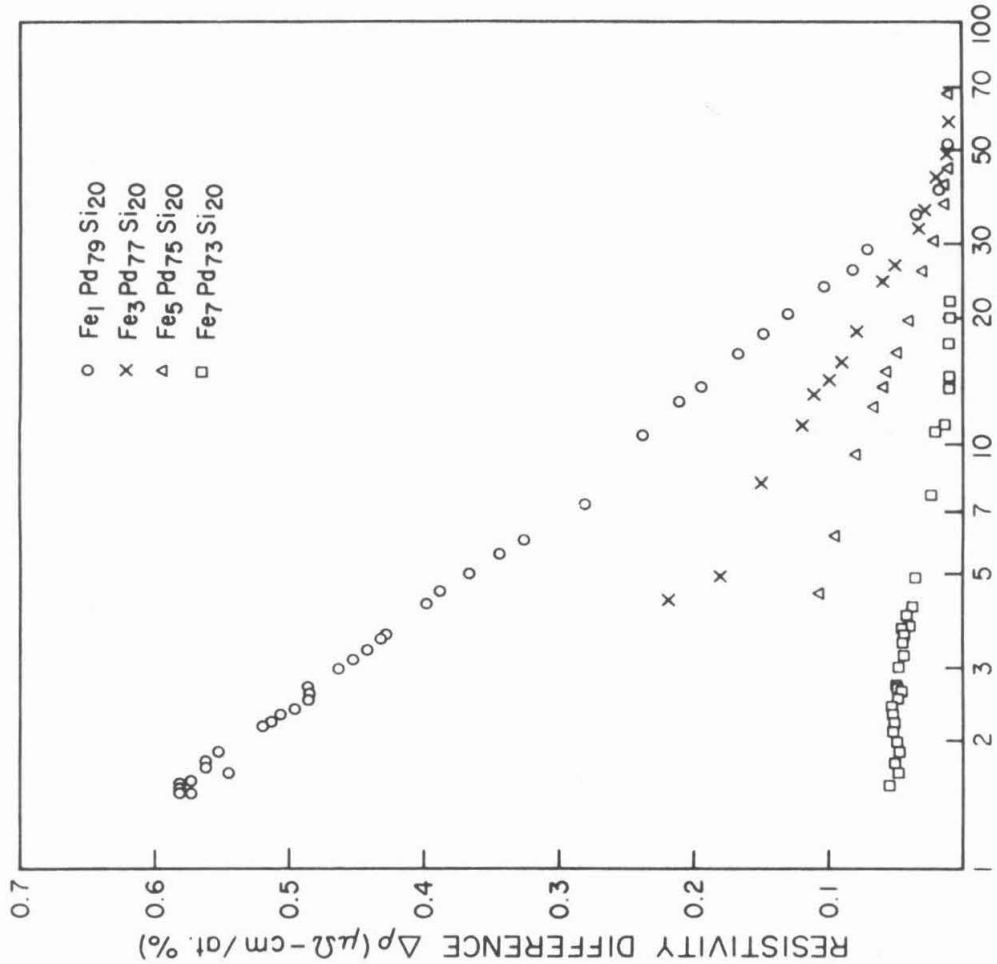

Fig. 6. Resistivity difference per at.% Fe vs temperature for the $Fe_xPd_{80-x}Si_{20}$ alloys

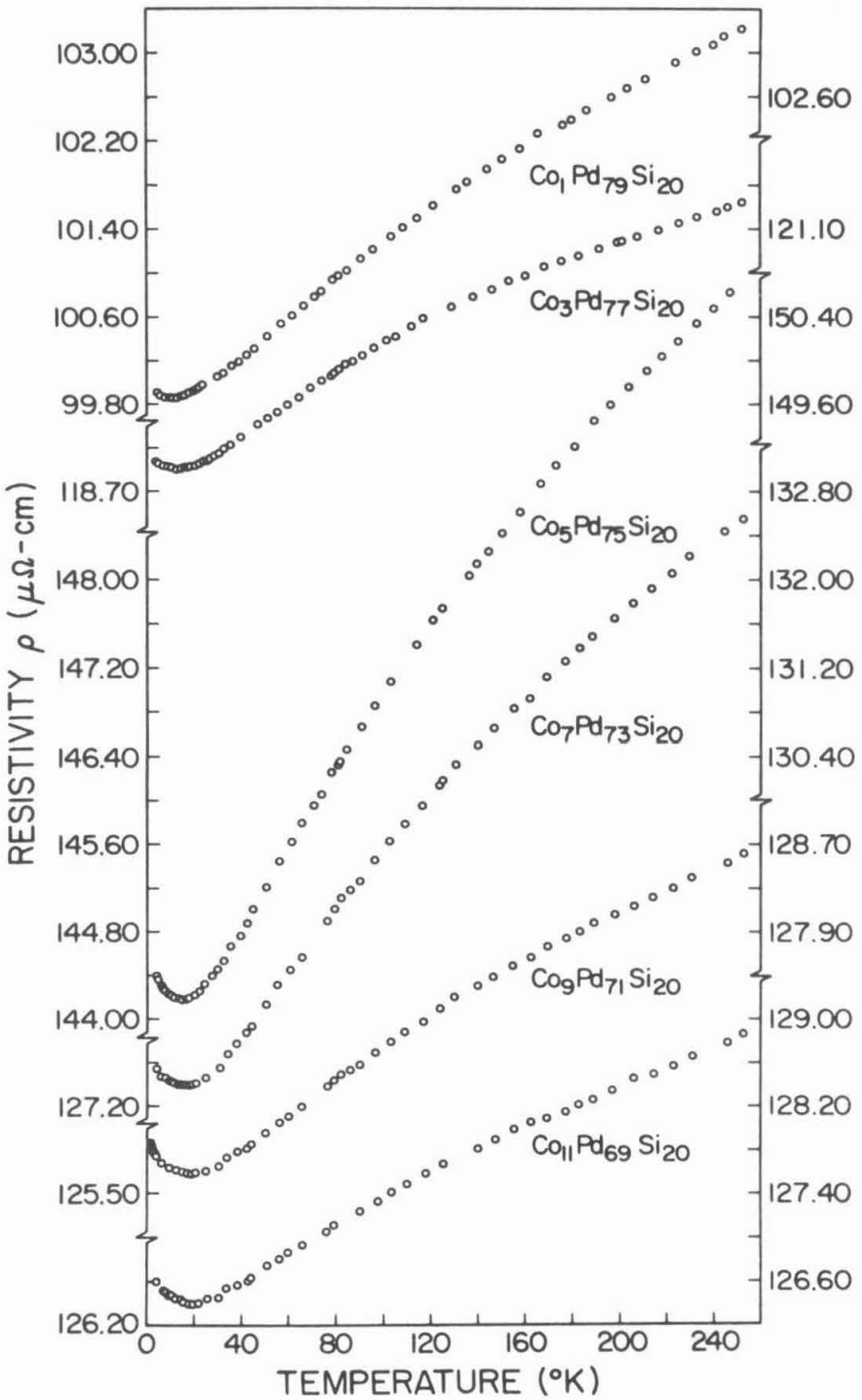

Fig. 7. Resistivity vs temperature curves for the $Co_xPd_{80-x}Si_{20}$ alloys

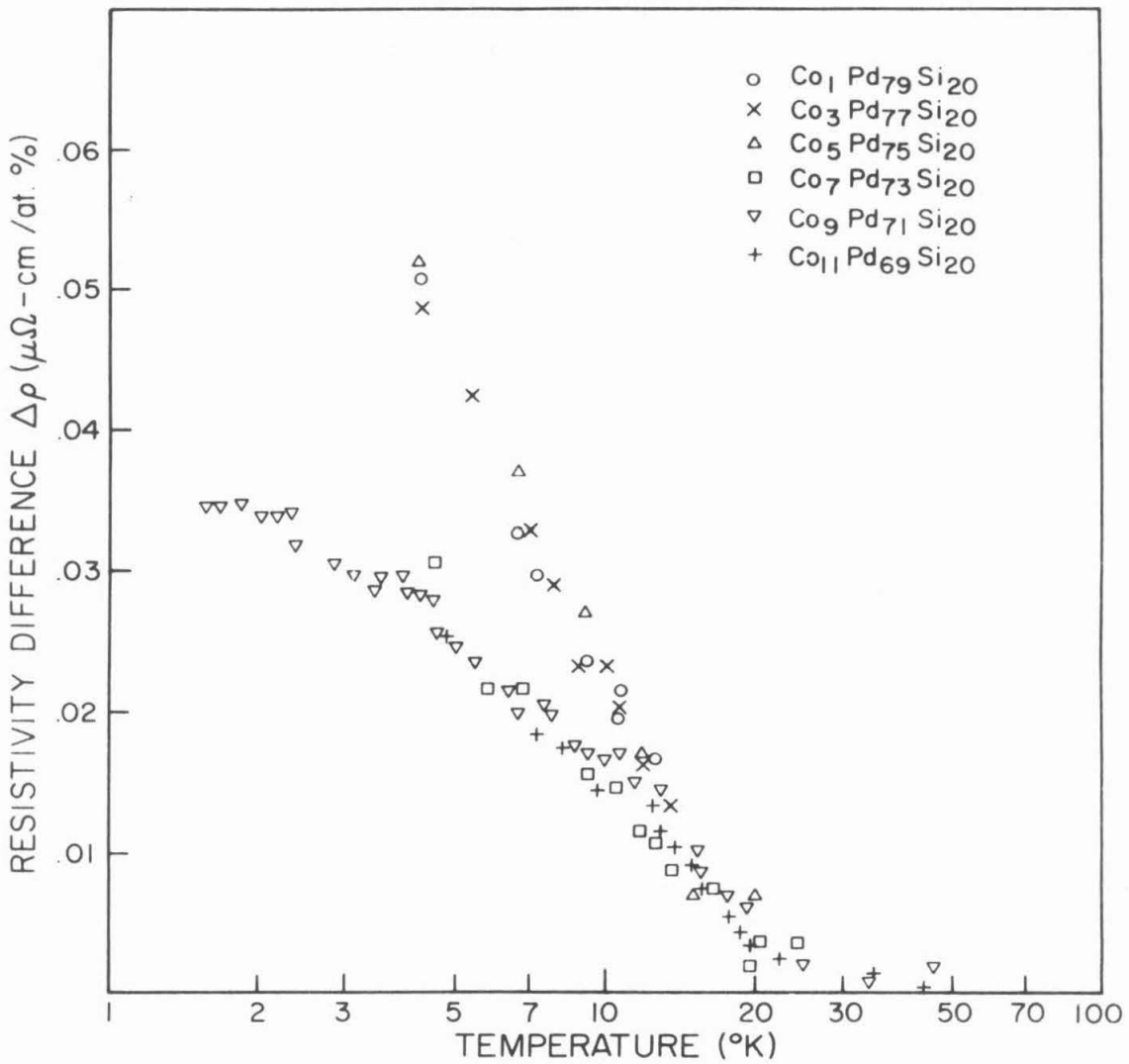

Fig. 8. Resistivity difference per at.% Co vs temperature curves for the $Co_xPd_{80-x}Si_{20}$ alloys

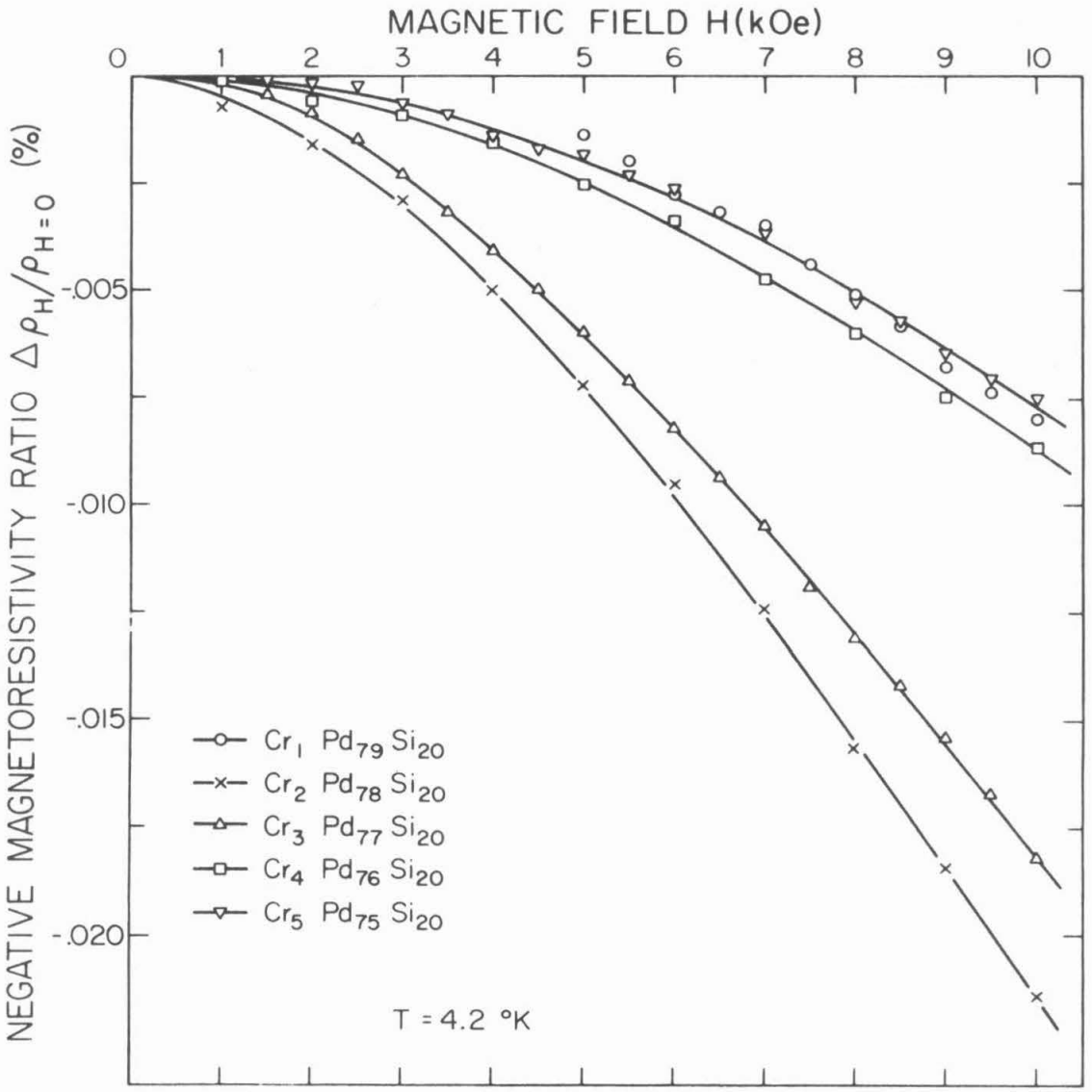

Fig. 9. Negative magnetoresistivity ratio vs magnetic field curves at 4.2°K for the $Cr_xPd_{80-x}Si_{20}$ alloys

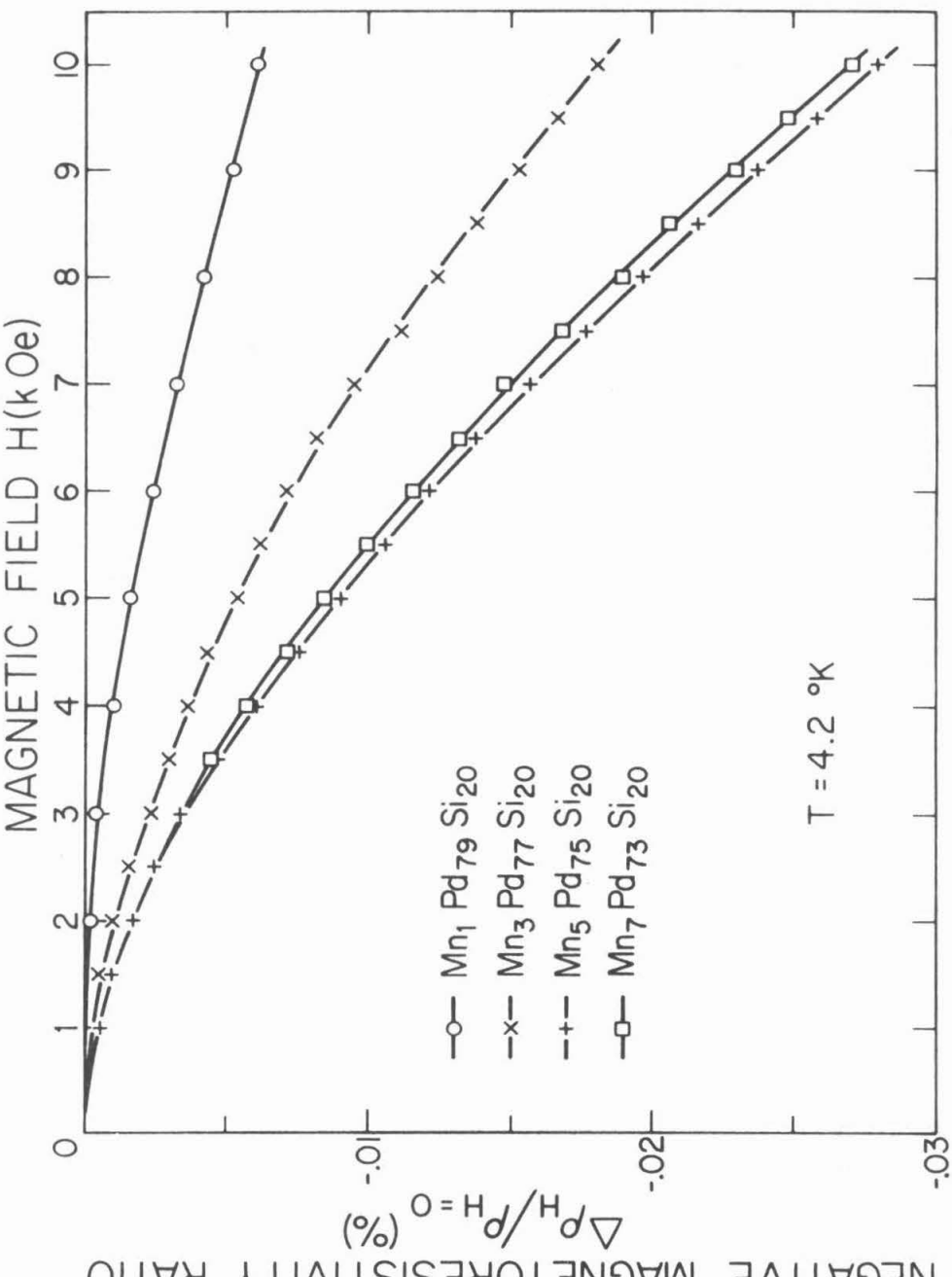

Fig. 10. Negative magnetoresistivity ratio vs magnetic field curves at 4.2°K for the $Mn_x Pd_{80-x} Si_{20}$ alloys

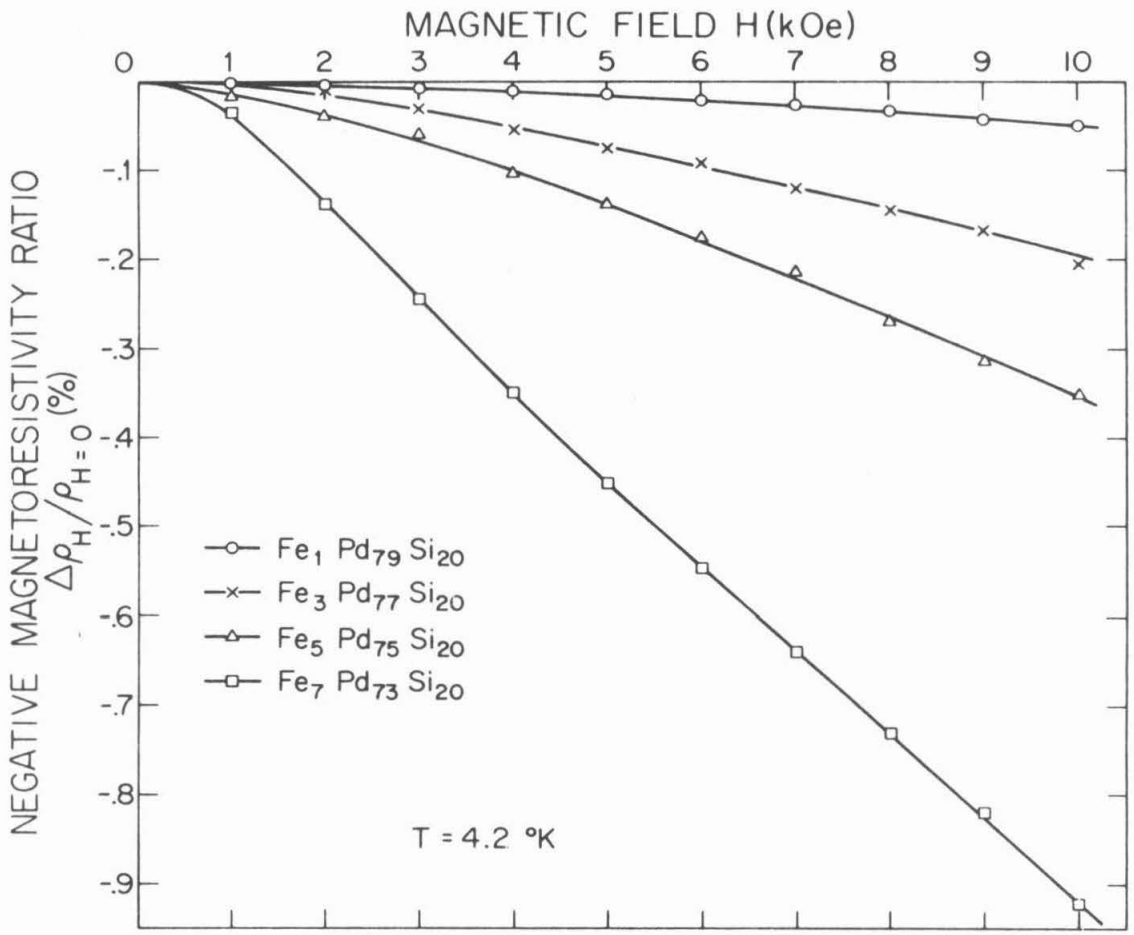

Fig. 11. Negative magnetoresistivity ratio vs magnetic field curves at 4.2°K for the $Fe_xPd_{80-x}Si_{20}$ alloys

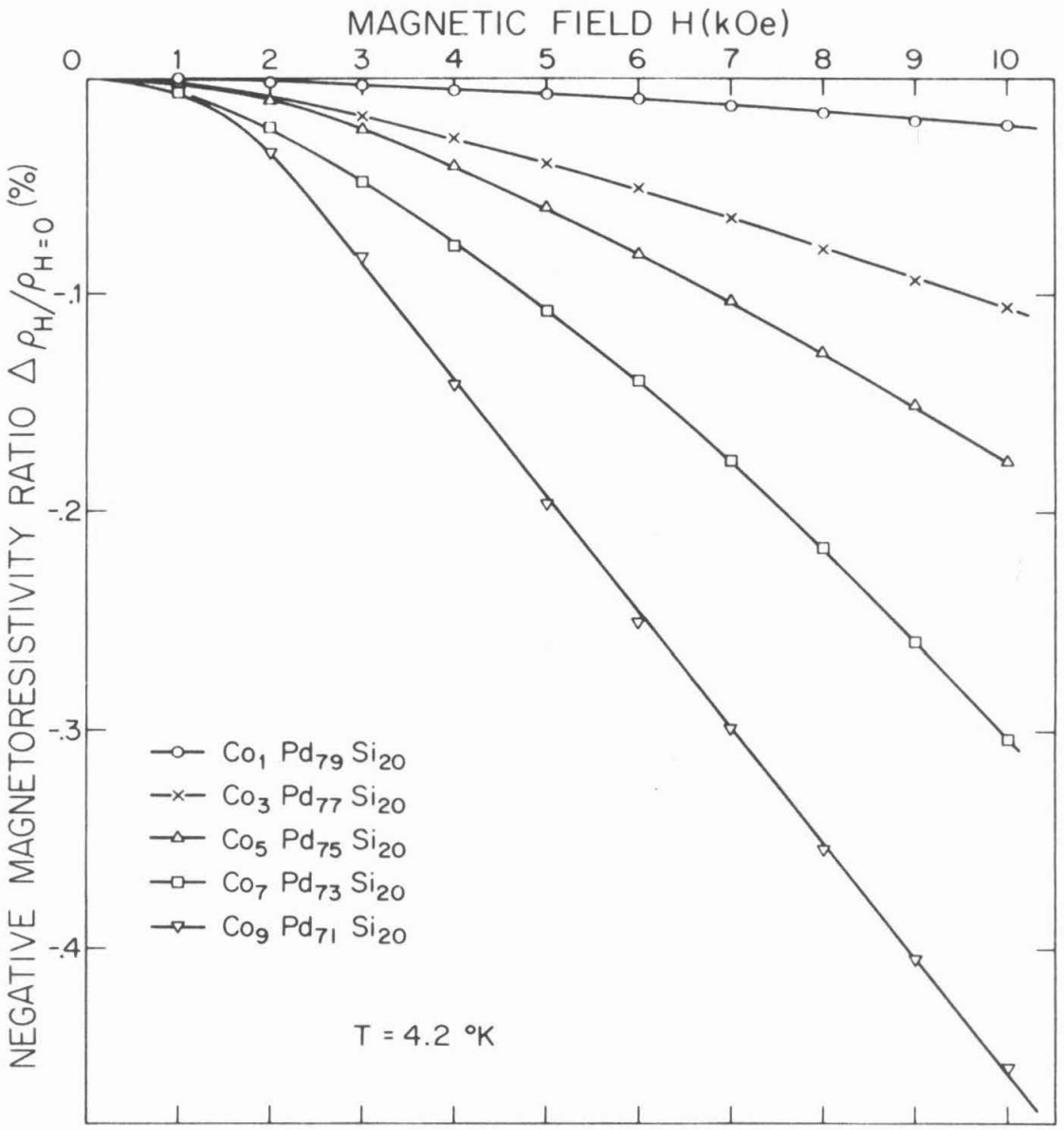

Fig. 12. Negative magnetoresistivity ratio vs magnetic field curves at 4.2°K for the $Co_xPd_{80-x}Si_{20}$ alloys

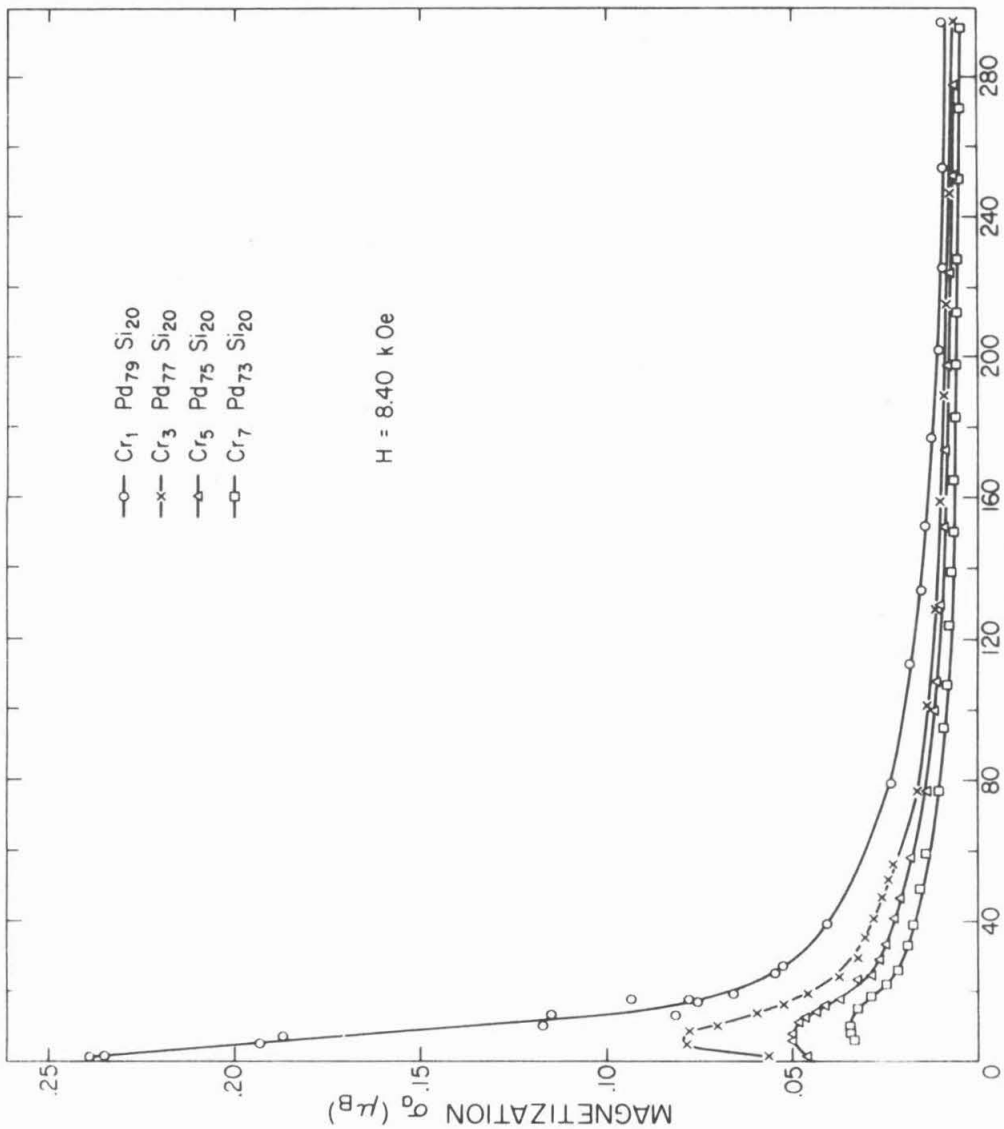

Fig. 13. Magnetization per Cr atom vs temperature curves at H=8.40kOe for the $Cr_x Pd_{80-x} Si_{20}$ alloys

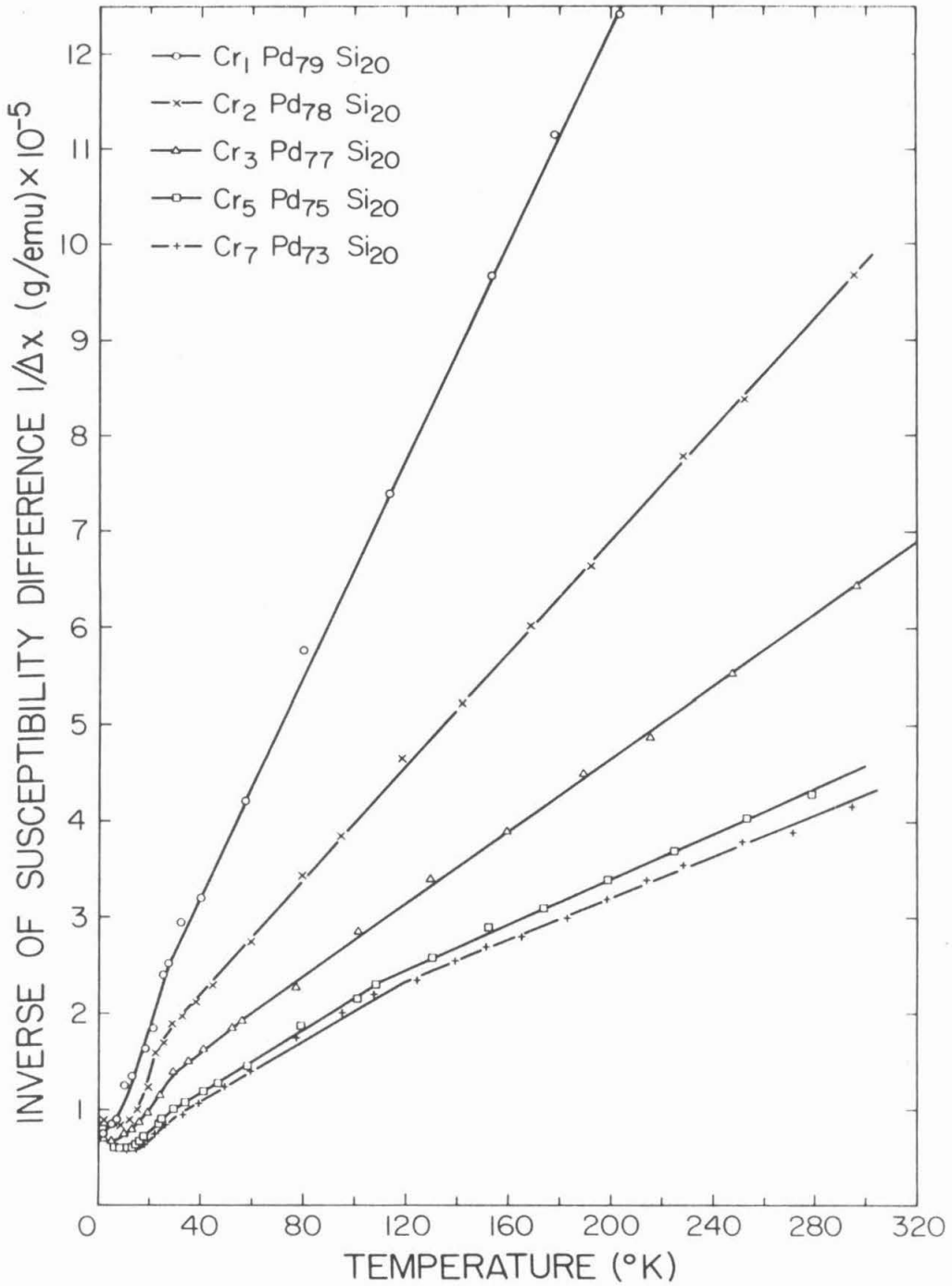

Fig. 14. Inverse of the susceptibility difference per gram of the $Cr_xPd_{80-x}Si_{20}$ alloys vs temperature curves

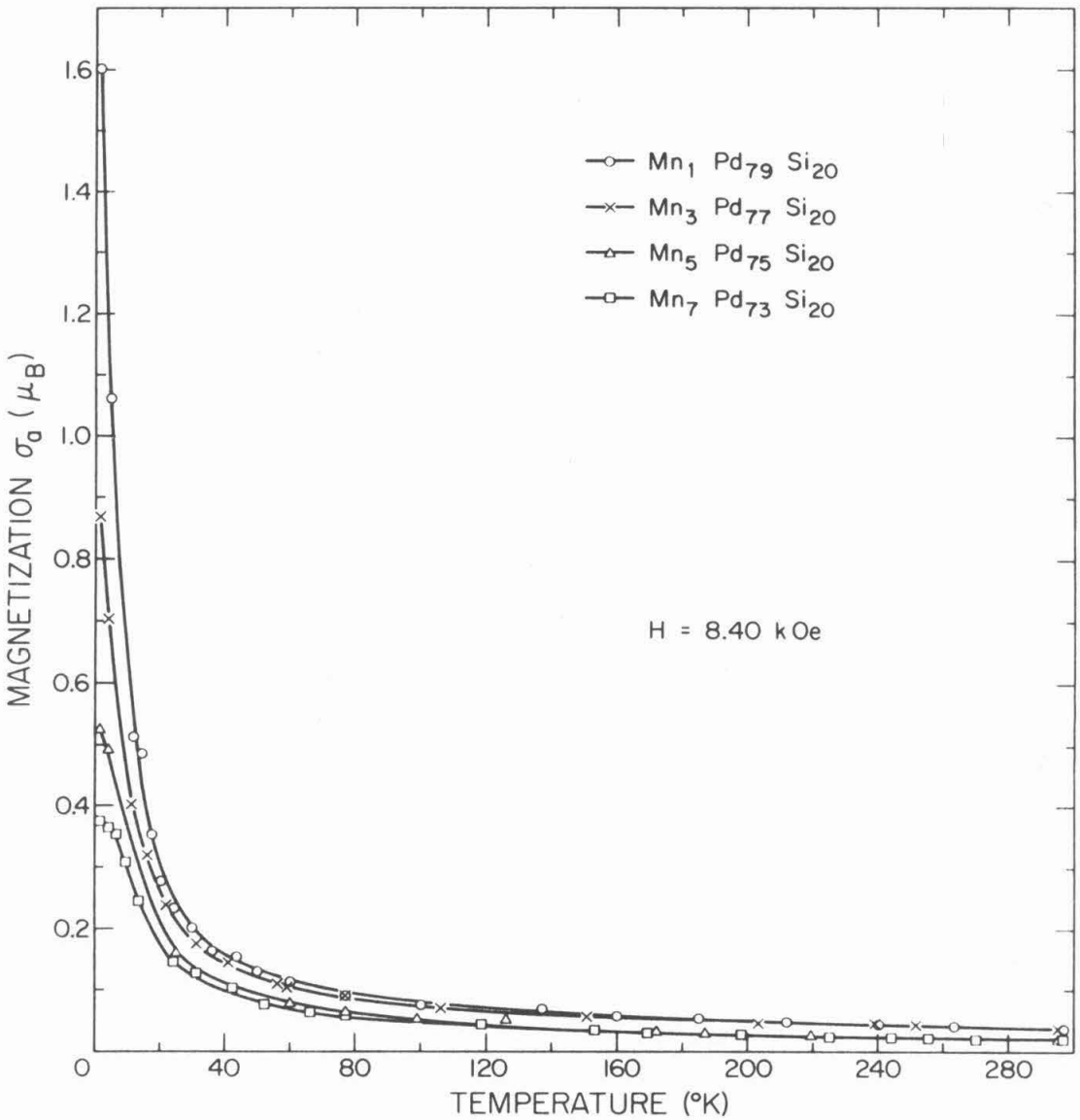

Fig. 15. Magnetization per Mn atom vs temperature curves at H=8.40kOe for the $Mn_xPd_{80-x}Si_{20}$ alloys

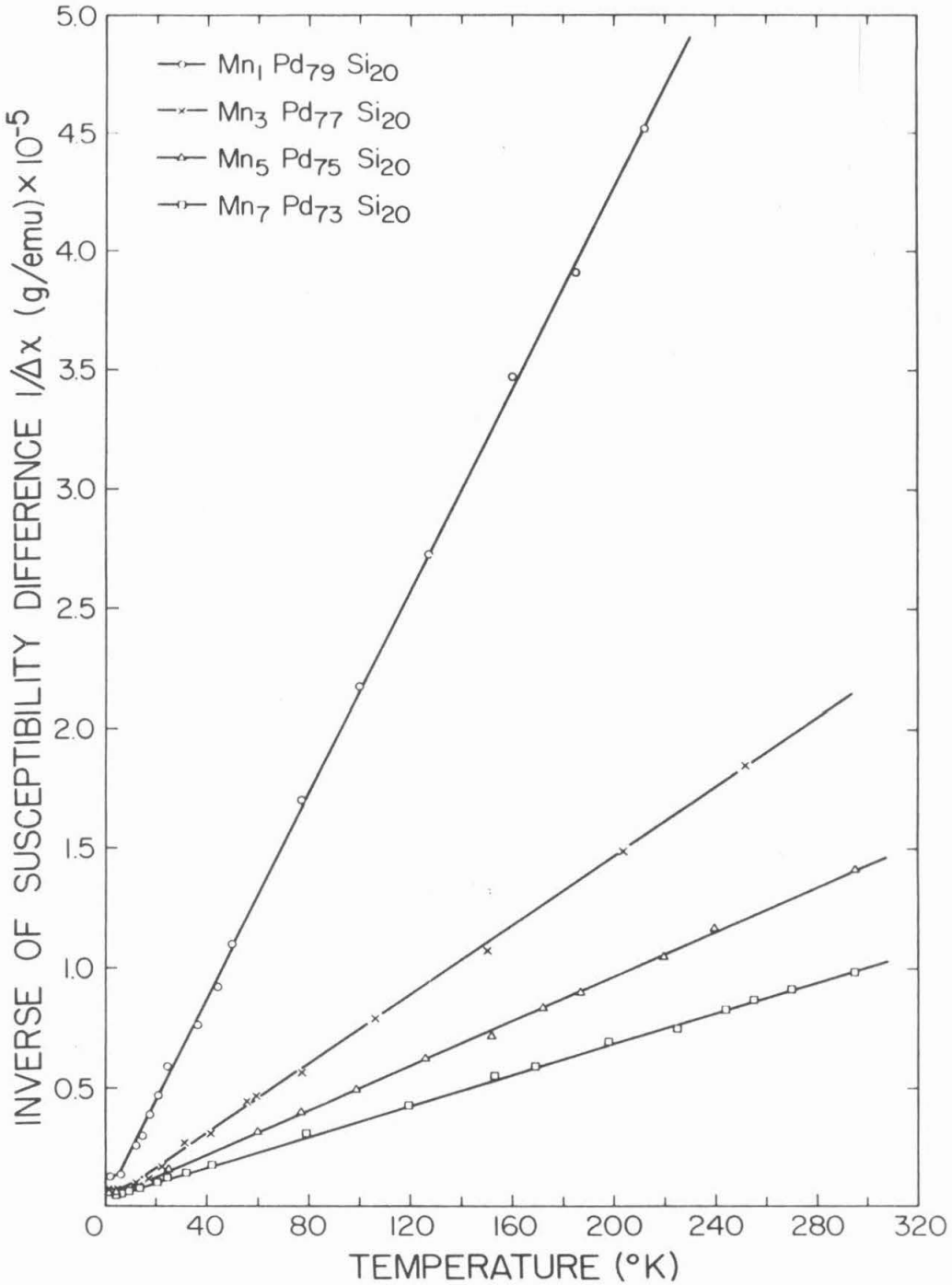

Fig. 16. Inverse of the susceptibility difference per gram of the $Mn_xPd_{80-x}Si_{20}$ alloy vs temperature curves

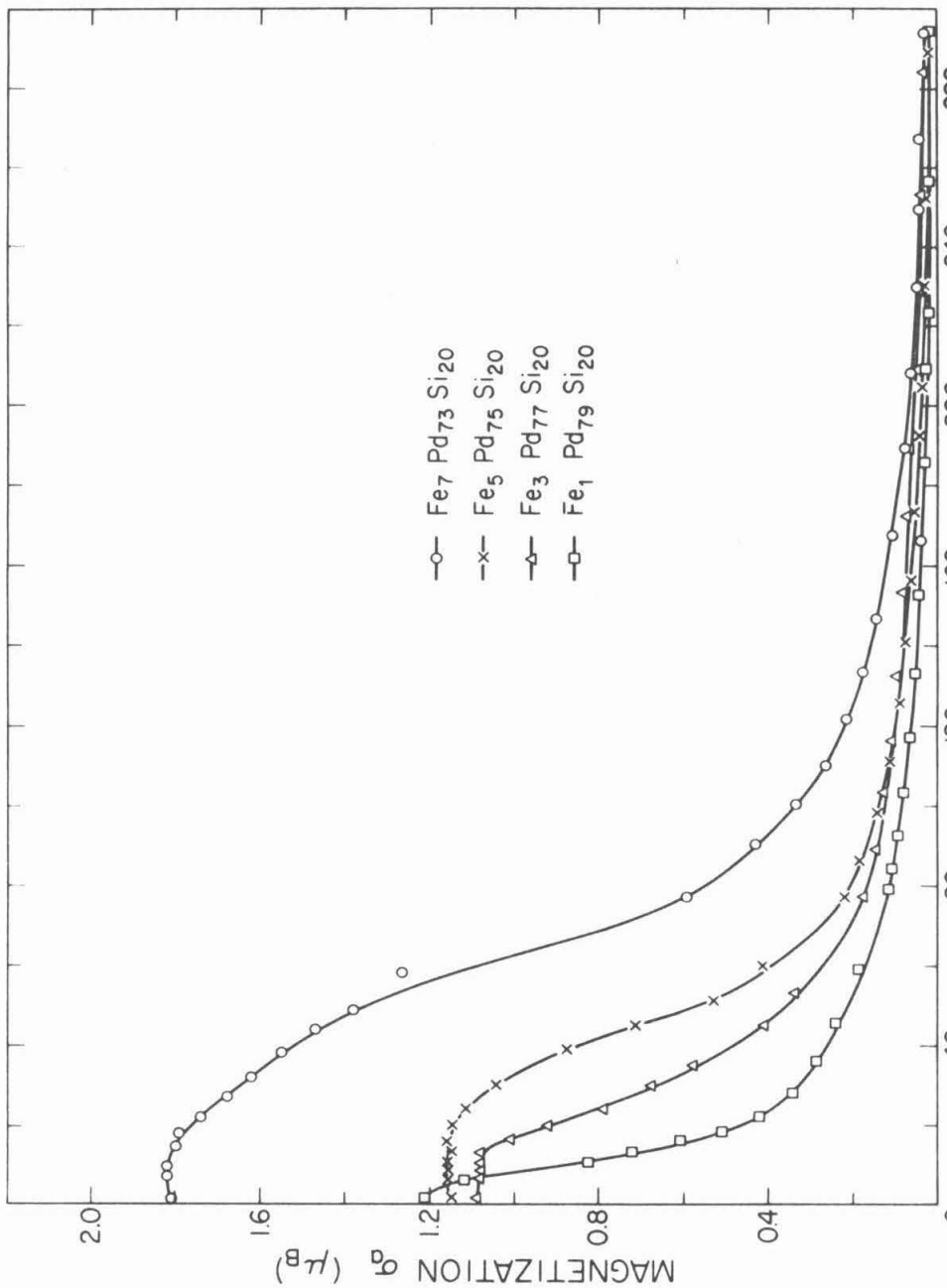

Fig. 17. Magnetization per Fe atom vs temperature curves at H=8.40kOe for the $Fe_xPd_{80-x}Si_{20}$ alloys

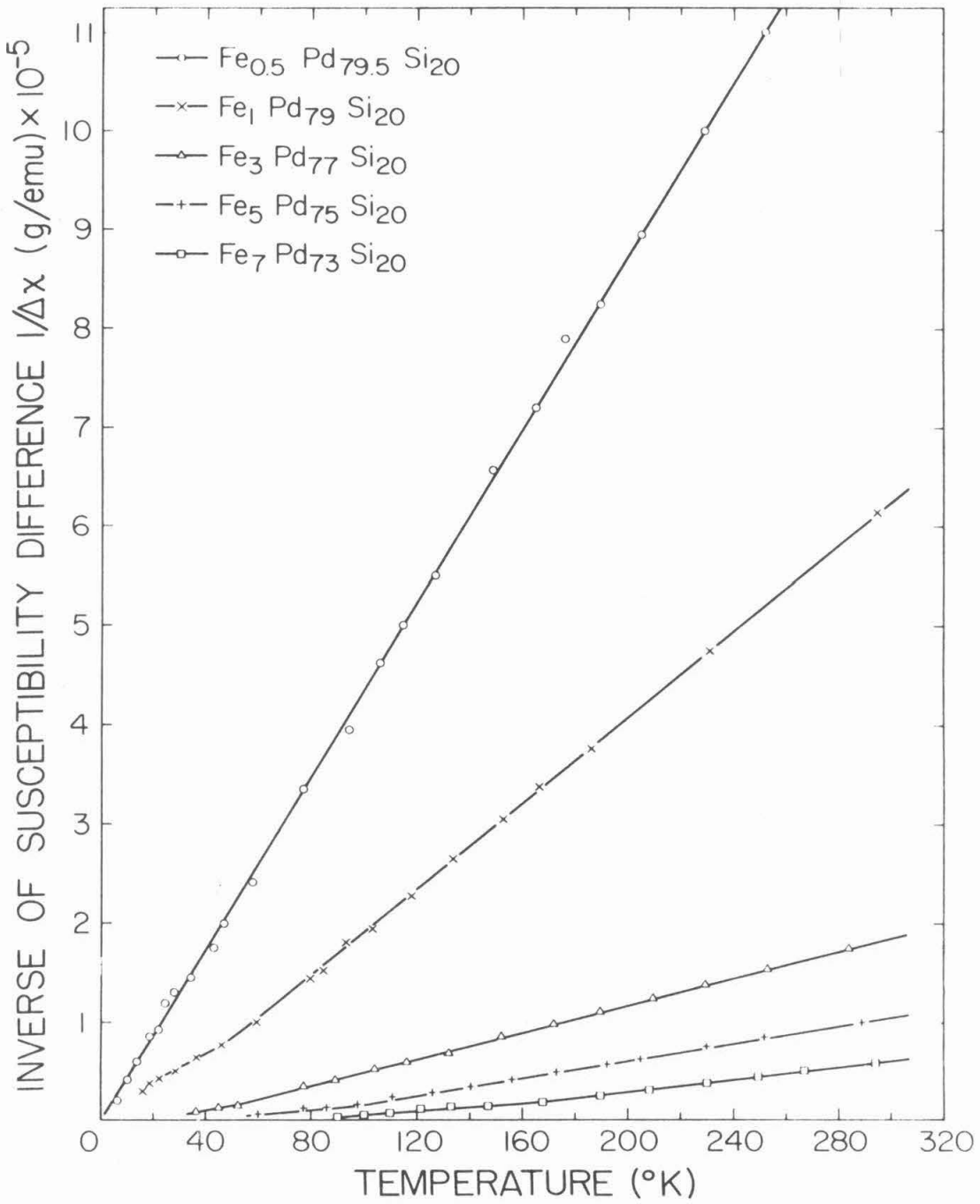

Fig. 18. Inverse of the susceptibility difference per gram of the $Fe_xPd_{80-x}Si_{20}$ alloy vs temperature curves

IV. ANALYSIS

(1) The Kondo Effect

When a transition metal is introduced into an alloy, the following three processes are expected to contribute to the resistivity: (a) direct s-s transitions; (b) s-d transitions in which the final states are non-conducting "d" states; (c) indirect s-d transitions via the "d" states. The first process is the same as in normal metals and the second process is important for the resistivity of pure transition metals. These two processes, therefore, are not of interest here. It is the third process that leads to the resistivity minimum phenomenon.

Kondo[15] interpreted the resistivity minimum phenomena by supposing that the interaction between spins $\vec{s}$ of the conduction electrons and spins $\vec{S}$ of the localized electrons has the form

$$H' = -2 J_{sd} \vec{s} \cdot \vec{S} \qquad (1)$$

where J_{sd} is the s-d exchange integral. He further considered the following four processes for the indirect s-d transitions depending on the intermediate "d" states:

(i) the electron with spin up, $k^{\uparrow}$, is first scattered to the unoccupied d state ($q'^{\uparrow}$) and then to another conduction electron state $k'^{\uparrow}$;

(ii) the occupied electron $q^{\uparrow}$ is first scattered to $k'^{\uparrow}$ and the electron $k^{\uparrow}$ fills up the state $q^{\uparrow}$;

(iii) the intermediate state is changed to $q'^{\downarrow}$ in process (i);

(iv) the intermediate state is changed to $q^{\downarrow}$ in process (ii).

By calculating the transition probability for the above four processes to the second Born approximation, Kondo obtained the spin resistivity

$$\rho_{spin} = x\rho_M\{1 + (3\ p\ J_{sd}/E_F)\ \ell n\ T\} \qquad (2)$$

where x is the concentration of the transition metal, ρ_M the temperature independent part of the spin resistivity, p the number of conduction electron per host atom and E_F the Fermi energy. Thus the total resistivity is

$$\rho = \rho_L + x\rho_A + x\ \rho_M + x\ (3\ p\ J_{sd}\ \rho_M/E_F)\ \ell n\ T \qquad (3)$$

where ρ_L is the lattice resistivity and ρ_A the resistivity due to the potential introduced by the transition metal. If $J_{sd} < 0$, corresponding to an antiferromagnetic coupling between conduction and localized electron spins, Eq. (3) gives a minimum. Assuming $\rho_L = a\ T^5$, the temperature at which the minimum occurs is given by

$$T_m = (3pJ_{sd}\rho_M/5E_Fa)^{1/5}\ x^{1/5} \qquad (4)$$

The above theory has been applied with success to the case of crystalline alloys.

Kondo's perturbational treatment, however, has a drawback; i.e. the resistivity diverges as T goes to zero. The first attempt to solve this problem was done by Nagaoka[16]. He has shown that, if $J_{sd} < 0$, the perturbational treatment breaks down below a critical temperature T_K (called Kondo temperature) and that near the Fermi surface there appears a quasi-bound state between the conduction electron spins and the localized spins. This quasi-bound state is a result of a collective effect,

in the sense that the moment of the conduction electrons in the vicinity of the transition metal atom compensates the moment of the localized spins, rather than that of a singlet spin state in which a single electron is bound to the transition metal atom. As a consequence, the resistivity begins to saturate for $T \ll T_K$. The Kondo temperature has been defined by

$$T_K \approx T_F \exp\left(- 1/N(0)|J_{sd}|\right) \tag{5}$$

where T_F is the Fermi temperature and $N(0)$ the density of states of one spin per atom. Physically T_K is a measure of the quasi-bound state energy ($\sim kT_K$). As pointed out by Schrieffer[27], T_K could range from millidegrees to beyond the melting point of metals since $\exp(-1/N(0)|J_{sd}|)$ varies rapidly with $N(0)|J_{sd}|$.

Several experimental evidences of the quasi-bound state have been reported[17-21]. However, the resistivity data at higher temperatures ($T > T_K$) can be explained by the Kondo theory but not by the Nagaoka theory. Some attempts[22, 23] have been made to formulate a theory valid at all temperature and at present it appears that the Nagaoka theory is satisfactory for $T \ll T_K$ and the Kondo theory is applicable for $T_K < T < T_m$. The theoretical result given by Nagaoka for the resistivity is, for $T \ll T_K$

$$\Delta\rho = \Delta\rho_o \{1 - (T/T_R)^2\} \tag{6}$$

where $\Delta\rho_o = mx/e^2\pi\hbar N(0)$, m and e being the mass and the charge of an electron and $\hbar$ the Planck's constant. Nagaoka also has shown that $T_R \sim T_K$. Eq. (6) implies that $\Delta\rho$ approaches the residual resistivity $\Delta\rho_o$

as T goes to zero.

(2) Negative Magnetoresistivity

In metals the presence of a magnetic field increases the resistivity. This positive magnetoresistivity generally obeys the Kohler rule quite accurately[28]. The situation is quite different when a non-magnetic metal contains small concentrations of a transition metal. The effect of the magnetic field is to decrease the resistivity. It has been found[4, 10, 11] that this negative magnetoresistivity is usually proportional to the square of the magnetization and arises from the s-d exchange interaction. Physically the negative magnetoresistivity is due to the freezing-out of the internal degrees of freedom of the localized spin. Since this dynamical characteristic of the spin system is attributed mainly to Kondo's logarithmic divergence of resistivity, one can expect a decrease of resistivity by applying a magnetic field.

The theoretical basis of the negative magnetoresistivity is rather simple. Suppose the interaction between spins $\vec{s}$ of the conduction electrons and spins $\vec{S}$ of the localized electrons can be expressed by

$$H' = \sum_i \sum_n V - 2 \sum_i \sum_n J_{sd} \vec{s}_i \cdot \vec{S}_n \qquad (7)$$

where V is the potential due to the dilute concentration of a transition metal and J_{sd} the s-d exchange integral. The transition probability per unit time from the initial state i to the final state f is given by

$$W_{i \to f} = \frac{2\pi}{\hbar} \left| \langle f | H' | i \rangle \right|^2 D(E_f)$$

where $D(E_f)$ is the density of the final state. Substituting Eq. (7) into the above formula, we obtain

$$W_{i \to f} = W_o \pm c|J_{sd}|\ \sigma_a$$

where W_o is the sum of the transition probability due to the potential V only and that due to J_{sd} only, c is a constant and σ_a is the magnetization of the transition metal. The sign in front of the second term depends on the spin of the conduction electron. Thus the transition probability for the s-electrons with spin-up and -down may be written as

$$W_\uparrow = W_o + c|J_{sd}|\ \sigma_a \quad \text{(for spin-up)}$$

$$W_\downarrow = W_o - c|J_{sd}|\ \sigma_a \quad \text{(for spin-down)}.$$

If the number of conduction electrons with spin-up and -down is identical, the net conductivity is proportional to $(1/W_\uparrow + 1/W_\downarrow)$. Thus the resistivity is given by

$$\rho \propto \frac{W_o}{2} - \frac{c^2}{2W_o} J_{sd}^2\ \sigma_a^2 \quad .$$

Since $\sigma_a \propto H$ for a paramagnet, the resistivity difference $\Delta\rho_H$ between the resistivity in the presence of a magnetic field and that in zero field is given by

$$\Delta\rho_H \propto - J_{sd}^2\ \sigma_a^2 \quad .$$

The proportionality constant has been recently calculated by Béal-Monod and Weiner[29]. Their results give

$$\Delta\rho_H = - \frac{3\pi m}{2E_F e^2 \hbar} \times V_o\ J_{sd}^2\ \sigma_a^2 \left\{1 + \left(\frac{\mu_B}{\mu_{eff}}\right)^2\right\} \qquad (8)$$

where e and m are the charge and mass of the electron, E_F the Fermi energy, x the atomic concentration of the transition metal, V_o is the atomic volume, σ_a the magnetization of the transition metal in μ_B per atom and μ_{eff} the effective magnetic moment. Eq. (8) is valid for $T > T_K$, but can be extended[29] to the case where $T \sim T_K$ if σ_a is the measured magnetization.

(3) Magnetic Properties

Magnetic moment measurements provide some basic informations about the magnetic state of the alloy containing a transition metal and the electronic structure of the magnetic atom. The temperature dependence of the magnetic susceptibility obtained from the observed magnetic isothermals (magnetization vs magnetic field with temperature as a parameter) gives a direct evidence of whether or not an alloy exhibits localized moments. When localized moments exist in an alloy, the measured susceptibility obeys the Curie-Weiss law. For the present alloys, the observed susceptibility can be expressed by a general formula

$$\chi_{M\text{-}Pd\text{-}Si} = N \mu_{eff}^2 / 3k(T+\theta_p) + \chi_{Pd\text{-}Si}$$

where N is the number of the transition metal atom, μ_{eff} the effective magnetic moment, k the Boltzmann constant, θp the paramagnetic Curie temperature, and $\chi_{Pd\text{-}Si}$ the susceptibility of the host $Pd_{80}Si_{20}$ alloy. It is assumed that only the electron spins contribute to the magnetic moment, so that $\mu_{eff} = g \mu_B \sqrt{S(S+1)}$ and g = 2.0. We are interested in the susceptibility contribution $\Delta\chi$ from the transition metal in the

alloy. Thus we use

$$\Delta\chi = \chi_{M\text{-}Pd\text{-}Si} - \chi_{Pd\text{-}Si} = N\,\mu_{eff}^2/3k(T+\theta_p). \tag{9}$$

The sign of θ_p depends on the type of long range interaction between transition metal atoms. Blandin and Friedel[30] considered the d-d spin interaction of the form $-(J_{dd})_{ij}\vec{S}_i\vec{S}_j$ and obtained the susceptibility to the order of J_{dd}^2. Their results give

$$\theta_p = -2S(S+1)J_{dd}x/3k \tag{10}$$

where S and x are the spin and the concentration of the transition metal and $J_{dd} = \sum_j (J_{dd})_{ij}$ is the exchange integral for the d-d spin interaction.

The existing theories[16,23,31] predict that as T goes to zero the magnetic moment should vanish due to the formation of the quasi-bound state while the susceptibility becomes finite. This gives another way of writing $\Delta\chi$ where μ_{eff} is temperature dependent. Then we have

$$\Delta\chi = N\mu_{eff}^2(T)/3kT. \tag{11}$$

Recently Anderson[32] has suggested that the susceptibility varies like $(T/T_K)^{-\frac{1}{2}}$ when the quasi-bound state is formed. Thus we have

$$\mu_{eff}^2\,(T) = \mu_{eff}^2 f(T) \tag{12}$$

where

$$f\,(T) = 1 \qquad T \gg T_K$$
$$f\,(T) \propto (T/T_K)^{\frac{1}{2}} \qquad T \ll T_K\ .$$

The present data which indicate the existence of localized moments, were analyzed by using Eqs. (9) ~ (12) for the temperature range where these expressions hold. For the temperature range where the magnetically ordered state exists, we analyzed the magnetization-temperature curves to obtain magnetic transition temperatures.

(4) Virtual Bound State Model

The concept of virtual bound states is known in the case of free electrons scattered by atoms in a gas[33]. This concept was applied by Friedel[12, 13] to atoms in alloys.

Consider a spherically symmetric, attractive potential which can accommodate a bound state with quantum number ℓ. Suppose that the potential is reduced slightly so that it can no longer accommodate the bound state and that this reduced potential corresponds to the actual potential around an atom in an alloy. Then the bound state increases in energy and merges into the conduction band. This state is no longer a true bound state, but corresponds to a wave packet, localized around the atom, having a broad energy band with its central level above the bottom of the conduction band. Thus these "virtual" bound states will resonate with the conduction states. More specifically the scattering amplitude of the ℓ-th spherical component for these states is extremely large and the excess charge density summed over the entire virtual states is approximately equal to that of the initial ℓ-th bound state (Friedel's sum rule).

When a metal contains a small amount of a transition metal, it is expected that the d-states of the transition metal shift from above to

below the Fermi level. For some transition metals, the d-states coincide with the Fermi level or levels near it, which accompanies the appearance of the virtual bound d-states. To satisfy the Hund's rule, the exchange interactions within the d-shell must be such that the shell is split into two halves of opposite spin directions. This splitting can only occur if the energy gained by the splitting is larger than the width W of the virtual states; i.e.

$$W < p\Delta E \tag{13}$$

where p is the number of electrons or holes in the d-shell, and ΔE is the energy gained by flipping one d-electron from an antiparallel to a parallel position. The value of ΔE is known to be $0.6 \sim 0.7$ eV and W is proportional to the Fermi energy[12].

When the d-states split into two halves, the Friedel sum rule can be written as

$$\frac{1}{\pi} \sum_{\ell} (2\ell + 1)\, \eta_{\ell}\, (E_F) = Z \tag{14}$$

where Z is the number of d electrons in one of the split d-states below the Fermi level and $\eta_{\ell}(E_F)$ is the phase shift for the ℓ-th spherical component. Using η_{ℓ} Blandin and Friedel[30] have obtained the residual resistivity (in atomic units)

$$\Delta\rho_o = \frac{2\pi x}{p\, k_F} \sum_{\ell} \ell \left\{\sin^2(\eta^{\uparrow}_{\ell-1} - \eta^{\uparrow}_{\ell}) + \sin^2(\eta^{\downarrow}_{\ell-1} - \eta^{\downarrow}_{\ell})\right\} \tag{15}$$

where p is the number of electrons per atom, x the atomic concentration of the transition metal, k_F the Fermi wave number and the arrows show the direction of the spins in the d-states.

V. DISCUSSION OF RESULTS

(1) Electrical Resistivity

The linear temperature dependence of the resistivity for the amorphous $Pd_{80}Si_{20}$ alloy is consistent with the result calculated from the quasi-gas model[34, 35]. The quadratic temperature dependence of the resistivity for $T \leq 40^{o}K$ is not due to the electron-electron U-process[36] since reciprocal lattice vector cannot be defined for an amorphous alloy. It has been shown[37] recently that the spin density fluctuation leads to a low temperature resistivity term which varies as AT^2 where A is proportional to the square of the spin susceptibility. This may be the case with the present result since the observed susceptibility for the $Pd_{80}Si_{20}$ alloy is Pauli-like.

The resistivity data shown in Part III-(1) are interpreted and described in the following for each transition metal case.

(i) Chromium-palladium-silicon alloys

Typical resistivity vs temperature curves for $Cr_xPd_{80-x}Si_{20}$ alloys ($0<x \leq 7$ at.%) are shown in Fig. 1. It is noticed that the Kondo type resistivity anomaly becomes very pronounced when the Cr concentration is large. This wide change of the resistivity anomaly with the transition metal concentration is unusual and has never been observed in the case of crystalline alloys. Thus the most striking result here is that the resistivity minimum is observed at very high (as high as $580^{o}K$) temperatures and in concentrated alloys (up to 7 at.% Cr). The position of the minimum T_m is plotted as a function of Cr concentration

in Fig. 19. It is evident that T_m is not proportional to $x^{1/5}$ as in Eq. (4). This is due to the fact that the resistivity minimum occurs at temperatures where $\rho_L \propto T$. Thus we can write a phenomenological formula for the resistivity of the $Cr_xPd_{80-x}Si_{20}$ alloys as

$$\rho = \alpha + \beta T + \gamma \ln T \qquad (x \geq 0.5). \tag{16}$$

Eq. (16) gives a resistivity minimum at

$$T_m = - \frac{\gamma}{\beta} . \tag{17}$$

It is found that β is approximately constant at $7.5 \cdot 10^{-3}$ $\mu\Omega$-cm. Typical values of γ are obtained from Fig. 2 and are listed in Table 1. Then using Eq. (17) with $\gamma = - 0.629\ x$ $\mu\Omega$-cm, we find

$$T_m = 84\ x \quad (^oK); \ (x \text{ in at.\%}).$$

Thus T_m is proportional to the Cr concentration which is consistent with Fig. 19. For $x < 0.5$ (corresponding to $T_m < 50^oK$), we should use $\rho_L \propto T^2$. In this case T_m is expected to vary as $\sqrt{x}$. This is, however, difficult to confirm due to the scattering of T_m data.

The temperature variation of $\Delta\rho$, shown in Fig. 2, depends on Cr concentration but generally follows the prototype where $\Delta\rho$ obeys the logarithmic law of Kondo at higher temperatures and becomes temperature independent at the lower temperature limit. This agrees qualitatively with the theories by Nagaoka[16], Suhl-Wong[22] and Hamann[23]. However as in the case of crystalline alloys[21], these theories do not give a good $-\ln T$ fit to the present results for a wide temperature range.

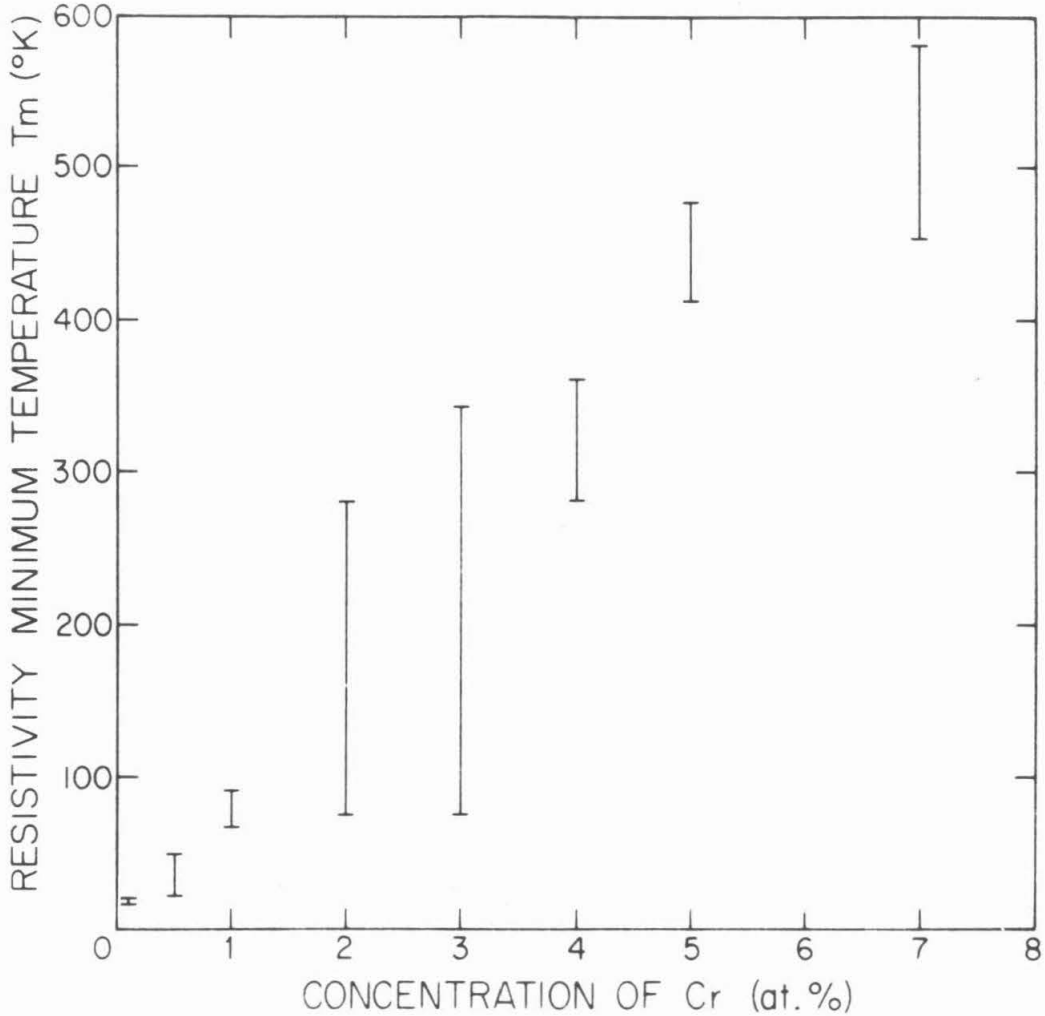

Fig. 19. Resistivity minimum temperature vs Cr concentration for the $Cr_xPd_{80-x}Si_{20}$ alloys

TABLE 1

Results of the resistivity measurement for the $Cr_xPd_{80-x}Si_{20}$ alloys

Alloy Composition	γ ($\mu\Omega$-cm)	Δ ($\mu\Omega$-cm)	$\Delta\rho_o$ ($\mu\Omega$-cm)	T_R (^oK)
$Cr_1Pd_{79}Si_{20}$	-0.767	2.5	22.6	21
$Cr_3Pd_{77}Si_{20}$	-2.17	7.2	52.5	76
$Cr_5Pd_{75}Si_{20}$	-3.25	10.0	54.7	123
$Cr_7Pd_{73}Si_{20}$	-4.36	10.1	46.8	115

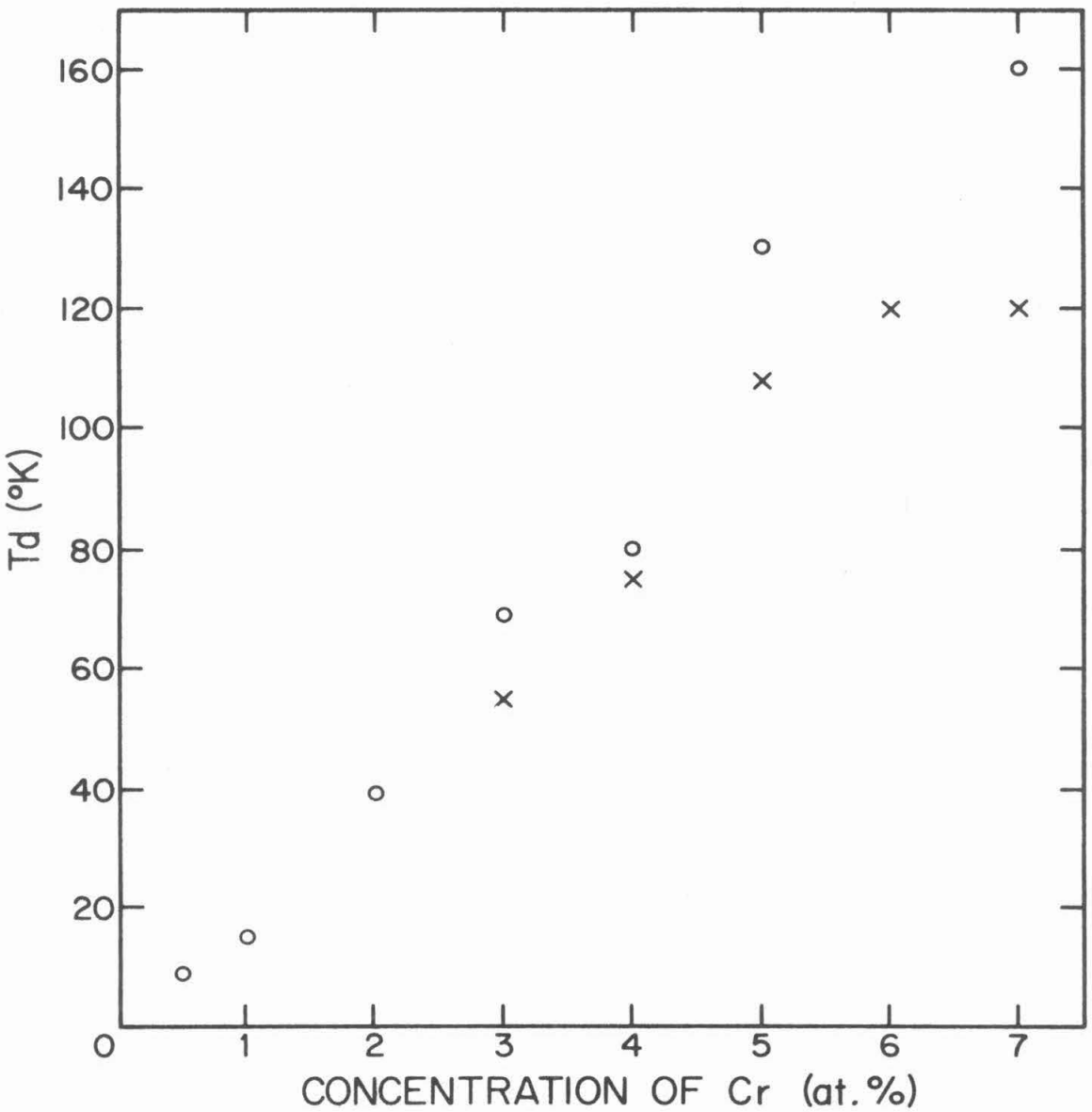

Fig. 20. Temperature at which $\Delta\rho$ deviates from the $-\ell n\ T$ law vs Cr concentration for the $Cr_xPd_{80-x}Si_{20}$ alloys (o). The points (x) are taken from Table 8.

The temperature range where $\Delta\rho$ follows the logarithmic law of Kondo depends upon Cr concentration. Immediately below the resistivity minimum temperature T_m, $\Delta\rho$ obeys the $-\ell n\ T$ law and starts to deviate from it below some temperature T_d. The critical temperature T_d depends upon Cr concentration and is shown in Fig. 20. In the same figure are plotted the temperatures at which the magnetic susceptibility deviates from the Curie-Weiss law. Below T_d, $\Delta\rho$ increases slower than $-\ell n\ T$, approaching a constant value at the lower temperature limit. The constant temperature dependence of $\Delta\rho$ at low temperature ($T < 2^{o}K$) can be explained by the formation of the quasi-bound state. (Further evidence of the quasi-bound state formed in $Cr_xPd_{80-x}Si_{20}$ alloys is given in Sec. (3)-(i)). Using Eq. (6), $\Delta\rho_o$ and T_R are obtained from the resistivity data at the lower temperatures and are listed in Table 1. It is noticed that the concentration dependence of T_R is similar to that of T_d (Fig. 20). Since $T_K \sim T_R$[16], the present result indicates that the Kondo temperature increases with Cr concentration. This is different from the case of crystalline alloys where T_K is independent of concentration. However, unlike the crystalline alloy case, the Cr concentration could be increased to rather large values and this might result in some change of the density of states N(0). This, as mentioned in Part IV-(1), leads to a change of T_K. In fact the observed $\Delta\rho_o$(Table 1) is constant at $\sim 50\ \mu\Omega$-cm for $x \geq 3$ which leads to a linear concentration dependence of N(0). Then from Eq. (5) T_K should increase with the Cr concentration, as is observed. Since there is some ambiguity in

determining N(0), no quantitative argument is given here. The connection between T_R, T_d and T_K is discussed in Sec. (3)-(i).

The depth of the resistivity minimum which is conveniently defined as the difference between the resistivity at $T = T_o \sim 0$ and that at $T = T_m$ is given from Eq. (16) by

$$\Delta = \rho_{T_o} - \rho_{T_m} = \gamma \ln \left(\frac{T_o}{T_m}\right) . \qquad (18)$$

We have $T_m = 84 \times {}^oK$, $T_o \sim 2^oK$ and $\gamma = -0.629 \times \mu\Omega$-cm from the resistivity data for $Cr_xPd_{80-x}Si_{20}$ alloys. Thus we obtain

$$\Delta = 2.35 \left(1 + \frac{\ln x}{3.74}\right) x \ \mu\Omega\text{-cm}.$$

Since $1 > \frac{\ln x}{3.74}$ for $0.5 \leq x \leq 3$, the depth Δ is approximately proportional to Cr concentration, as is observed (Table 1). For $5 \leq x \leq 7$, the depth Δ is constant at ~ 10 $\mu\Omega$-cm. The fact that Δ is not proportional to Cr concentration for $x \geq 5$ suggests that the d-d spin interaction creates some internal field which suppresses the Kondo effect. This is consistent with the experimental results[21] where Δ is decreased by applying a magnetic field.

(ii) Manganese-palladium-silicon alloys

In light of the resistivity minimum problem, a study of alloys containing Mn is of interest, since Mn has a half-filled d-band ($3d^5 4S^2$) and gives the lowest residual resistivity[12] in alloys. In fact in the present study, $Mn_xPd_{80-x}Si_{20}$ alloys played an important role. As

explained in Sec. (4) Mn alloys are used as a basis to determine E_F of the present $M_xPd_{80-x}Si_{20}$ alloys.

The results of the resistivity measurement for $Mn_xPd_{80-x}Si_{20}$ ($0 < x \leq 7$ at.%) alloys are shown in Fig. 3. Three characteristics are noticed in this figure: (a) the resistivity minimum is not as pronounced as in the case of $Cr_xPd_{80-x}Si_{20}$ alloys; (b) the resistivity-temperature coefficient β at higher temperatures changes with Mn concentration; in other words Matthiessen's rule is not satisfied; (c) the resistivity minimum temperature T_m seems to increase with Mn concentration. The first characteristic indicates the fact that both the s-d exchange energy J_{sd} and the Kondo temperature T_K for $Mn_xPd_{80-x}Si_{20}$ alloys are much smaller than those for $Cr_xPd_{80-x}Si_{20}$ alloys. The second feature is found only in the alloys containing Mn. It is found that β is approximately proportional to the inverse of Mn concentration. To account for this, the electron mean free path should be proportional to Mn concentration. The third characteristic is shown in Fig. 21. To interpret these data, we write the empirical formula for the resistivity of $Mn_xPd_{80-x}Si_{20}$ alloys as

$$\rho = \alpha + \delta T^2 + \gamma \ln T \qquad (19)$$

where $\rho_L = \delta T^2$ is used since the resistivity of the host $Pd_{80}Si_{20}$ alloy changes as T^2 for $T < 50^oK$ and the values of T_m for the $Mn_xPd_{80-x}Si_{20}$ alloys are less than 50^oK. It is found that the coefficient δ is inversely proportional to Mn concentration. The origin of this fact may be the same as that of the concentration dependence of β.

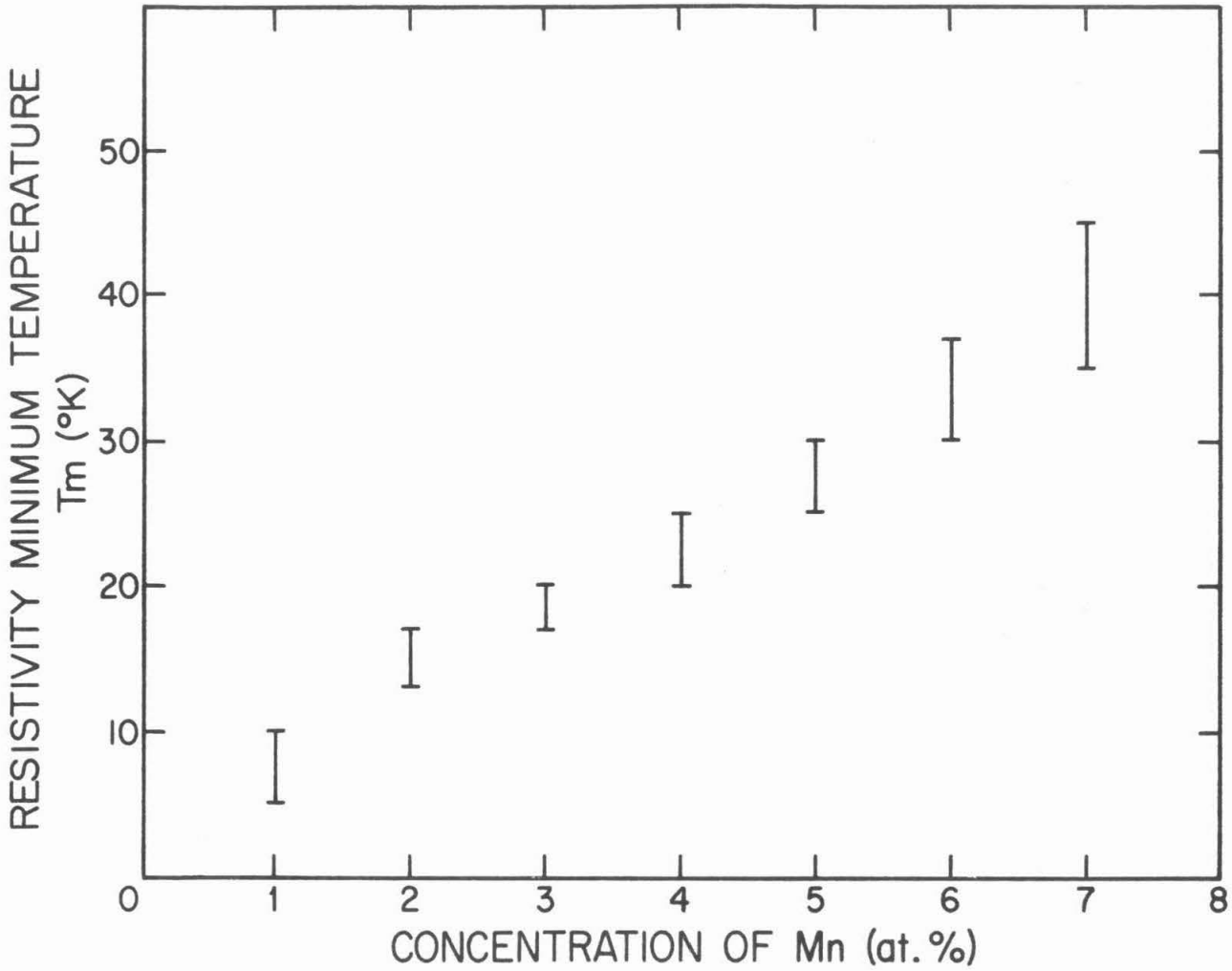

Fig. 21. Resistivity minimum temperature vs Mn concentration for the $Mn_xPd_{80-x}Si_{20}$ alloys

Eq. (19) gives a resistivity minimum temperature at

$$T_m = \sqrt{-\frac{\gamma}{2\delta}} \tag{20}$$

From the resistivity data in Figs. 3 and 4, we have $\gamma = -2.3 \cdot 10^{-2}$ x $\mu\Omega$-cm, x $\delta = 2.9 \cdot 10^{-4}$ $\mu\Omega$-cm. Then we find

$$T_m \sim 6.1 \text{ x } (^oK), \quad (x \leq 7 \text{ at.\%});$$

which is in good agreement with the data in Fig. 21.

It is seen in Fig. 4 that the temperature variation of $\Delta\rho$ is independent of Mn concentration. The $-\ell n\ T$ dependence of $\Delta\rho$ is observed down to $T \sim 4^oK$, below which $\Delta\rho$ becomes temperature independent indicating the formation of quasi-bound states. Since the temperature variation of $\Delta\rho$ undergoes such an abrupt change around 4^oK, Eq. (6) cannot be applied to the present data to determine T_K. The value of T_K is estimated to be $\sim 4^oK$, at which $\Delta\rho$ starts to deviate from the $-\ell n\ T$ law (see Fig. 4). It is found that $\Delta = 7 \cdot 10^{-2}$ $\mu\Omega$-cm/at.% and $\Delta\rho_o \sim$ 3.8 $\mu\Omega$-cm/at.% (from Fig. 4). The value of $\Delta\rho_o$ is compared with the theoretical result in Sec. (5).

(iii) Iron-palladium-silicon alloys

The purpose of this study is to investigate the resistivity minimum problem in both dilute Fe alloys and in concentrated Fe alloys which tend to be ferromagnetic at low temperature. Kondo's theory predicts that the $-\ell n\ T$ dependence of the resistivity should vanish when magnetic ordering occur. In fact several authors[38-41] have reported that the maximum of the resistivity which occurs below T_m can be attributed to

the onset of magnetic ordering.

The resistivity measured for $Fe_xPd_{80-x}Si_{20}$ ($0 < x \leq 7$ at.%) alloys is plotted in Fig. 5 as a function of temperature. It is noticed that the resistivity minimum effect becomes smaller when Fe concentration is high, which is different from the case of alloys containing Cr or Mn. The resistivity minimum temperature T_m also decreases with increasing Fe concentration for $x > 3$ at.%, which is shown in Fig. 22. As shown in Sec. (3)-(iii), $Fe_xPd_{80-x}Si_{20}$ alloys become ferromagnetic at low temperature. A comparison of Fig. 22 with Table 10 shows that $T_m < T_c$ (ferromagnetic Curie temperature) for $x > 3$. This means that Kondo's resistivity minimum phenomena can coexist with ferromagnetism. This fact seems to contradict the Kondo prediction and the theories of Suhl[38] and Abrikosov[39]. However, if we consider the possibility of localized moments in magnetically ordered alloys[42, 43], we can expect Kondo's logarithmic divergence of resistivity in these alloys. No maximum of the resistivity was observed at $T = T_c$ for $Fe_1Pd_{79}Si_{20}$ alloys for which $T_m > T_c$, which is different from the case of crystalline alloys. This may indicate that localized moments are well screened. However, the decrease of T_m with increasing Fe concentration for $x > 3$ suggests that density of localized moments might decrease with increasing Fe concentration. A change of slope in the resistivity-temperature curve was observed at $T \sim T_c$ for $Fe_xPd_{80-x}Si_{20}$ alloys with $x > 3$, whose Curie temperatures were above T_m. Such an anomaly has been known to be essential for ferromagnetic metals, and was considered[8] to be due to

the s-d transition where the final state of the scattered electron is a non-conducting d-state.

The concentration dependence of T_m is difficult to interpret because of the existence of ferromagnetic state in the alloys. However, for dilute Fe alloys ($x \leq 1$) we may write the resistivity in the form of Eq. (19). Using $\gamma = -0.17\ x\ \mu\Omega$-cm and $\delta = 2.8 \cdot 10^{-4}\ \mu\Omega$-cm, we find from Eq. (20)

$$T_m \sim 18 \sqrt{x}\ \ (^oK),\ (x \leq 1\ \text{at.\%}),$$

which is consistent with the data for $x = 1$.

The temperature variation of the resistivity difference $\Delta\rho$, as shown in Fig. 6, depends on Fe concentration. Both γ (the slope of $\Delta\rho$ vs $\ell n\ T$) and Δ (the depth of the resistivity minimum) are not proportional to Fe concentration for large concentration, as seen in Table 2. This again indicates a decrease of the "effective" density of the localized moments as Fe concentration is increased, i.e., more Fe atoms participate in forming the ferromagnetically ordered state. The saturation of $\Delta\rho$ occurs at $T \lesssim 3^oK$, which may give an approximate Kondo temperature for the Fe alloys. The residual resistivity obtained for the $Fe_1Pd_{79}Si_{20}$ alloy is 19 $\mu\Omega$-cm (from Fig. 6). This is compared with the value (21.4 $\mu\Omega$-cm) calculated in Sec. (5).

A resistivity minimum has been recently found[44] in amorphous $Fe_xPd_{80-x}P_{20}$ ($23 \leq x \leq 44$) in the temperature range where the alloys are ferromagnetic. The general characteristics of these alloys are

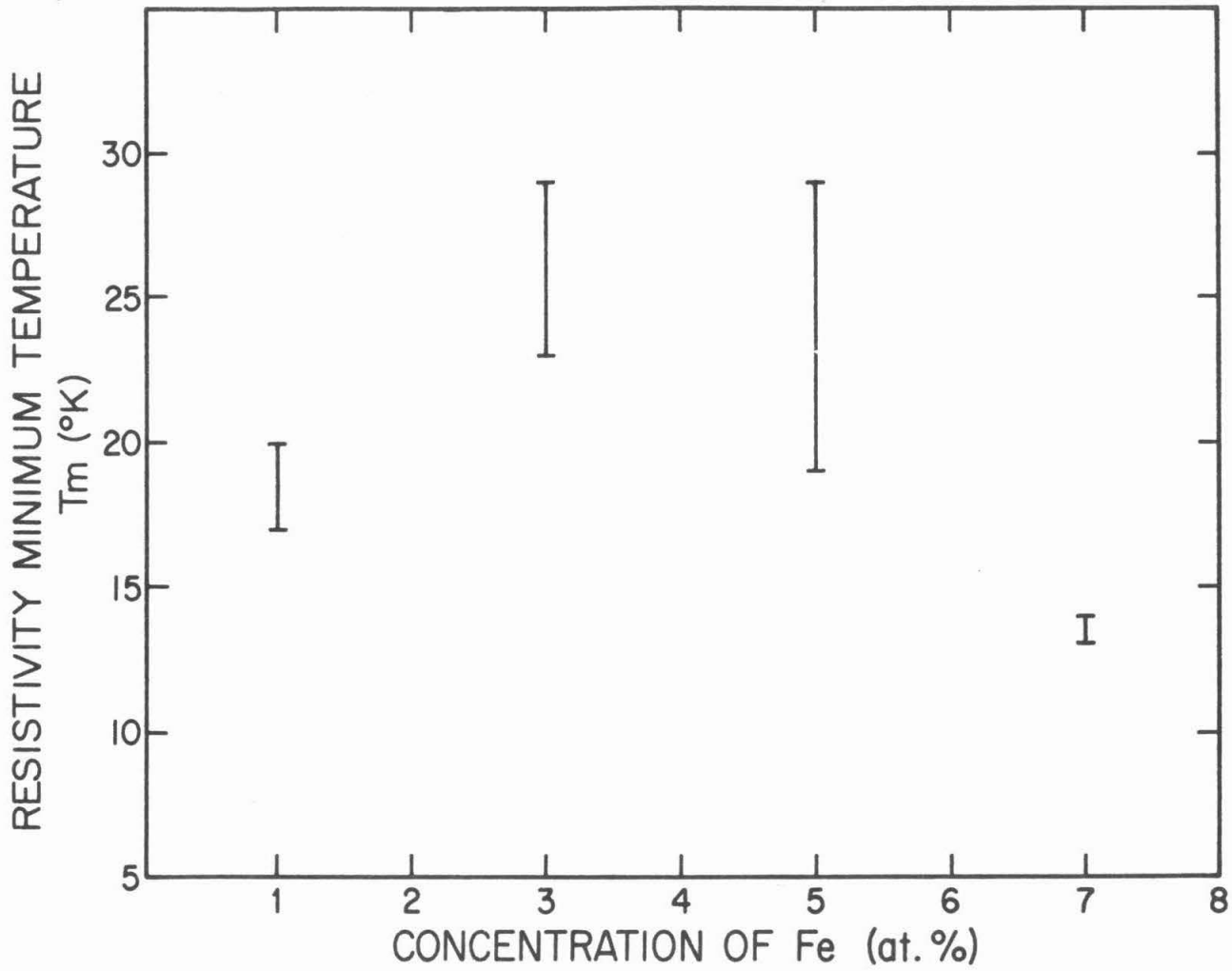

Fig. 22. Resistivity minimum temperature vs Fe concentration for the $Fe_xPd_{80-x}Si_{20}$ alloys

TABLE 2

Values of γ and Δ for the $Fe_xPd_{80-x}Si_{20}$ alloys

Alloy Composition	γ ($\mu\Omega$-cm)	Δ ($\mu\Omega$-cm)
$Fe_1Pd_{79}Si_{20}$	-0.174	0.4
$Fe_3Pd_{77}Si_{20}$	-0.260	0.7
$Fe_5Pd_{75}Si_{20}$	-0.286	0.6
$Fe_7Pd_{73}Si_{20}$	-0.163	0.3

similar to those of $Fe_xPd_{80-x}Si_{20}$ alloys with higher Fe concentration. This provides another evidence for the coexistence of ferromagnetism and Kondo effect.

(iv) Cobalt-palladium-silicon alloys

The study of alloys containing Co is of interest for the following two reasons: (a) the d-band of Co is 70% filled ($3d^7\ 4s^2$) which makes it difficult to form localized states in alloys. In fact not many alloys containing Co show localized moments and (b) Co atoms in $Co_xPd_{80-x}Si_{20}$ alloys[26] form a superparamagnetic clustering and the alloys become ferromagnetic at low temperature.

The results of the resistivity measurements for $Co_xPd_{80-x}Si_{20}$ ($0 < x \leq 11$) alloys are shown in Fig. 7. It is noticed that the resistivity minimum is well defined up to x = 11 at.%. The resistivity minimum temperatures T_m, shown in Fig. 23, are found to be insensitive to Co concentration for $x > 1$. A comparison of this figure with Table 11 indicates that the Kondo effect can coexist with ferromagnetism in $Co_xPd_{80-x}Si_{20}$ alloys, since $T_m < T_c$ for $x > 3$. The gradual change of slope in the resistivity-temperature curve around T_c indicates that the onset of ferromagnetism is not well-defined (see Sec. 3-(iv)).

For alloys with $x \leq 1$ at.%, it is found that $T_m > T_c$. The theory of Kondo, therefore, can be applied to these alloys. The minimum temperature T_m for $x \leq 1$ may be estimated by using Eq. (20) with $\gamma = -4.3 \cdot 10^{-2}\ x$ $\mu\Omega$-cm and $\delta = 2.8 \cdot 10^{-4}$ $\mu\Omega$-cm. Thus we find

$$T_m \sim 8.7 \sqrt{x}\ (^oK)$$

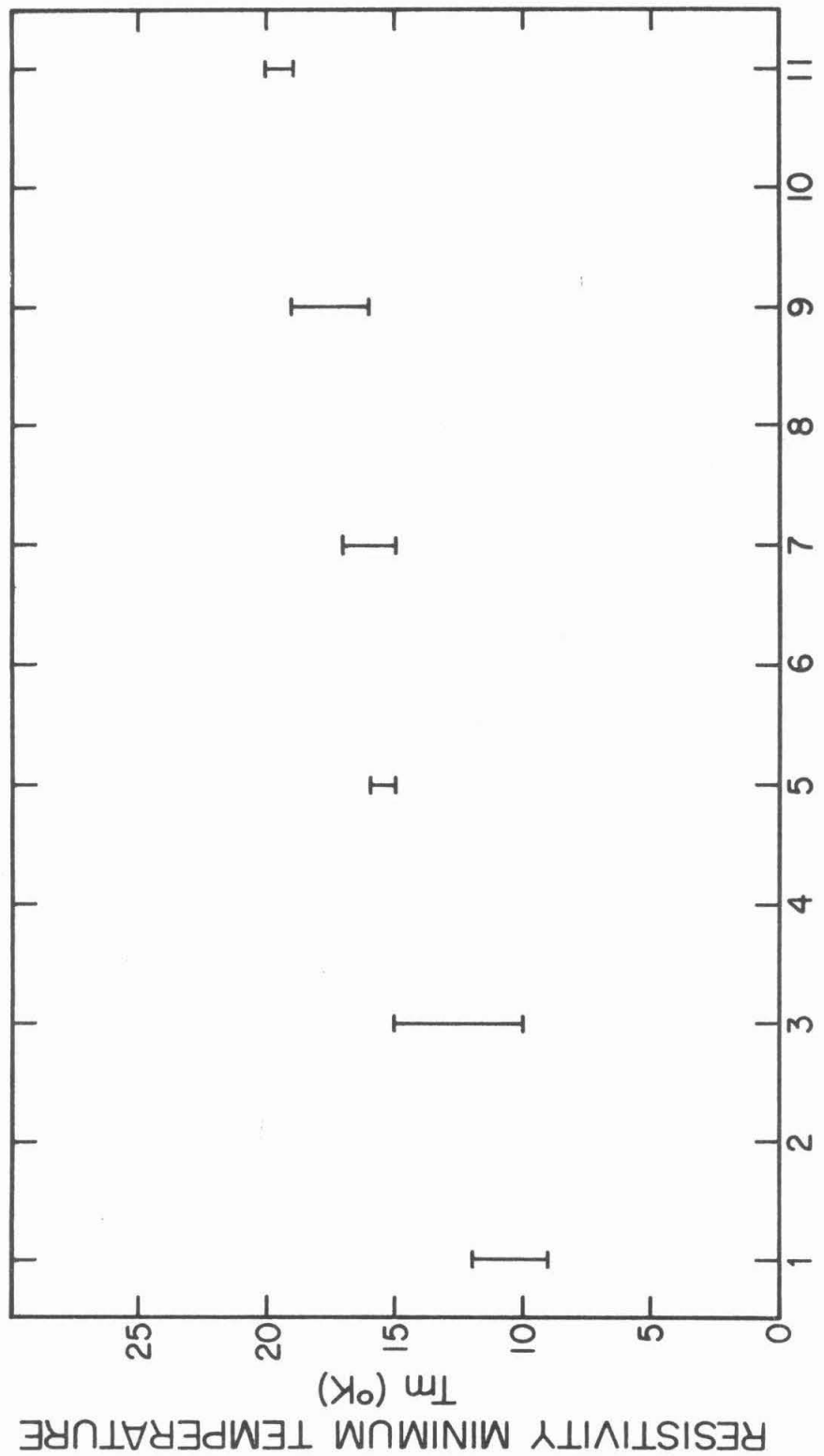

Fig. 23. Resistivity minimum temperature vs Co concentration for the $Co_x Pd_{80-x} Si_{20}$ alloys

TABLE 3

Values of γ and Δ for the $Co_xPd_{80-x}Si_{20}$ alloys

Alloy Composition	γ ($\mu\Omega$-cm)	Δ ($\mu\Omega$-cm)
$Co_1Pd_{79}Si_{20}$	-0.040	0.04
$Co_3Pd_{77}Si_{20}$	-0.143	0.15
$Co_5Pd_{75}Si_{20}$	-0.197	0.23
$Co_7Pd_{73}Si_{20}$	-0.139	0.20
$Co_9Pd_{71}Si_{20}$	-0.142	0.24
$Co_{11}Pd_{69}Si_{20}$	-0.181	0.29

which gives a good estimation for T_m up to x = 3 (Fig. 23).

The temperature variation of $\Delta\rho$, shown in Fig. 8, is independent of Co concentration for $x \leq 5$ at.% and depends on Co concentration for $x > 5$. The slope γ and the depth Δ are listed in Table 3. Both $|\gamma|$ and Δ vary as $4.3 \cdot 10^{-2}$ x $\mu\Omega$-cm for $x \leq 5$ at.% and are constant at $\gamma \sim -0.18$ $\mu\Omega$-cm and $\Delta \sim 0.25$ $\mu\Omega$-cm for $x > 5$ at.%. The fact that γ and Δ are constant for $x > 5$ may indicate that the density of localized Co atoms is independent of Co concentration. The Kondo temperature is estimated to be $\sim 2^{\circ}K$, since the saturation of $\Delta\rho$ takes place below this temperature. The residual resistivity obtained from Fig. 8 is 4.2 $\mu\Omega$-cm/at.%, which is compared with the value (7.4 $\mu\Omega$-cm/at.%) calculated in Sec. (5).

(2) Magnetoresistivity

The results of the magnetoresistivity measurements are analyzed and described in the following for each transition metal case. As mentioned in Part III-(2), the positive magnetoresistivity for the $Pd_{80}Si_{20}$ alloys is negligibly small. Thus the subtraction of the positive part from the net observed magnetoresistivity is not such a problem as it is for crystalline alloys. The absence of a positive magnetoresistivity indicates that the conduction electrons behave like free electrons in amorphous alloys. This makes the analysis much easier.

(i) Chromium-palladium-silicon alloys

As shown in Fig. 9, the negative magnetoresistivity of the $Cr_xPd_{80-x}Si_{20}$ alloys is appreciable at $T = 4.2^{\circ}K$. The absence of

negative magnetoresistivity at 77^{o} and 295^{o}K is probably due to the fact that the magnetization σ_a is very small at these temperatures (see Fig. 13). The net negative magnetoresistivity is found to vary as $-b\sigma_a^n$ with b and n given in Table 4. The deviation of n from 2 [the theoretical result as seen in Eq. (8)] indicates that T = 4.2^{o}K is already in the temperature region where the quasi-bound state is present.

The concentration dependence of the negative magnetoresistivity has been studied. Fig. 24 shows $\Delta\rho_{H=10k0e}/\rho_{H=0}$ vs Cr concentration at T = 4.2^{o}K. Two characteristics are noticed: (a) there is a large scattering of $\Delta\rho_H/\rho_{H=0}$ for the alloys of the same concentration of Cr for $x < 4$ at.%; (b) despite the scattering of the data, it is seen that $|\Delta\rho_H/\rho_{H=0}|$ increases with Cr concentration for $x \leq 2$ at.% and decreases with increasing Cr concentration for $x > 2$ at.%. The first characteristic is consistent with the resistivity results, since an alloy specimen with a small T_m always has a large negative magnetoresistivity and vice versa. Since the negative magnetoresistivity is proportional to $-\sigma_a^2$, some change of σ_a from specimen to specimen would result in an appreciable scattering of $\Delta\rho_H/\rho_{H=0}$. The variation $\Delta\sigma_a$ of σ_a in different specimens with the same nominal composition can be estimated by using a Brillouin function of the form $B_s(g\mu_B SH/k(T+\theta_B))$ with S = 3/2 and with the appropriate error in θ_B (see Table 8). An example of comparison of this estimation with the experimental results is given in Table 5, which shows a reasonable agreement. Since $T_m \propto T_K \propto \theta_B$ as discussed in Sec. (3)-(i), it is reasonable to expect that the specimen with a low T_m exhibits a large σ_a resulting

in a large negative magnetoresistivity. This clearly explains the correlation between the resistivity and magnetoresistivity data.

The scattering of $\Delta\rho_H/\rho_{H=0}$ for a fixed concentration of Cr indicates that the spatial distribution of σ_a is somewhat different in each specimen. One may suspect that the actual concentration of Cr in the specimen may be different in spite of the same nominal composition. To check this possibility, two specimens were prepared from the same foil ($Cr_3Pd_{77}Si_{20}$ alloy). One specimen showed a large negative magnetoresistivity ($\Delta\rho_{H=10k0e}/\rho_{H=0} = -0.02\%$) with a low T_m($\sim 75^oK$) and the other a small negative magnetoresistivity ($\Delta\rho_{H=10k0e}/\rho_{H=0} = -0.0073\%$) with a high T_m ($\sim 280^oK$). Since the quenched foil is considered to be uniform, the possibility of a large concentration change from specimen to specimen is unlikely.

The second characteristic of Fig. 24 has been noticed in crystalline alloys. Gerritsen[4] has reported that the negative magnetoresistivity of Au-Mn is strongly influenced by annealing, indicating the influence of microstructure. The concentration dependence of $\Delta\rho_H/\rho_{H=0}$ for the $Cr_xPd_{80-x}Si_{20}$ alloys ($x > 2$ at.%) can be interpreted along a similar line. As mentioned in Sec. (3)-(i), the magnetization σ_a is inversely proportional to the concentration of Cr for $x > 2$ at.% due to the Cr-Cr interaction (see Fig. 13). Thus Eq. (8) gives $\Delta\rho_H/\rho_{H=0} \propto x^{-1}$ for $x > 2$ at.%, which is actually observed in the present experiment (see Fig. 24).

There is a minimum in the $\Delta\rho_H/\rho_{H=0}$ vs concentration curve. In the case of $Cr_xPd_{80-x}Si_{20}$ alloys, this minimum occurs around $x = 2$ at.% when

TABLE 4

Typical values of b and n at $T = 4.2^{o}K$ in the expression $\Delta\rho_H/\rho_{H=0} = -b\sigma_a^n$ for the $Cr_xPd_{80-x}Si_{20}$ alloys

Alloy Composition	$b(\%/\mu_B^n)$	n
$Cr_1Pd_{79}Si_{20}$	0.15	1.89
$Cr_2Pd_{78}Si_{20}$	1.30	1.95
$Cr_3Pd_{77}Si_{20}$	2.25	1.67
$Cr_4Pd_{76}Si_{20}$	1.82	1.80
$Cr_5Pd_{75}Si_{20}$	2.50	1.88
$Cr_6Pd_{74}Si_{20}$	3.61	1.65
$Cr_7Pd_{73}Si_{20}$	4.66	1.53

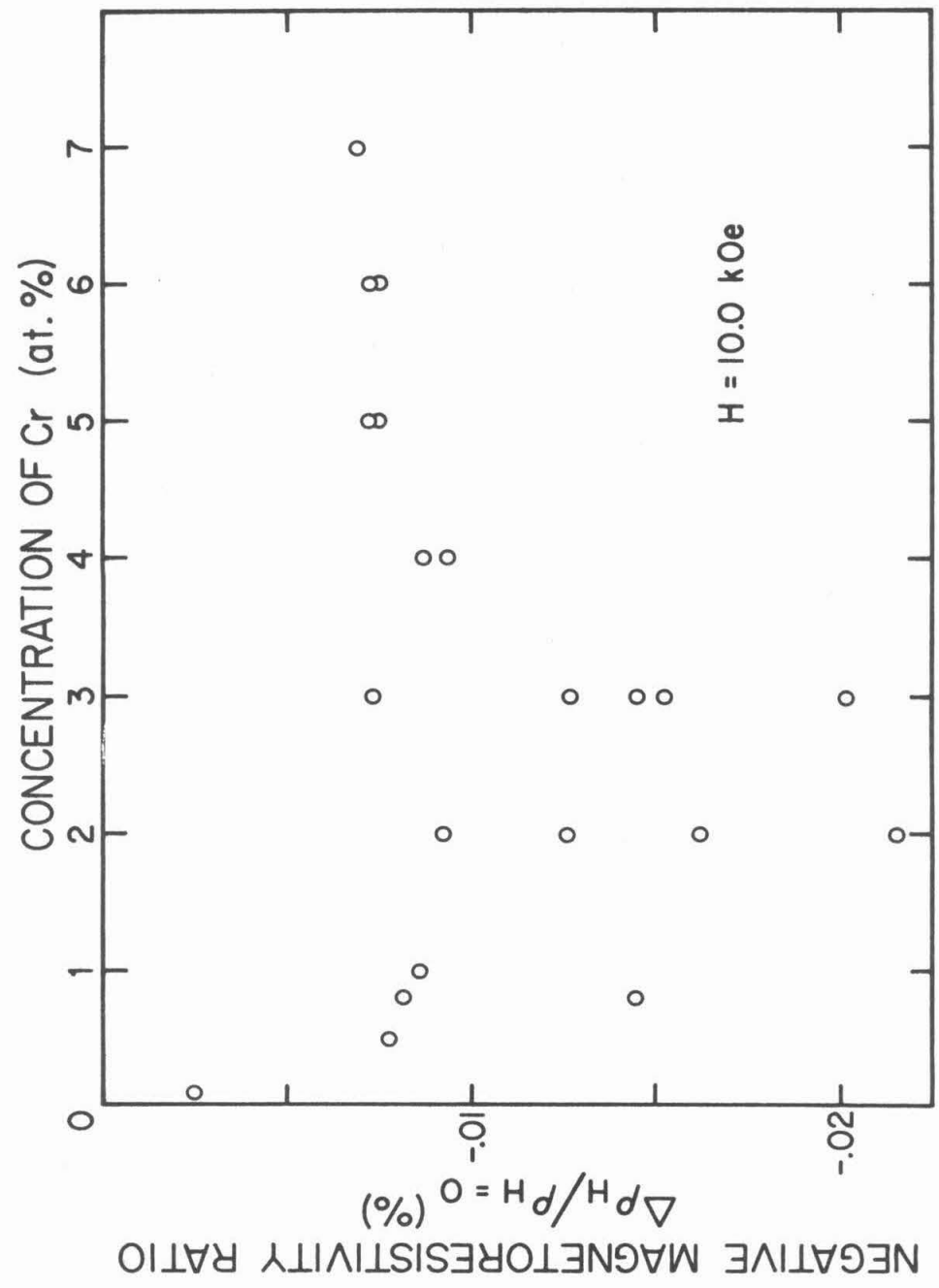

Fig. 24. Negative magnetoresistivity ratio vs Cr concentration at H=10.0 kOe and T = 4.2°K for the $Cr_x Pd_{80-x} Si_{20}$ alloys

TABLE 5

Comparison between the estimated and the experimental error in $\Delta\rho_{H=10k0e}/\rho_{H=0}$ at T = 4.2°K

Alloy Composition	$(\Delta\sigma_a/\sigma_a)_{H=10k0e}$	$\Delta(\Delta\rho_{H=10k0e}/\rho_{H=0})_{est.}$	$\Delta(\Delta\rho_{H=10k0e}/\rho_{H=0})_{exp.}$
$Cr_2Pd_{78}Si_{20}$	±17%	±34%	±40%
$Cr_6Pd_{74}Si_{20}$	±5 %	±10%	±3%

$T = 4.2^{o}K$ and $H = 10.0$ kOe. Similar minima have been observed in crystalline alloys[4], but the transition metal concentration at which the minimum occurs are very small, i.e., of the order of less than 0.1 at.%. This fact indicates that the d-d spin interaction between transition metal atoms is weaker in amorphous alloys than in crystalline alloys.

(ii) Manganese-palladium-silicon alloys

The curves for $\Delta\rho_H/\rho_{H=0}$ at $T = 4.2^{o}K$ against H, shown in Fig. 10, resemble those found in the case of the Cr alloys. The absence of a negative magnetoresistivity at $T = 77^{o}$ and $295^{o}K$ is due to a small value of σ_a at these temperatures (see Fig. 15) as in the case of Cr alloys. The results for $Mn_xPd_{80-x}Si_{20}$ alloys can be fitted to the general function $\Delta\rho_H/\rho_{H=0} = -b\,\sigma_a^n$ with b and n given in Table 6. That $n \sim 2$ implies the quasi-bound states are not fully formed at $4.2^{o}K$, i.e., $T_K \lesssim 4.2^{o}K$. This assures that the application of Eq. (8) to the present results is valid.

The general profile of the plot $\Delta\rho_{H=10kOe}/\rho_{H=0}$ at $4.2^{o}K$ against Mn concentration, as shown in Fig. 25, is similar to that for the Cr alloys. It is noticed that (a) the absolute value of the negative magnetoresistivity increases with Mn concentration for $x < 6$ at.% and decreases for $x > 6$ at.%, and that (b) the scattering of the data is very small compared with that of the Cr alloys. The first characteristic is reasonably consistent with the dependence of σ_a on Mn concentration (see Fig. 15). From Fig. 15 we have $\sigma_a \propto x^{-\frac{1}{2}}$ for $x \leq 5$ at.%. Thus we obtain $\Delta\rho_H/\rho_{H=0} \propto -x$

TABLE 6

Values of b and n at T = 4.2°K in the expression $\Delta\rho_H/\rho_{H=0} = -b\,\sigma_a^n$ for the $Mn_xPd_{80-x}Si_{20}$ alloys

Alloy composition	$b(\%/\mu_B^n)$	n
$Mn_1Pd_{79}Si_{20}$	.0035	2.00
$Mn_3Pd_{77}Si_{20}$	.0235	2.04
$Mn_5Pd_{75}Si_{20}$	.0760	1.91
$Mn_7Pd_{73}Si_{20}$	.110	1.68

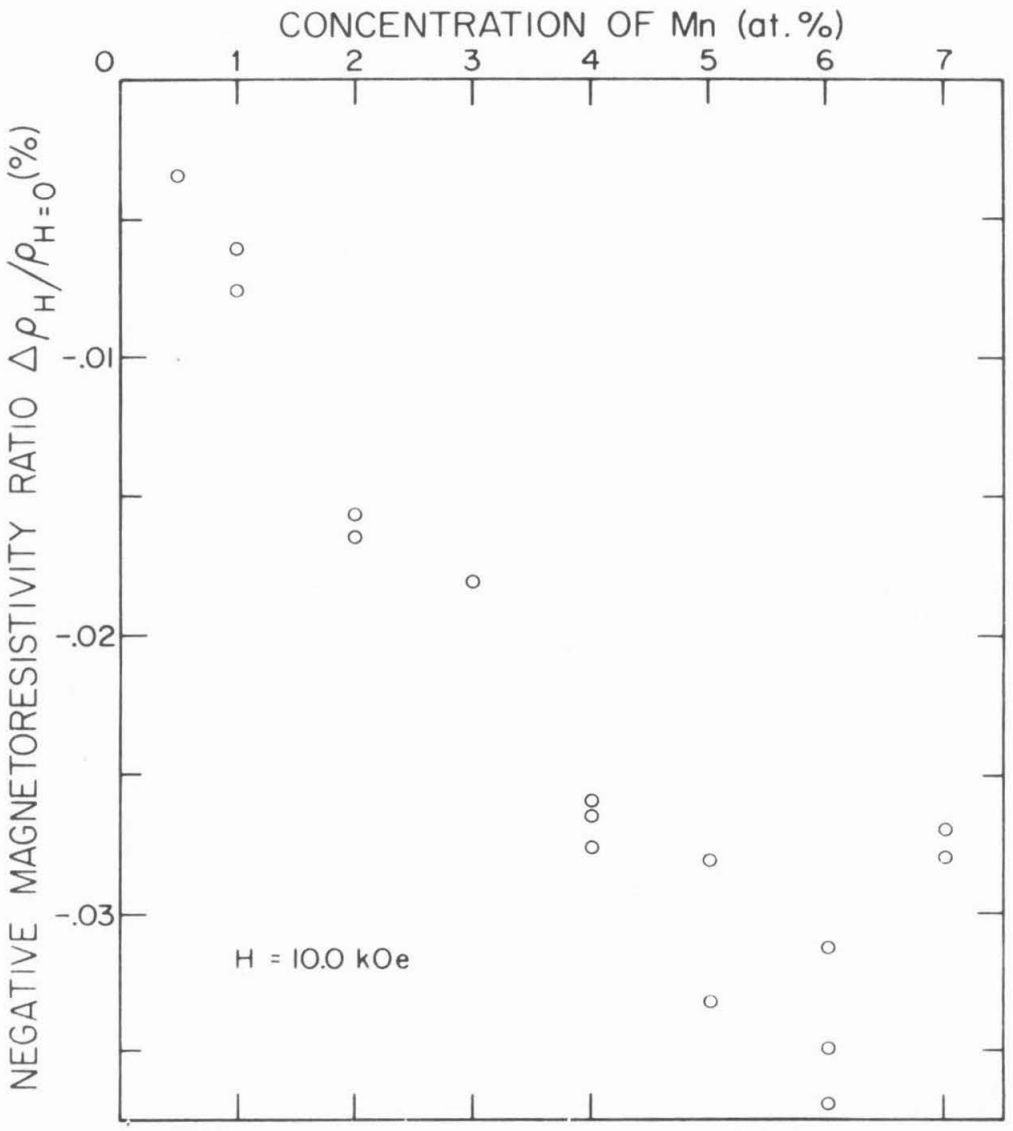

Fig. 25. Negative magnetoresistivity ratio vs Mn concentration at H=10.0 kOe and T=4.2°K for the $Mn_xPd_{80-x}Si_{20}$ alloys

since b varies like x^2 for ≤ 5 (from Table 6). For $x > 6$, $\Delta\rho_H/\rho_{H=0}$ probably varies like $-x^{-1}$ since $\sigma_a \propto x^{-1}$ for $x > 6$. The striking result is that the concentration where $|\Delta\rho_H/\rho_{H=0}|$ is maximum is very large, i.e., ~ 6 at.%, indicating the d-d spin interaction betweeen Mn atoms is very weak in the $Mn_xPd_{80-x}Si_{20}$ alloys.

The small scattering of the data for the alloys of the same Mn concentration indicates that the magnetization does not vary very much from specimen to specimen. This is confirmed by fitting the magnetization data to a Brillouin function of the form $B_s(g\mu_B SH/k(T+\theta_B))$ with $S = 5/2$ and with the results of θ_B listed in Table 9. For example, the estimated error on $\Delta\rho_H/\rho_{H=0}$ due to the error on σ_a is found to be $\pm$ 6% for the $Mn_3Pd_{77}Si_{20}$ alloys. The small error on σ_a is also reflected in the small scattering of T_m (see Fig. 21). Thus, the $Mn_xPd_{80-x}Si_{20}$ alloys seem to be less sensitive to structural inhomogeneities than the Cr alloys.

(iii) Iron-palladium-silicon alloys

The results of $\Delta\rho_H/\rho_{H=0}$ vs H for the $Fe_xPd_{80-x}Si_{20}$ alloys, shown in Fig. 11, are somewhat different from those found for the alloys containing Cr or Mn. It is noticed that the negative magnetoresistivity is much larger than that for the Cr or Mn alloys and that $\Delta\rho_H/\rho_{H=0}$ varies as $\sim H$ for alloys with higher Fe concentrations. It is found, however, that $\Delta\rho_H/\rho_{H=0}$ varies as $-b\,\sigma_a^n$ with b and n given in Table 7. The large value of n for $x \geq 1$ at $T = 4.2^oK$ seems to be due to the appearance of ferromagnetism, since 4.2^oK is well below the Curie temperature for these alloys (see Table 10).

TABLE 7

Values of b and n in the expression $\Delta\rho_H/\rho_{H=0} = -b\ \sigma_a^n$ for the $Fe_xPd_{80-x}Si_{20}$ alloys

Alloy Composition	$b\ (\%/\mu_B^n)$ ($T=4.2^oK$)	n ($T=4.2^oK$)	$b\ (\%/\mu_B^2)$ ($T=77^oK$)	n ($T=77^oK$)
$Fe_{0.5}Pd_{79.5}Si_{20}$	.0127	1.85		
$Fe_1Pd_{79}Si_{20}$	.0270	2.61		
$Fe_3Pd_{77}Si_{30}$	.127	2.32		
$Fe_5Pd_{75}Si_{20}$	.195	2.48	.0540	1.80
$Fe_7Pd_{73}Si_{20}$	.145	2.74	.0520	1.83

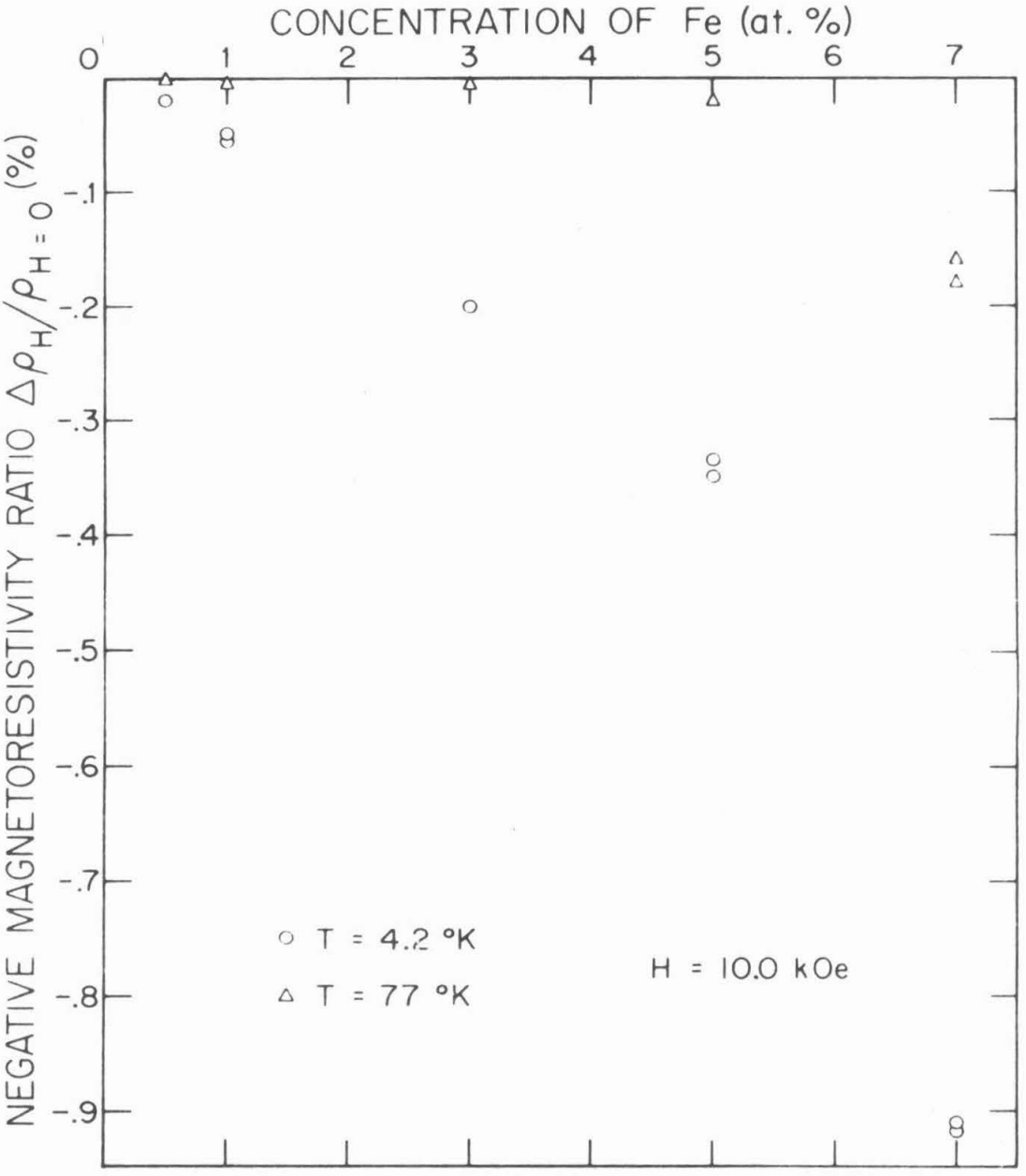

Fig. 26. Negative magnetoresistivity ratio vs Fe concentration at H= 10.0 kOe and T=4.2°K(o) and 77°K (Δ) for the $Fe_xPd_{80-x}Si_{20}$ alloys

The concentration dependence of $\Delta\rho_H/\rho_{H=0}$ is also different from that for the Cr or Mn alloys. A plot of $\Delta\rho_{H=10k0e}/\rho_{H=0}$ vs Fe concentration for T = 4.2° and 77°K is shown in Fig. 26. It is noticed that the absolute value of the negative magnetoresistivity increases somewhat linearly with Fe concentration x for $x < 5$ and more rapidly with x for $x > 5$. This is consistent with the concentration dependence of the magnetization (from Fig. 17), i.e., σ_a is approximately constant for $0.5 \leq x < 5$ and σ_a is proportional to x for $x \geq 5$.

Although the quantitative analysis of the negative magnetoresistivity for the $Fe_xPd_{80-x}Si_{20}$ alloys is complicated by the existence of ferromagnetism, the observed data obey Eq. (8) qualitatively if σ_a is the measured magnetization.

(iv) Cobalt-palladium-silicon alloys

The results obtained for the $Co_xPd_{80-x}Si_{20}$ alloys, shown in Fig. 12 for T = 4.2°K, resemble those for the $Fe_xPd_{80-x}Si_{20}$ alloys in many ways. The negative magnetoresistivity at 4.2°K for the $Co_1Pd_{79}Si_{20}$ alloy varies like $\Delta\rho_H/\rho_{H=0} = -b\,\sigma_a^n$ with b = 0.099 $(\%/\mu_B^n)$ and n = 1.90. An appreciable negative magnetoresistivity was observed at higher concentrations of Co at T = 77° and 295°K. This is probably due to the large magnetization arising from the d-d spin clustering[26] among Co atoms in the alloys.

The concentration dependence of $\Delta\rho_{H=10k0e}/\rho_{H=0}$ at T = 4.2°, 77° and 295°K is shown in Fig. 27. These data are consistent with the concentration dependence of the magnetization obtained in Ref. 26. It

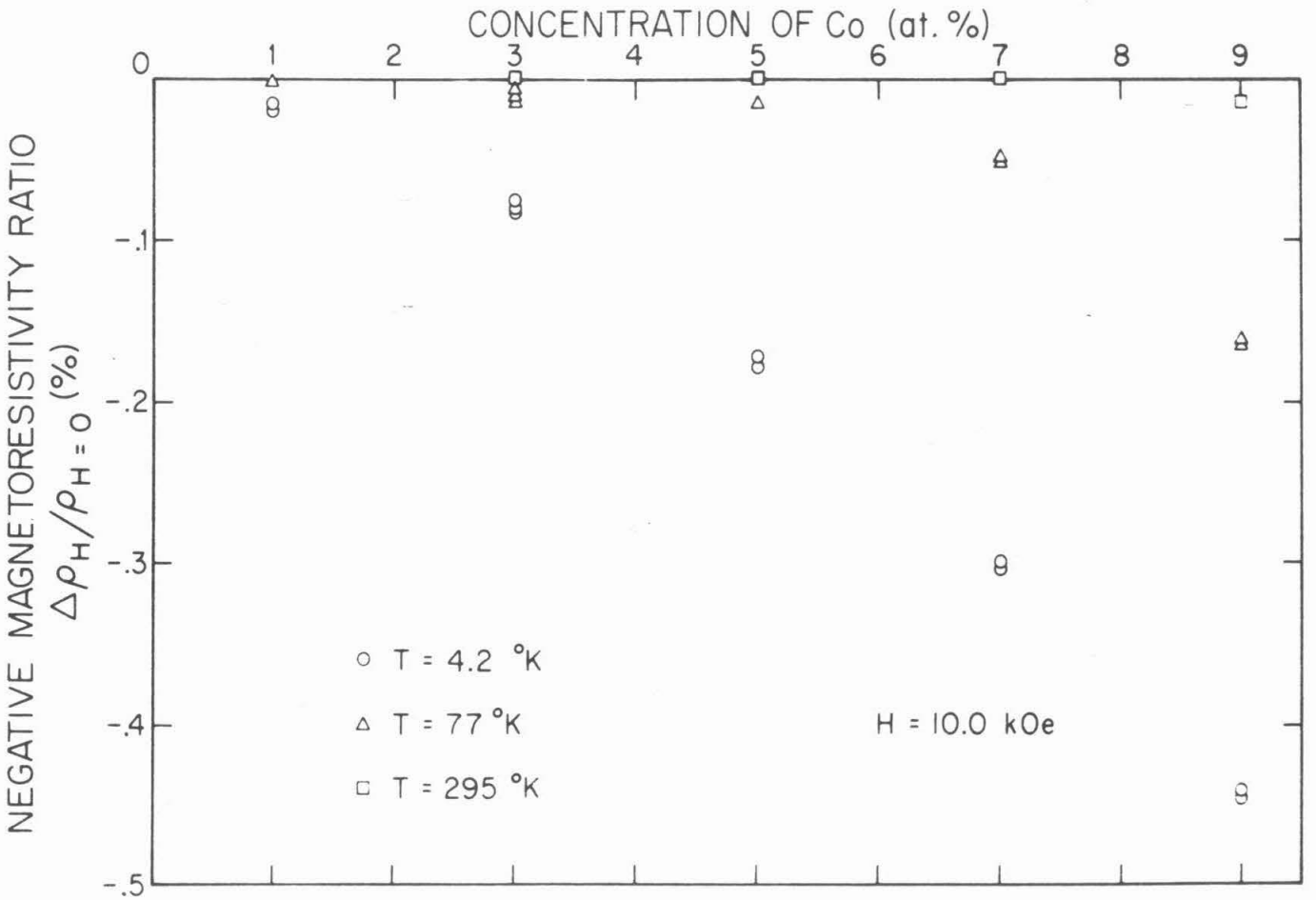

Fig. 27. Negative magnetoresistivity ratio vs Co concentration at H= 10.0 kOe, and T=4.2°K (o) 77°K (Δ) and 295°K (□) for the $Co_xPd_{80-x}Si_{20}$ alloys

is found from Fig. 12 that $\Delta\rho_{H=8.4kOe}/\rho_{H=0} \propto -x^{1.6}$. On the other hand we find in Ref. 26 that $\sigma_a \propto x^{0.3}$. Thus we have $\Delta\rho_H/\rho_{H=0} \propto -x\,\sigma_a^2 \propto -x^{1.6}$ from Eq. (8). As in the case of the $Fe_xPd_{80-x}Si_{20}$ alloys, T = 4.2°K is already in the temperature range where the $Co_xPd_{80-x}Si_{20}$ ($1 \leq x \leq 9$) alloys behave like ferromagnets (see Table 11). This means that Eq. (8) is still qualitatively valid in spite of the fact that the negative magnetoresistivity due to the s-d exchange interaction coexists with ferromagnetism.

(3) Magnetic Properties

(i) Chromium-palladium-silicon alloys

The results of the magnetic isothermals for the $Cr_xPd_{80-x}Si_{20}$ alloys show that the magnetization is proportional to the magnetic field in the temperature range between 1.7° and 300°K, i.e., the alloys behave like paramagnets. The magnetization vs temperature curves are shown in Fig. 13. It is seen that for a given temperature and a given field, the magnetization decreases with increasing Cr concentration. At H = 8.40 kOe and T = 4.2°K, for example, the magnetization σ_a is found to vary as $\sim 0.24\ x^{-1}\ \mu_B$/atom for $2 \leq x \leq 4$ at.%. This variation of σ_a with Cr concentration suggests some antiferromagnetic interaction between Cr atoms.

The difference between the susceptibility of the Cr alloy and that of the host alloy ($\Delta\chi$) follows the Curie-Weiss law or Eq. 9. This is shown in Fig. 14, where $1/\Delta\chi$ is plotted against temperature. The susceptibility difference deviates from the Curie-Weiss law below about

$25^{o}K$ and undergoes a maximum at $T = T_N$. Above $25^{o}K$, curves of $1/\Delta\chi$ vs T seem to consist of two straight lines with a change in slope at some temperature T_d which depends on Cr concentration. As a consequence, the values of μ_{eff} and θ_p in Eq. (9) are not the same below and above T_d. The results are summarized in Table 8. The temperature dependence of $\mu_{eff}(T)$ is obtained through Eq. (11) and shown in Fig. 28. Anderson[32] suggested that for $T \ll T_K$ the value of $\Delta\chi$ would be proportional to $T^{-\frac{1}{2}}$. As shown in Fig. 29, this law seems to be obeyed between T_N and T_d.

The value obtained for μ_{eff} in Table 8 leads to $S = \frac{1}{2}$ (2.6), which suggests that there are 2.6 holes in the d-band of Cr. The effective magnetic moment of Cr in crystalline Pd has been measured by Burger[45] and is about 4.5 μ_B/atom which is larger than the present result. The difference between the S value of 3/2 (assuming Cr^{3+}) and the experimentally determined value of 1.3 suggests that the conduction electrons partly fill the unfilled d-band of Cr. The fact that μ_{eff} is approximately independent of Cr concentration indicates that the spin clustering observed in $Co_xPd_{80-x}Si_{20}$ alloys[26] is probably absent in the Cr alloys. The fact that θ_p is larger than T_N which is positive suggests that the present results could be discussed by using the molecular field model[7]. In light of this model, the fact that $0 < T_N < \theta_p$ implies that the nearest neighbors Cr-Cr interaction (proportional to $\theta_p - T_N$) is as strong as the next nearest neighbors one (proportional to $\theta_p + T_N$). Thus the appearance of antiferromagnetism in the Cr alloys is most likely due to the superexchange interaction through Pd and Si atoms.

TABLE 8

Results of the magnetic measurements for the $Cr_xPd_{80-x}Si_{20}$ alloys

Alloy Composition	$\mu_{eff}(\mu_B/atom)$ ($T_d < T \leq 300^oK$)	$\theta_p(^oK)$ ($T_d < T \leq 300^oK$)	$\mu_{eff}(\mu_B/atom)$ ($25^oK < T < T_d$)	$\theta_p(^oK)$ ($25^oK < T < T_d$)	$T_N(^oK)$	$T_d(^oK)$	$\theta_B(^oK)$
$Cr_1Pd_{79}Si_{20}$	3.58	19	3.58	19	< 2	25	16 ~ 24
$Cr_2Pd_{78}Si_{20}$	3.49	35	3.49	35	6	30	25 ~ 44
$Cr_3Pd_{77}Si_{20}$	3.58	50	3.32	36	5	55	42 ~ 56
$Cr_4Pd_{76}Si_{20}$	3.56	67	2.94	30	10	75	54 ~ 74
$Cr_5Pd_{75}Si_{20}$	3.48	80	2.93	32	10	108	67 ~109
$Cr_6Pd_{74}Si_{20}$	3.31	90	2.71	35	11	120	93 ~120
$Cr_7Pd_{73}Si_{20}$	2.98	91	2.46	28	13	120	102 ~127

This implies that the 2.6 holes are not completely localized on the Cr atom but some of those are contributed by the Pd and Si atoms. The strength of the Cr-Cr interaction can be estimated by obtaining J_{dd} from Eq. (10) with θ_p in Table 8. It is found that $J_{dd} \sim -0.074$ eV. Since $|J_{dd}| < |J_{sd}|$ (see Sec. (4) for the value of J_{sd}), the susceptibility at higher temperatures might be influenced by the s-d exchange interaction. As seen in Ref. 7, the change of θ_p due to the s-d exchange interaction is proportional to the susceptibility χ_e of the conduction electrons. Thus θ_p is not much influenced by the s-d exchange interaction since $\chi_e \sim 10^{-6}$ emu $\ll 1$.

It is found that the value of μ_{eff} for the temperature range between 25°K and T_d is smaller than that above T_d, and this may be due to the existence of the quasi-bound state. It might be concluded that $T_K \sim \theta_p$ (for $T < T_d$), since this θ_p is insensitive to Cr concentration. However, T_d is prcbably the Kondo temperatur e for the following reasons:

(a) As mentioned in Sec. (1)-(i) (see Fig. 20), T_d is very close to the temperature at which the resistivity difference $\Delta\rho$ deviates from the $-\ell n\ T$ dependence. It is found also that T_d is approximately the same as T_R which is obtained from Eq. (6).

(b) The effective magnetic moment decreases below T_d as seen in Fig. 28 and Table 8.

(c) The susceptibility difference $\Delta\chi$ (see Fig. 29) obeys Eq. (11) with $\mu_{eff}^2(T)$ having the temperature dependence of Eq. (12) where a general function $f(T) = (0.60 \pm 0.05)\ (T/T_d)^{\frac{1}{2}}$ is obtained for $T_N < T \ll T_d$.

(d) The observed magnetization fits a Brillouin function of the form $B_s(g\mu_B SH/k(T+\theta_B))$ with $S = 3/2$ and θ_B listed in Table 8. It has been suggested[21] that $\theta_B \sim T_K$. Since $\theta_B \sim T_d$ as seen in Table 8, it is concluded that $T_K \sim T_d \sim \theta_B$.

The deviation of $\Delta\chi$ from the Curie-Weiss law for $T_N < T < 25^oK$ is probably due to the existence of the quasi-bound state, since this is the temperature range where $\Delta\chi \propto (T/T_K)^{-\frac{1}{2}}$. The value of $\Delta\chi$ undergoes a maximum at $T = T_N$ below which $\Delta\chi$ decreases very slowly with decreasing temperature (see Fig. 29). It seems that $\Delta\chi$ approaches a constant value at $\sim 1.3 \cdot 10^{-5}$ emu/g (or $2.1 \cdot 10^{-5}/x$ in μ_B/atom; x in at.% Cr) at the lower temperature limit. It has been suggested[46, 47] that $\Delta\chi/\text{atom} \propto \mu_{eff}^2/kT_K$ as T goes to zero. Then this relation gives $T_K \propto x$, which is consistent with the concentration dependence of T_d. This provides another evidence for the conclusion that Kondo temperature is proportional to Cr concentration.

Below T_N, $\mu_{eff}(T)$ decreases rapidly with decreasing temperature, approaching the value of zero moment at the absolute zero temperature (see Fig. 28). This is consistent with the theoretical prediction of Nagaoka[16], Yosida[48], Takano-Ogawa[31] and Hamann[23]. Hence T_N may not be the antiferromagnetic transition temperature in the usual sense but rather the temperature at which a complete spin compensation starts to occur. This is probably the case for the Cr alloys since the resistivity difference $\Delta\rho$ is almost saturated below T_N as seen in Fig. 2. The fact that $\Delta\chi$ becomes maximum and $\Delta\rho$ levels off at $T = T_N$ was predicted theoretically by Yosida and Okiji[49].

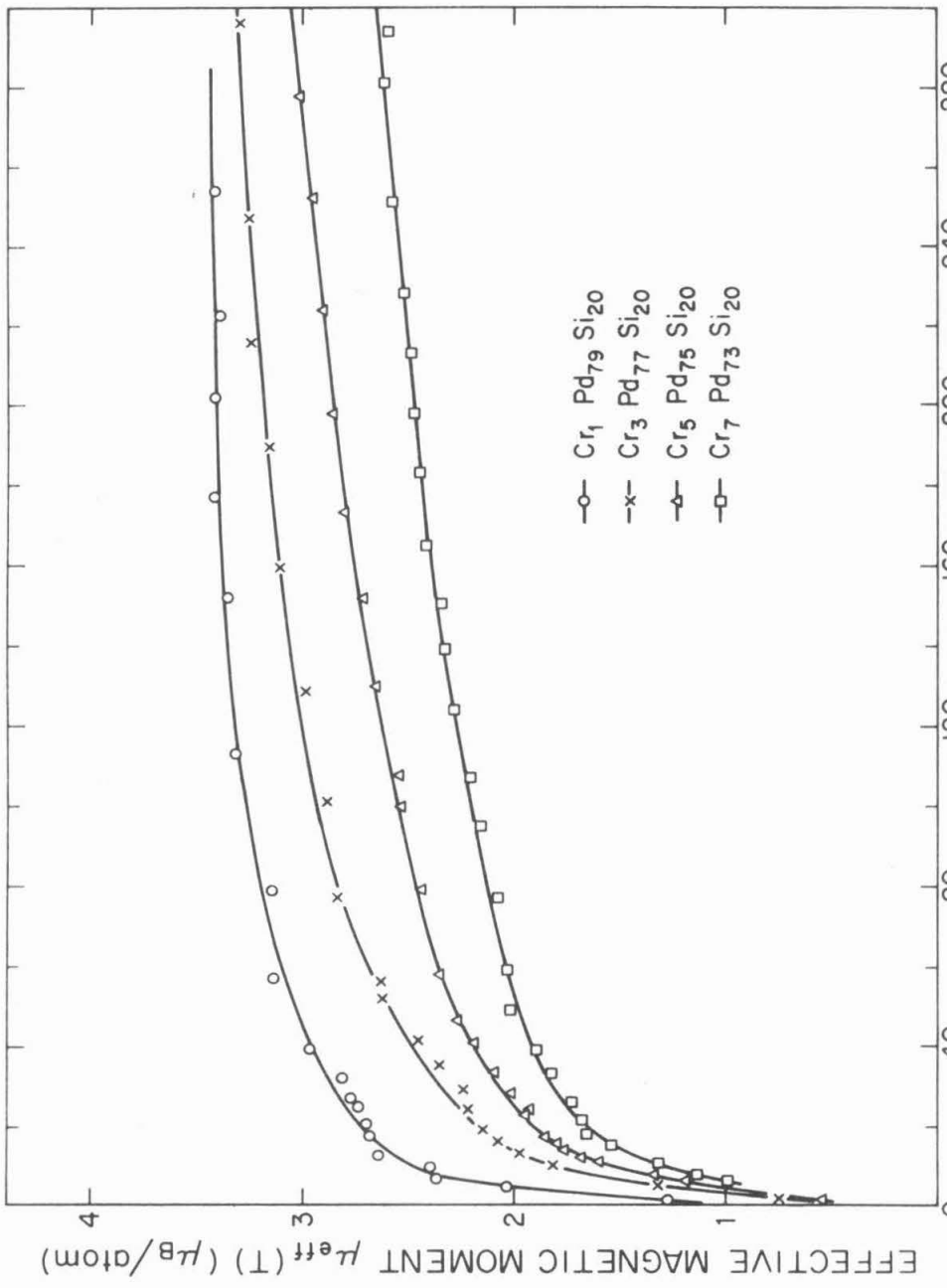

Fig. 28. Effective magnetic moment per Cr atom vs temperature curves for the $Cr_x Pd_{80-x} Si_{20}$ alloys

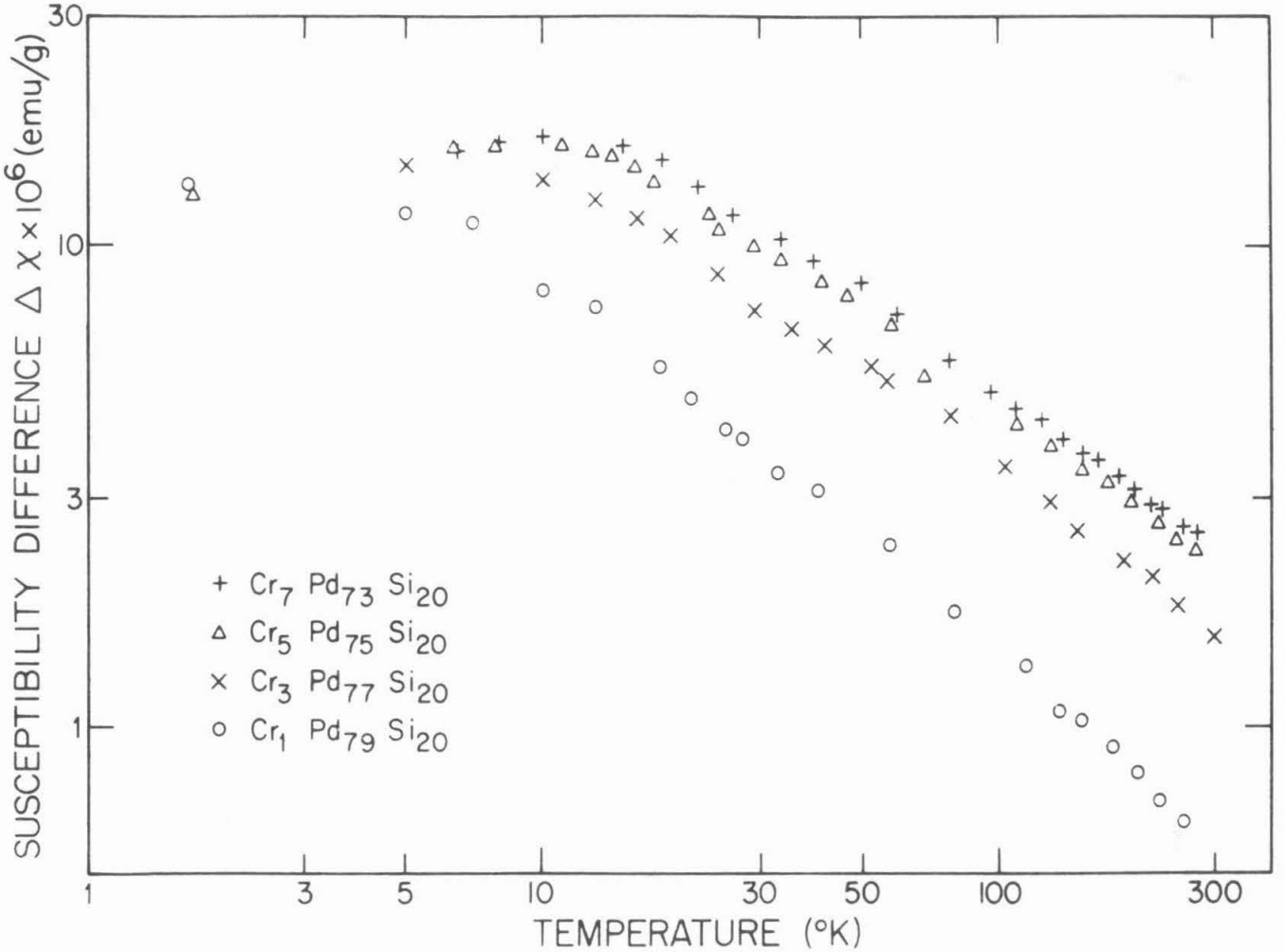

Fig. 29. Susceptibility difference per gram of the $Cr_xPd_{80-x}Si_{20}$ alloys vs temperature

(ii) Manganese-palladium-silicon-alloys

The magnetic behavior of the $Mn_xPd_{80-x}Si_{20}$ alloys resembles that of the Cr alloys, as expected. The magnetization varies linearly with the magnetic field between 1.7° and 300°K, indicating the paramagnetic behavior of the alloys. The concentration dependence as well as the temperature dependence of the magnetic moments were studied. It is found that the magnetization σ_a varies like $1.15\ x^{-\frac{1}{2}}(\mu_B/\text{atom})$ for $1 \leq x \leq 5$ and $2.50\ x^{-1}\ (\mu_B/\text{atom})$ for $5 \leq x \leq 7$ at $T = 4.2^oK$ and $H = 8.40$ kOe (Fig. 15). The decrease in the magnetization with respect to Mn concentration suggests that the Mn-Mn interaction is antiferromagnetic.

The magnetic susceptibility differences $\Delta\chi$ obey the Curie-Weiss law in a temperature range from $\sim 4^oK$ to 300^oK as shown in Fig. 16. No change in the slope of the $1/\Delta\chi$ vs T curve was observed for the Mn alloys. The results from the susceptibility analysis are found in Table 9.

The invariance of μ_{eff} with respect to Mn concentration suggests that the Mn atoms do not form clustering. The observed values for μ_{eff} give S = 4.9/2 or 4.9 d-holes per Mn atom, and this indicates that the Mn atom behaves as Mn^{2+} ion in the alloy. The fact that S is very close to 5/2 shows that the d-band of the Mn atom is hardly filled with the conduction electrons. Burger[45] has obtained $S \sim 5/2$ for Mn in crystalline Pd, which indicates that the electronic structure of Mn is not very much altered by the presence of Pd atoms.

The Mn alloys behave like antiferromagnets for $T \leq T_N$. However the transition temperature T_N may not be the usual antiferromagnetic

Nēel temperature since T_N is approximately 4^oK and independent of Mn concentration. The occurrence of the positive θ_p and probably very small Nēel temperature is possible in light of the molecular field model mentioned before. As in the case of the Cr alloys, the Mn-Mn nearest neighbors interaction is as strong as the Mn-Mn next nearest neighbors one. The strength of the Mn-Mn interaction is estimated from $J_{dd} \sim -0.0022$ eV obtained through Eq. (10). As in the case of the Cr alloys, the influence of the s-d exchange interaction on θ_p is negligible even if $|J_{dd}| < |J_{sd}|$ (see Sec. 4 for the value of J_{sd}). It is found that θ_p/at.% for the amorphous Mn-Pd-Si alloys is about 1.2^oK which is smaller than that for the crystalline Mn-Pd alloys ($\sim 4.5^oK$). This implies that the d-d spin correlation is weaker in the amorphous alloys than in the crystalline alloys. It is concluded that the Mn-Mn interaction is antiferromagnetic due to the superexchange interaction via Pd and Si atoms.

The magnetic moments observed in the Mn alloys can be expressed by a Brillouin function of the form $B_S(g\mu_B SH/k(T+\theta_B))$ with $S = 5/2$ and θ_B listed in Table 9. It is noticed that $\theta_p \sim \theta_B$, which is to be expected since the Curie-Weiss law holds between 4^o and 300^oK.

The susceptibility difference ($\Delta\chi$) has a maximum at T_N and then decreases with decreasing temperature. Due to the lack of points of $\Delta\chi$ below 4.2^oK, an analysis by means of $\Delta\chi(0) \propto \mu_{eff}^2/kT_K$ is not possible. The invariance of T_N with respect to Mn concentration suggests that T_N may not be the usual antiferromagnetic transition temperature but the temperature at which the quasi-bound state begins to be complete. The

TABLE 9

Results of the magnetic measurements for the $Mn_xPd_{80-x}Si_{20}$ alloys

Alloy Composition	$\mu_{eff}(\mu_B/atom)$ $T_N < T < 300^oK$	$\theta_p(^oK)$ $T_N < T < 300^oK$	$T_N(^oK)$	$\theta_B(^oK)$
$Mn_1Pd_{79}Si_{20}$	5.84	1	2	1.0 ± 0.3
$Mn_3Pd_{77}Si_{20}$	5.73	4	4	4.2 ± 0.4
$Mn_5Pd_{75}Si_{20}$	5.56	9	4	7.5 ± 1
$Mn_7Pd_{73}Si_{20}$	5.76	12	4	12.5 ± 1

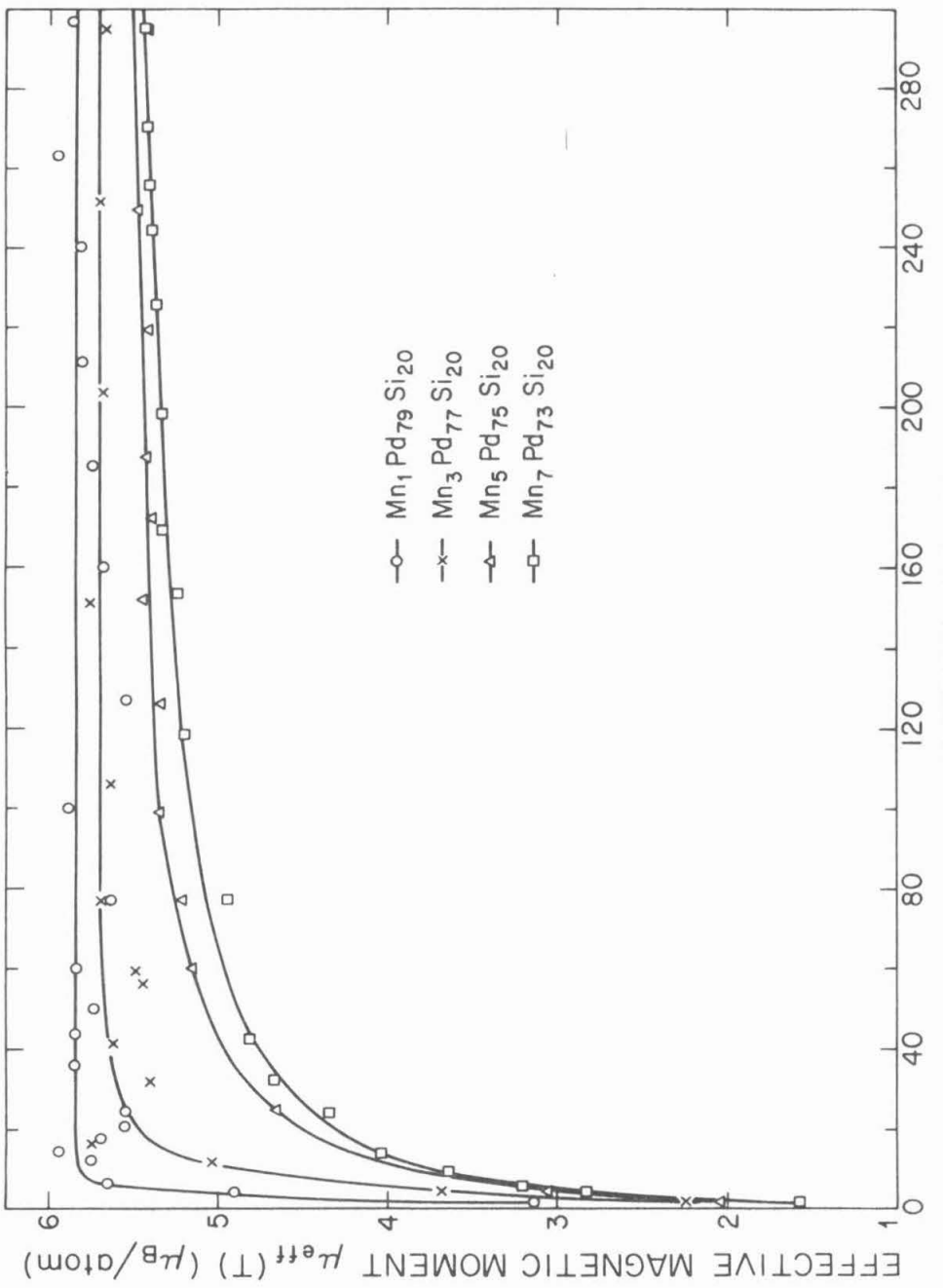

Fig. 30. Effective magnetic moment per Mn atom vs temperature for the $Mn_x Pd_{80-x} Si_{20}$ alloys

rapid decrease of $\mu_{eff}(T)$ below T_N, as seen in Fig. 30, supports this suggestion.

(iii) Iron-palladium-silicon alloys

It is to be expected that the $Fe_xPd_{80-x}Si_{20}$ alloys behave like ferromagnets at low temperature considering the fact that ferromagnetism persists down to 0.15 at.% Fe in crystalline Pd-Fe alloys[50]. The results of the magnetic isothermals show that the magnetization is proportional to the magnetic field only at higher temperatures and tends to saturate at lower temperatures and at higher magnetic fields. The magnetization vs temperature curves, shown in Fig. 17, implies the ferromagnetic behavior of the Fe alloys.

The magnetic isothermals obtained can be expressed by

$$\sigma_a (H, T) = \Delta\chi H + \sigma_a (0,T),$$

where $\sigma_a (H,T)$ is the magnetization per transition metal atom at a temperature T and field H and $\sigma_a (0,T)$ is the spontaneous magnetization. It is found that above some temperature T_d the spontaneous magnetization $\sigma_a(0,T)$ is approximately zero and that $\Delta\chi$ obeys the Curie-Weiss law with the paramagnetic temperature $-\theta_p$. Below the temperature $|\theta_p|$ the alloys behave like ferromagnets. The ferromagnetic Curie temperatures T_c were obtained by plotting $\sigma_a^2 (0,T)$ vs T and extrapolating the linear part to the temperature axis. The results obtained through this analysis are summarized in Table 10.

The main features of the Fe alloys are (a) that μ_{eff} is approximately independent of Fe concentration between 0.5 and 7 at.% and (b)

that the alloys behave like ferromagnets below $T_c \sim |\theta_p| \sim 10.2$ x (^oK). The first characteristic is different from the Pd-Fe case[57] where μ_{eff} varies with Fe concentration and becomes as large as 12 μ_B/atom at 0.28 at.% Fe. It is also different from the case of amorphous Co-Pd-Si alloys[26] where μ_{eff} increases with Co concentration (see Table 11). The unusually large values of μ_{eff} obtained for crystalline Pd-Fe alloys have been considered to be due to the spin polarization of Pd atoms surrounding a Fe atom. The situation may be the same in the amorphous Fe-Pd-Si alloys, since the value of μ_{eff} (~ 5.7 μ_B/atom) is too large to assign all the moments to one Fe atom. Cable et al.[51] have obtained the effective moment per Fe atom and found 2.9 μ_B and 3.0 μ_B for PdFe and Pd_3Fe respectively. The moment on the Pd atom was 0.30 μ_B. Therefore it is assumed here that $\mu_{Fe} = 3.0\ \mu_B$ and $\mu_{Pd} = 0.30\ \mu_B$. It has been shown[52], on the other hand, that in an amorphous $Pd_{80}Si_{20}$ alloy a Pd atom has an average of 11.6 nearest neighbors of either Pd or Si atom. Then it is reasonable to assume that each Fe atom in an amorphous Fe alloy has, on the average, 11.6 nearest neighbors of either Pd or Si atom for a small Fe concentration, and that the ratio of the number of Pd atoms to that of Si atoms for each Fe atom is kept at (80-x):20. In other words, each Fe atom is assumed to have 11.6 $(\frac{80-x}{100-x})$ Pd atoms as its neighbors. Thus we obtain for a small x

$$\mu_{eff} \sim \mu_{Fe} + 11.6\ (\frac{80-x}{100-x})\ \mu_{Pd} \sim 5.8\ \mu_B/\text{atom}$$

which agrees with our experimental results. The present result also indicates that the Pd atoms in the vicinity of a Fe atom also contribute to the measured moment. The invariance of μ_{eff} with respect to Fe concentration suggests that each Fe atom is surrounded by an atmosphere of Pd and Si atoms to form magnetic single domains which do not interact with each other (in the short range order) up to a Fe concentration of 7 at.% at temperatures well above the paramagnetic Curie temperature.

The susceptibility difference $\Delta\chi$ starts to deviate from the Curie-Weiss law below T_d, implying a ferromagnetic ordering starts to take place. The occurrence of ferromagnetism at lower temperatures is clearly manifested in the magnetization-temperature curve (Fig. 17). However the magnetization σ_a behaves somewhat differently from the crystalline case in the temperature range where σ_a approaches its saturation value, which is clearly seen for the $Fe_7Pd_{73}Si_{20}$ alloy (Fig. 17). Tsuei et al.[53] have observed a similar behavior in an amorphous Fe-P-C alloy. These observations have been recently explained theoretically by Handrich[54]. The somewhat different behavior of the magnetization with respect to temperature in amorphous ferromagnets may create difficulty in determining the ferromagnetic Curie temperatures by conventional methods. However, it is noticed that the temperature where the resistivity deviates from linearity is in the vicinity of $T_c \sim |\theta_p|$ (Fig. 5), which supports the present determination of T_c.

The paramagnetic Curie temperature per at.% Fe is found to be approximately $10^{o}K$ compared with $18^{o}K$ for crystalline Pd-Fe alloys[45].

TABLE 10

Results of the magnetic measurements for the $Fe_xPd_{80-x}Si_{20}$ alloys

Alloy Composition	$\mu_{eff}(\mu_B/atom)$ $T_d < T < 300^oK$	$\lvert\theta_p\rvert(^oK)$	$T_d(^oK)$	$T_c(^oK)$
$Fe_{0.5}Pd_{79.5}Si_{20}$	5.73	1	1.7	< 4
$Fe_1Pd_{79}Si_{20}$	5.78	11	45	11
$Fe_3Pd_{77}Si_{20}$	5.85	30	50	30
$Fe_5Pd_{75}Si_{20}$	5.60	64	95	51
$Fe_7Pd_{73}Si_{20}$	5.60	110	160	72

The smaller value of θ_p/at.% Fe for the amorphous alloys may suggest that the long-range Fe-Fe interaction is smaller in these alloys. It is found from Eq. (10) that $J_{dd} \sim 0.018$ eV which gives an approximate value for the long range Fe-Fe interaction energy in the present alloys. These results seem to be consistent with Handrich's theory[54]. His result indicates that J_{dd} in amorphous alloys can be written as

$$J_{dd} = \frac{4\pi}{V} \int r^2 g(r)\ J(r)\, dr$$

where V is the volume in which the above integration is performed, g(r) the radial distribution function and J(r) the d-d exchange integral in crystalline alloys. Using Crewdson's results[52], i.e., $4\pi r^2 g(r) \sim 23 \exp\{-\frac{1}{2}(\frac{r-r_o}{0.212})^2\}$ and $r_o \sim 2.79$Å, we obtain $(J_{dd})_{amorphous} \sim 0.6\ (J_{dd})_{crystalline}$, which is quite consistent with the values for θ_p mentioned above.

Due to the existence of ferromagnetism, the Kondo temperature for the $Fe_xPd_{80-x}Si_{20}$ alloys could not be estimated from the susceptibility results.

(iv) Cobalt-palladium-silicon alloys

The magnetic properties of the $Co_xPd_{80-x}Si_{20}$ alloys have been studied[26] for $x \geq 3$. Results are summarized in Table 11 together with the present results for the $Co_1Pd_{79}Si_{20}$. Weiner[26] has explained the large moments for the concentrated Co alloys in terms of the super-exchange clustering model, where more than one cobalt atom form a cluster to attain the large moments. For the dilute Co alloys, the situation may be somewhat different. As it is noticed, μ_{eff} does not vary

TABLE 11

Values of μ_{eff} and T_c for the $Co_xPd_{80-x}Si_{20}$ alloys*

Alloy Composition	μ_{eff} (μ_B/atom)	T_c (^oK)
$Co_1Pd_{79}Si_{20}$	4.29	6
$Co_3Pd_{77}Si_{20}$	4.3	15
$Co_5Pd_{75}Si_{20}$	7.4	36
$Co_7Pd_{73}Si_{20}$	10.0	41
$Co_9Pd_{71}Si_{20}$	16.8	59
$Co_{10}Pd_{70}Si_{20}$	20.1	95
$Co_{11}Pd_{69}Si_{20}$	11.7	105

*Results are taken from Ref. 26 except those for the $Co_1Pd_{70}Si_{20}$ alloys.

in alloys containing less than 3 at.% of Co, which suggests that the cluster model is not applicable to these alloys. Yet the magnetic moments per Co atom are still larger than the Co moment (1.7 μ_B/atom).

Thus it must be assumed that Pd atoms surrounding a Co atom contribute to the magnetic moments. If it is assumed[26] that μ_{Co} = 1.7 μ_B/atom and μ_{Pd} = 0.30 μ_B/atom and that each Co atom has $11.6(\frac{80-x}{100-x})$ nearest neighbors of Pd, then

$$\mu_{eff} \sim \mu_{Co} + 11.6\ (\frac{80-x}{100-x})\ \mu_{Pd} \sim 4.5\ \mu_B/\text{atom},$$

which agrees with the values obtained for alloys containing less than 3 at.% Co.

As pointed out by Weiner[26], the ferromagnetic transition temperatures (T_c) are not well-defined in the amorphous alloys. However T_c is estimated from the temperature at which σ_a vs T^{-1} curve deviates from a straight line. The Kondo temperature could not be estimated from the susceptibility results due to the existence of ferromagnetism as in the case of Fe alloys.

(4) Determination of the Fermi Energy and the s-d Exchange Integrals

Eqs. (2) and (8) indicate that a combination of electrical resistivity, magnetoresistivity and magnetic measurements leads to a determination of the Fermi energy (E_F) and of the s-d exchange integral (J_{sd}). In the case of most crystalline alloys, whose Fermi energies are known, either Eq. (2) or (8) has been used to determine J_{sd}. Some of the previously reported values for J_{sd} are given in Table 12 for the metals of the first transition series alloyed with various host metals.

Table 12

Values of J_{sd}(eV) in different host metals

Transition Metal	$Pd_{80}Si_{20}$ (E_F=3.5eV)	Pd (E_F=5eV)	Au (E_F=5.5eV)	Cu (E_F=7.0eV)	Mg (E_F=7.1eV)	Zn (E_F=10eV)	Al (E_F=12eV)
Sc							
Ti							
V			-0.60(14)				
Cr	-2.3	-0.55(59)				-1.4(56)	
Mn	-0.11	0.007 to 0.017(55)		-0.40(57)	-0.30(58)	-0.94(62) -1.4(56)	
Fe	-0.95		-0.15(15) -0.064 to -0.1(61)	-1.2(60) -0.91(57) -0.6(21)			
Co	-0.20						
Ni							

(The numbers in the parenthesis are the reference numbers.)

Since both Eqs. (2) and (8) are valid only in the paramagnetic temperature range, it is expected that a simultaneous application of these formulae to the observed results would be limited. As discussed in Sec. (3), only the $Mn_xPd_{80-x}Si_x$ alloys were paramagnetic down to 4.2°K. Therefore the results for the $Mn_xPd_{80-x}Si_{20}$ alloys were used to determine E_F of the alloys. The Fermi energy obtained in this way was assumed to be the same for all the other amorphous alloys.

The Fermi energy and the value of J_{sd} for the $Mn_3Pd_{77}Si_{20}$ alloy were determined from Eqs. (2) and (8) by using the following numerical values, i.e., ρ_M = 57.3 μΩ-cm, γ = -0.071 μΩ-cm, $\Delta\rho_{H=8.40kOe}$ = 0.0134 μΩ-cm, σ_a(8.40kOe, 4.2°K) = 0.691 μ_B/atom and μ_{eff} = 5.73 μ_B. The results were E_F = 4.0 eV and J_{sd} = -0.096 eV. Similar computations for the other Mn alloys gave approximately the same values, and the average values were

$$E_F = (3.5 \pm 0.5) \text{ eV}$$

$$(J_{sd})_{Mn} = (-0.11 \pm 0.01) \text{ eV}.$$

The uncertainty in J_{sd} is mainly due to the uncertainty in E_F, but is usually very small since $J_{sd} \propto \sqrt{E_F}$.

Similar computations were carried out for the Cr alloys. From the slope of $\Delta\rho$ vs $\ell n\ T$ plot (γ) and with E_F = 3.5 eV and $\rho_M \sim 69$ μΩ-cm, we find

$$(J_{sd})_{Cr} = (-2.3 \pm 0.5) \text{ eV}.$$

The $Fe_xPd_{80-x}Si_{20}$ alloys behave like ferromagnets at T = 4.2°K, and the resistivity minimum temperature T_m is below the ferromagnetic Curie temperature (T_c) for all the alloys except for the $Fe_1Pd_{79}Si_{20}$ alloys. Thus Eq. (2) is valid for $T_c < T < T_m$. Using E_F = 3.5 eV, ρ_M = 46 μΩ-cm and γ = -0.174 μΩ-cm we find

$$(J_{sd})_{Fe} = (-0.95 \pm 0.05) \text{ eV}.$$

The situation is similar for the $Co_xPd_{80-x}Si_{20}$ alloys. Eq. (2) is valid only for $T_c < T < T_m$ for $Co_1Pd_{79}Si_{20}$ alloys. Using E_F = 3.5 eV, ρ_M = 50 μΩ-cm and γ = -0.04 μΩ-cm, we find

$$(J_{sd})_{Co} = (-0.20 \pm 0.01) \text{ eV}.$$

The present results are summarized in Table 12 together with the previously reported results of J_{sd} for different host metals. Two interesting features are noticed in Table 12: (i) the value of J_{sd} for a given transition metal seems to depend on the host metal; (ii) the possibility of having a resistivity minimum phenomena in alloys increases with decreasing Fermi energy. These two features can be explained by Friedel's model (see Sec.5). It is noticed that J_{sd} for Mn-Pd crystalline alloys is positive. The low temperature resistivity for these alloys showed no resistivity minimum[55], indicating the consistency of the Kondo theory.

The large value of J_{sd} for the Cr alloys may be responsible for the large resistivity minimum depth discussed in Sec. (1).

(5) Localized d-states

Friedel's virtual bound state model described in Part IV-(4) gives

an empirical rule concerning the existence of localized moments. If we take $W \sim 1.5$ eV (from $E_F = 3.5$ eV) and $\Delta E \sim 0.6$ eV in Eq. (13), we obtain $p > 2$. This means that transition metals V, Cr, Mn, Fe or Co can form localized moments in the amorphous palladium-silicon base alloys while Sc, Ti or Ni cannot, which is consistent with the present results. From this rule it is expected that $V_xPd_{80-x}Si_{20}$ alloys should exhibit localized moments. However, this was not confirmed due to the difficulty of obtaining an amorphous state for this alloy system.

From the results of the magnetic measurements it is found that the atoms surrounding a transition metal atom contribute to the measured magnetic moments. This means that the virtual bound d-states spread over the neighboring Pd and Si atoms. In addition, the fact that the values of effective magnetic moments are invariant for a wide range of transition metal concentrations suggests that one of the split d-states is near the Fermi level and the other is below it. These observations are summarized in Fig. 31 for the alloys containing Cr, Mn Fe or Co (with less than 3 at.% Co). It is noticed that one of the d-states of Cr has its center at the Fermi level. This may indicate that the interaction of the d-electrons of Cr and the conduction electrons is large, resulting in a large value of J_{sd} (see Table 12). Similarly a large value of J_{sd} (- 1.4 eV) for a crystalline Zn-Mn[56] alloy may be due to the fact that S = 3/2 and a small value of J_{sd} (- 0.4 eV) for a crystalline Cu-Mn[57] alloy to the fact that S = 5/2.

The absence of localized moments in the $Ni_xPd_{80-x}Si_{20}$ alloys

indicates that the 0.6 holes of Ni are filled by free electrons mainly from Si. The virtual d-states, therefore, exist below the Fermi level and have no appreciable interactions with the conduction electrons which is revealed as the absence of Kondo effect and negative magnetoresistivity.

As Eq. (13) predicts, the splitting of the d-states becomes more likely as the Fermi energy is decreased. This agrees with the experimental results summarized in Table 12 which shows that with an increasing Fermi energy, the number of transition metals giving rise to anomalies due to the s-d exchange interaction seems to decrease. For example transition metals in Aℓ ($E_F \sim 12$ eV) do not show s-d exchange anomalies while such anomalies were observed for most of the transition metals in the amorphous alloys ($E_F = 3.5$ eV).

In Friedel's virtual bound state model, it is expected that the scattering amplitude for $\ell = 2$ is the largest since the virtual bound states are d-states. Then it can be assumed that η_o, η_1, $<< \eta_2$ and $\eta_\ell = 0$ for $\ell > 2$ in Eqs. (14) and (15). From the results of the magnetic measurements it is possible to estimate the phase shifts η_2 for the amorphous alloys by using Eq. (14). Thus we have $\eta_2^\uparrow \sim \pi/2$ and $\eta_2^\downarrow \sim 0$ for the Cr alloys, $\eta_2^\uparrow \sim \pi$ and $\eta_2^\downarrow \sim 0.1\ \pi/5$ for the Mn alloys, $\eta_2^\uparrow \sim \pi$ and $\eta_2^\downarrow \sim 2.8\ \pi/5$ for the Fe alloys and $\eta_2^\uparrow \sim \pi$ and $\eta_2^\downarrow \sim 4\ \pi/5$ for the Co alloys. With these values, the residual resistivities for these alloys can be obtained by using Eq. (15) and are given in Table 13 together with the experimental results found in Sec. (1). Table 13 shows a good agreement between the two results.

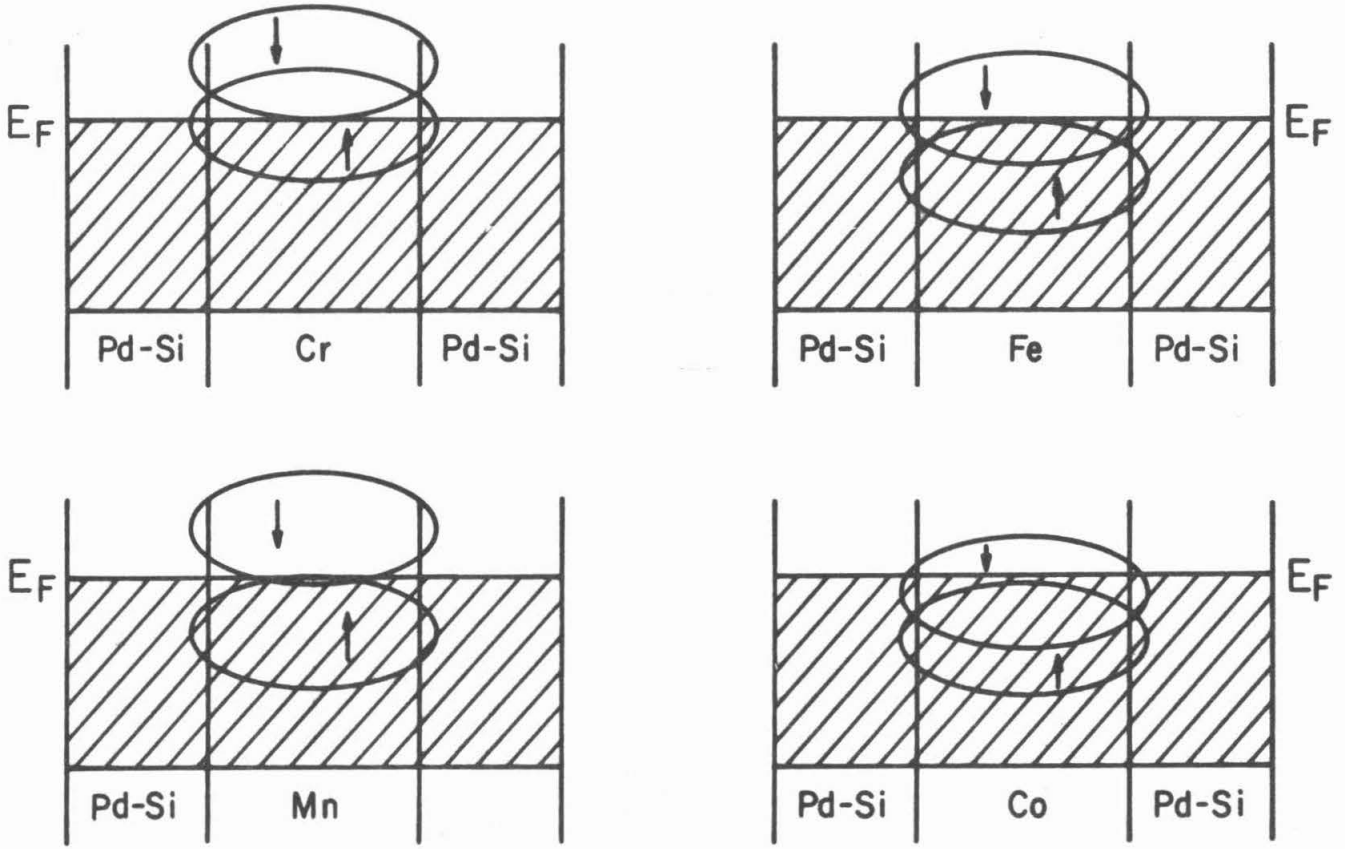

Fig. 31. Friedel's model of localized d-states for the amorphous Pd-Si alloys containing Cr, Mn, Fe or Co. The arrows show the direction of the spins in the d-states.

TABLE 13

Comparison between the theoretical $(\Delta\rho_o)_{th}$ and experimental $(\Delta\rho_o)_{exp}$ residual resistivities

Alloy Composition	$(\Delta\rho_o)_{th}$ μΩ-cm/at.%	$(\Delta\rho_o)_{exp}$ μΩ-cm/at.%
$Cr_xPd_{80-x}Si_{20}$	22.4	22
$Mn_xPd_{80-x}Si_{20}$	0.09	3.8
$Fe_xPd_{80-x}Si_{20}$	21.4	19
$Co_xPd_{80-x}Si_{20}$	7.4	4.2

VI. CONCLUSIONS

The electrical resistivity, the magnetoresistivity, the magnetic moments and the susceptibility of amorphous palladium-silicon base alloys containing Cr, Mn, Fe, Co or Ni were studied. A well-defined minimum in the resistivity vs temperature curve was obtained in the alloys containing Cr, Mn, Fe or Co but not in those containing Ni. Below the resistivity minimum temperature T_m, the resistivity varies as $-\ln T$ as the temperature decreases and tends to level off at lower temperature. In a temperature range just below the resistivity minimum temperature T_m, the resistivity-temperature relationship ($\rho \propto -\ln T$) can be explained by the Kondo theory. At lower temperatures the results can be interpreted on the basis of the theoretical treatments of Nagaoka, Suhl-Wong and Hamann. The deviation of the resistivity-temperature curve from the $-\ln T$ law is attributed to the appearance of quasi-bound states at lower temperatures. The temperature at which this deviation occurs gives an approximate Kondo temperature. It was also found that T_m is proportional to the transition metal concentration for the Cr and Mn alloys and proportional to the square root of concentration for the dilute Fe and Co alloys. This behavior of T_m is different from that found in crystalline alloys where T_m varies as the 1/5 power of concentration. For the Mn, Fe and Co alloys the difference between the two cases is attributed to the fact that the low temperature resistivity of the host amorphous alloy varies as T^2 while that of crystalline alloys varies as T^5. For the Cr alloys the difference is due to the fact that

the resistivity minimum occurs in a temperature range where the resistivity of the host amorphous alloy is proportional to T. A significant difference between crystalline and amorphous alloys is that in amorphous alloys the concentration of the transition metal can be as high as 11 at.%, whereas it is generally less than 1 at.% in crystalline alloys. Also the temperature at which the resistivity minimum occurs can be quite high in amorphous alloys, i.e., as high as 580^{o}K compared with less than 50^{o}K for crystalline alloys.

If the resistivity minimum is due to the s-d exchange interaction, which gives rise to a Kondo effect, it should be accompanied by a negative magnetoresistivity. This is indeed the case for all the amorphous alloys in which a resistivity minimum was found. The negative magnetoresistivity results were analyzed by making use of the theory of Béal-Monod and Weiner and the agreement between the theory and the experimental results was satisfactory.

The occurrence of both a resistivity minimum and a negative magnetoresistivity indicates the existence of magnetic moments localized on the transition metal atoms. A direct evidence for these localized moments was provided by the magnetic measurements. From the susceptibility data at higher temperatures, the effective magnetic moments per transition metal atom and the paramagnetic Curie temperature were obtained. These results lead to the conclusion that the Pd atoms surrounding the transition metal atom also contribute to the observed magnetic moments. The most astonishing result is that the resistivity

minimum coexists with ferromagnetism. This is inconsistent with the assumption on which the Kondo theory is based. It can be explained, however, if it is assumed that the d-d spin interaction is smaller in amorphous alloys than that in the crystalline alloys, so that the localized moments can coexist with the magnetic ordering. This assumption seems to be valid since the paramagnetic Curie temperatures for the amorphous alloys were approximately 1/2 of those for the crystalline alloys.

The Kondo temperature T_K was estimated from the susceptibility data at low temperature for the Cr alloys. It was found that T_K is proportional to Cr concentration and this result is in agreement with the resistivity data. The concentration dependence of T_K may be attributed to a small change in the density of states. The Kondo temperature T_K could not be estimated from the susceptibility data for the Mn alloys due to the lack of experimental points below $T = 4.2^{o}K$ and for the Fe and Co alloys because of the existence of ferromagnetism.

By using the results of the resistivity, magnetoresistivity, magnetic moment and susceptibility measurements, the Fermi energy and the s-d exchange integrals J_{sd} were determined for the amorphous alloys. It was found that the order of magnitude of J_{sd} is the same as that obtained for the crystalline alloys. The large value of J_{sd} obtained for the Cr alloys may explain the unusually large Kondo effect observed in these alloys.

Finally it was concluded on the basis of Friedel's virtual bound

state model that the occurrence of the s-d exchange anomalies in alloys containing Cr, Mn, Fe or Co and the absence of it in alloys containing Ni, are due to the fact that the host palladium-silicon alloy has a low Fermi energy of 3.5 eV. In addition, the residual resistivities calculated from the result of Friedel's model were found in good agreement with those obtained experimentally.

REFERENCES

1. C. Zener, Phys. Rev. 81, 440 (1951); 82, 403 (1951); 83, 299 (1951).
2. G. J. van den Berg, Proceedings of the 7th International Conference on Low Temperature Physics (Univ. of Toronto Press, 1961).
3. J. M. Ziman, Electrons and Phonons (Oxford Univ. Press, 1962) p. 346.
4. A. N. Gerritsen, Physica 19, 6 (1953).
5. J. Korringa and A. N. Gerritsen, Physica 19, 457 (1953).
6. J. Owen, M. Browne, W. D. Knight and C. Kittel, Phys. Rev. 102, 1501 (1956).
7. J. Owen, M. Browne, V. Arp and A. F. Kip, J. Phys. Chem. Solids 2, 85 (1957).
8. T. Kasuya, Progr. Theoret. Phys. (Japan) 16, 58 (1956).
9. R. W. Schmitt, Phys. Rev. 103, 83 (1956).
10. R. W. Schmitt and I. S. Jacobs, J. Phys. Chem. Solids 3, 324 (1957).
11. K. Yosida, Phys. Rev. 107, 396 (1957).
12. J. Friedel, Can. Journ. Phys. 34, 1190 (1956).
13. J. Friedel, Nuovo Cimento 7, 287 (1958).
14. K. Kume, J. Phys. Soc. Japan 23, 1226 (1967).
15. J. Kondo, Progr. Theoret. Phys. (Japan) 32, 37 (1964).
16. Y. Nagaoka, Phys. Rev. 138, A1112 (1965); Progr. Theoret. Phys. (Japan) 37, 13 (1967).
17. M. D. Daybell and W. A. Steyert, Phys. Rev. Letters 18, 398 (1967).
18. M. A. Jensen, A. J. Heeger, L. B. Welsh and G. Gladstone, Phys. Rev. Letters 18, 997 (1967).

19. R. B. Frankel, N. A. Blum, B. B. Schwartz and D. J. Kim, Phys. Rev. Letters 18, 1051 (1967).

20. C. M. Hurd, Phy. Rev. Letters 18, 1127 (1967).

21. M. D. Daybell and W. A. Steyert, Phys. Rev. Letters 20, 195 (1968).

22. H. Suhl and D. Wong, Physics 3, 17 (1967).

23. D. R. Hamann, Phys. Rev. 158, 570 (1967).

24. P. Pietrokowsky, J. Sci. Instr. 34, 445 (1962).

25. Pol Duwez, Rapid Quenching Techniques, Chapt. 7 in Techniques of Metals Research, edited by R. F. Bunshah (Interscience Publishers, 1968).

26. M. E. Weiner, Ph. D. Thesis, California Institute of Technology (1968).

27. J. R. Schrieffer, J. Appl. Phys. 38, 1143 (1967).

28. See for example Ref. 3, p. 491.

29. M. T. Bēal-Monod and R. A. Weiner, Phys. Rev. 170, 552 (1968).

30. A. Blandin and J. Friedel, J. Physique Rad. 20, 160 (1959).

31. F. Takano and T. Ogawa, Progr. Theoret. Phys. (Japan) 35, 343 (1966).

32. P. W. Anderson, Phys. Rev. 164, 352 (1967).

33. See for example L. I. Schiff, Quantum Mechanics (McGraw-Hill, 1955), p. 113.

34. See Ref. 3, p. 248.

35. A. I. Gubanov, Quantum Electron Theory of Amorphous Conductors (Consultant Bureau, 1965) p. 234.

36. See Ref. 3, p. 412.

37. M. J. Rice, Phys. Rev. 159, 153 (1967); J. Appl. Phys. 39, 958 (1968).

38. H. Suhl, Phys. Rev. 138, A515 (1965).

39. A. A. Abrikosov, Physics 2, 5 (1965).

40. R. J. Harrison and M. W. Klein, Phys. Rev. 154, 540 (1967).

41. W. M. Star, Phys. Letters 26A, 502 (1968).

42. T. Moriya, Teoria del magnetismo nei metalli di transizione, Rendiconti della Scuola Internazionale di Fisica "Enrico Fermi" 37 Corso (Academic Press, 1967), p. 251.

43. F. Gautier, Z. Angew. Phys. 24, 289 (1968).

44. P. L. Maitrepierre, Ph. D. Thesis, California Institute of Technology (1969).

45. J. P. Burger, J. Phys. Rad. 23, 530 (1962).

46. A. J. Heeger and M. A. Jensen, Phys. Rev. Letters 18, 488 (1967).

47. H. Ishii and K. Yosida, Progr. Theoret. Phys. (Japan) 38, 61 (1967).

48. K. Yosida, Phys. Rev. 147, 223 (1966).

49. K. Yosida and A. Okiji, Progr. Theoret. Phys. (Japan) 34, 505 (1965).

50. J. Crangle and W. R. Scott, J. Appl. Phys. 36, 921 (1965).

51. J. W. Cable, E. O. Wollan, W. C. Koehler and M. K. Wilkinson, J. Appl. Phys. 33, 1340 (1962).

52. R. C. Crewdson, Ph.D. Thesis, California Institute of Technology (1966).

53. C. C. Tsuei, G. Longworth and S.C.H. Lin, Phys. Rev. 170, 603 (1968).

54. K. Handrich, Physica Status Solidi (to be published).

55. M. P. Sarachik and D. Shaltiel, J. Appl. Phys. 38, 1155 (1967).

56. G. Boato, G. Gallinaro and C. Rizzuto, Phys. Rev. 148, 353 (1966).

57. P. Monod, Phys. Rev. Letters, 19,1113 (1967).

58. F. T. Hedgecock and W. B. Wuir, Phys. Rev. 136, A561 (1964).

59. R. Schwaller and J. Wucher, C. R. Acad. Sc. 264, 116 Série B (1967).

60. F. T. Hedgecock, W. B. Wuir, T. W. Randorf and R. Szmidt, Phys. Rev. Letters 20, 457 (1968).

61. H. Rohrer, J. Appl. Phys. 38, 1322 (1967).

62. E. W. Collins, E. T. Hedgecock and Y. Muto, Phys. Rev. 134, A1521 (1964).